NASA Contractor Report 3329

Improved Test Methods for Determining Lightning-Induced Voltages in Aircraft

K. E. Crouch and J. A. Plumer

NASA

NASA Contractor Report 3329

Improved Test Methods for Determining Lightning-Induced Voltages in Aircraft

K. E. Crouch and J. A. Plumer
Lightning Technologies, Inc.
Pittsfield, Massachusetts

NASA

National Aeronautics
and Space Administration

Scientific and Technical
Information Branch

1980

CONTENTS

CONTENTS - Continued

SYMBOLS

AWG	American wire gauge
BCS	backup control system
C	capacitance, farads
CT	current transformer
d	diameter of a conductor, meters
DFBW	digital fly by wire
DFCS	digital flight control system
e	voltage, volts
f	frequency, hertz
h	distance between conductors, m
i	current, amperes
I	peak current, amperes
i_L	simulated lightning current, amperes
L	inductance, henries
ℓ	length, meters
LTA	lightning transient analysis
MPC	mode and power control
R, R_F, R_R, R_s, R_t	resistance, ohms
t	time, seconds
T	period of oscillation, seconds
Z	impedance, ohms
Z_o, Z_L, $Z_{A/C}$	surge impedances (also characteristic impedances), ohms

SYMBOLS - continued

σ electrical conductivity, mhos/m

ε permittivity, F/m

μ permeability, H/m

τ traveling wave transit times, seconds

INTRODUCTION

The increasing use of solid state electronics to perform flight control and other critical functions in aircraft has led to increased concern about the reliability of such electronics under adverse environments. Among the potentially hazardous environments are the surge voltages induced in aircraft electrical wiring by lightning strikes. Electronic microcircuits operate at very low power levels and cannot tolerate surge voltages of the magnitude that can be induced by lightning.

To learn more about lightning-induced voltages and how to control them, a series of NASA-sponsored programs was conducted during the years 1967-72. This research led to a better understanding of how lightning causes interference in aircraft electrical circuits and development of a nondestructive method, known as the lightning transient analysis (LTA) test, for determining the magnitudes of possible lightning-induced voltages in various electrical circuits.

In response to a concern about fly-by-wire system vulnerability in particular, an LTA test was performed on the NASA-Dryden Flight Research Center (DFRC) F-8 digital fly-by-wire (DFBW) aircraft in 1974. The aircraft was subjected to electric currents which were similar in waveform to lightning return strokes but greatly reduced in amplitude. The test data were then extrapolated to correspond with severe lightning strike currents.

The F-8 data was widely studied and prompted positive efforts to design lightning protection into aircraft then being designed with fly-by-wire control systems, including the USAF/General Dynamics F-16 and the NASA space shuttle.

However, due to the lack of an apparent relationship between the driving test current and the voltages it induced in some electrical circuits, concern was expressed about the validity of the test method and the influence of the surrounding facility on results. Questions have also arisen about the validity of linear extrapolation of test data to predict induced voltages under full-scale lightning stroke conditions, and about whether the test current being driven through the aircraft is in fact the primary cause of most induced voltages.

The purposes of this program, therefore, were to obtain a better understanding of tne several cause-effect mechanisms inherent in LTA testing, develop ways to minimize unwanted facility

effects, and define improvements that enable a better simulation of natural lightning. The program was conducted in three experimental phases and utilized the NASA F-8 airplane as a test bed. Besides incorporating a typical flight-critical electronic system, the F-8 has been utilized in prior LTA tests and a large amount of data produced by the original LTA technique was available for baseline reference. The first and third experimental phases of this program were conducted on the F-8 at Dryden using transportable test equipment and instrumentation. The second experimental phase, which utilized a one-tenth scale model of the F-8, was conducted at Lightning Technologies, Inc. The program was conducted during the period February, 1979 through February, 1980.

OBJECTIVES

The primary objectives of this program were to obtain a better understanding of the basic mechanicms that related induced voltages appearing in aircraft electrical circuits to various test circuit parameters, and to utilize this knowledge to define improvements in the test method, such that overall validity is increased.

Of particular interest were the following relationships:

- The cause(s) of higher frequency oscillations that occur within a microsecond or so after current is applied to the aircraft.

- The effects of test circuit return conductors (not present in natural lightning but a necessity in most tests), and the nature of the transmission line thus formed.

- The nature and effects of traveling waves in the airframe.

The following improvements in simulation were also desired:

- Bring the test current and voltage into a proper relationship.

- Bring the traveling wave currents into proper relationship with the return-stroke currents.

- Enable simulation of lightning leader effects as well as the return stroke.

- Minimize unwanted facility effects.

2

BACKGROUND

Concern for the effects of lightning-induced voltages on aircraft electronic systems has been increasing with the advent of fly-by-wire flight controls and other systems which utilize electronics in flight-critical functions. Lightning strikes have already demonstrated an ability, on occasion, to disrupt aircraft electronics, and several trends in electronics and airframe design may aggravate the situation further unless designers are made aware of the lightning effects environment their equipment must survive in.

To learn more about lightning-induced voltages in aircraft electrical circuits and how to control them, a series of NASA-sponsored research programs was conducted during the years 1967-72. This research led to a better understanding of how lightning causes interference in aircraft electrical circuits (refs. 1 and 2) and development of a nondestructive method of simulating a lightning strike to the aircraft for the purpose of determining the susceptibility of particular circuits (ref. 3). This has become widely known as the LTA test.

Since the aircraft must be available before the susceptibility of its electrical circuits can be determined by the LTA test, a need exists for analytical techniques with which to predict this susceptibility during the design phase. Contractual efforts to develop such tools have been underway since 1972 (ref. 4) but these have borne little fruit thus far. The difficulty of solving this problem analytically is recognized, and proven techniques are not close at hand.

In response to the concern about fly-by-wire system vulnerability, an LTA test was performed on the NASA F-8 aircraft in 1974 (ref. 5). The aircraft was subjected to electric currents which were similar in waveform to lightning return strokes but greatly reduced in amplitude. The test data were extrapolated to correspond with average (30,000 A) and severe (200,000 A) lightning stroke currents. The extrapolated data is summarized in Table I.

The F-8 data was widely studied, and prompted positive efforts to design lightning protection into the aircraft then being designed with fly-by-wire control systems: the USAF/General Dynamics F-16 (ref. 6) and the NASA space shuttle (ref. 7). Nevertheless, the magnitude of the voltages measured in the F-8 and the apparent absence of a logical relationship to the injected test current has caused some skepticism regarding the validity of

the basic LTA test and the authenticity of the lightning strike amplitude and waveform simulated in the test.

TABLE I - RANGE OF PEAK INDUCED VOLTAGES IN NASA F-8 LTA TEST
(Scaled to 200 kA)

[From ref. 5]

INTERFACE	INDUCED VOLTAGE AMPLITUDE (Peak Volts)	
	MIN.	MAX.
Stick Trim and MPC Inputs to DFCS (J25)	233	900
Stick Transducer Inputs to DFCS (P4)	40	87
DFCS Control Outputs (J2)	233	400
BCS Control Inputs (J12)	222	422
Mode and Power Control (J15)	833	1132
Mode and Power Control (J14)	213	732
Power Dist. Bay (+28VDC Bus)	160	200
DFCS Ground to A/C Ground	0	666

The occurrence of return strokes, such as the one represented by the 2 x 50 microsecond waveform (time to reach crest x time to fall to 1/2 crest) used in the LTA test has been confirmed (ref. 8). Much less is known about the nature of streamer and leader currents occurring in the airframe, and no attempt was made during the LTA test development to simulate these currents. Whereas their amplitudes are almost certain to be less than return strokes, their rise and decay times may be considerably shorter, producing substantial rates of rise.

Flight research programs (ref. 9) are getting under way to learn more about these currents and other characteristics of lightning by flying instrumented aircraft near thunderstorms, but a number of years will be required to accumulate meaningful data.

In the meantime, the trend toward further miniaturization of electronics and use of nonconducting materials in airframes has increased the concern over induced voltages. This necessitates that questions of LTA test validity be resolved and the test improved, if necessary, so that it can be used with greater confidence.

Most of the questions about the validity of the LTA test have arisen because there appears to be little relationship between the test current and some of the voltages it induces, particularly in parallel-pair, single-point grounded circuits such as are employed in flight control systems.

A typical LTA test circuit is illustrated in Figure 1 and examples of voltages induced by the test current in two aircraft electrical circuits are shown in Figure 2.
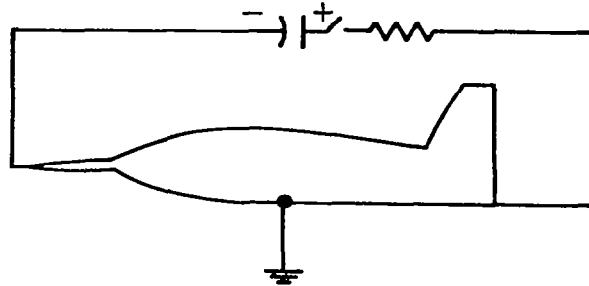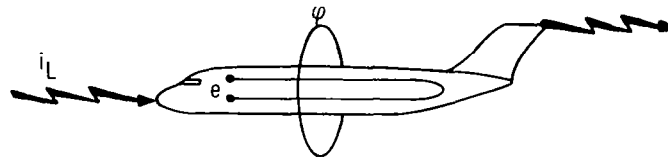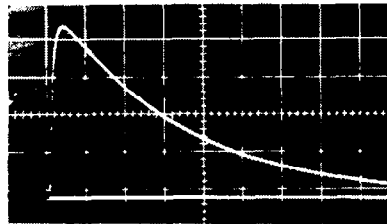
Figure 1 - Typical Lightning Transient
Analysis Test Circuit.

(a) Waveform of
lightning current
and magnetic flux.

(b) Induced voltage

$$e = \frac{d\varphi}{d\tau} + i_L R_S$$

= clear relationship.

(c) Induced voltage
$e = f(?)$
= unclear relationship.

10 µs

Figure 2 - Relationships between Test Current and
Induced Voltages.

The voltage measured in oscillogram (b) displays a structural voltage rise ($i_L R_s$) component that is in phase with the simulated lightning current, plus a magnetically induced component ($d\phi/dt$) which is proportional to its derivative. This is indicated by the shorter rise time and undershoot of the induced voltage waveform.

The voltage measured in oscillogram (c), however, oscillates at a high frequency about the zero-axis and bears no evident relationship to the lightning current. Circuits which display voltages such as shown in (b), where the familiar relationship exists, nearly always have a relatively large loop area, such as occurs when a single wire is used to transmit a signal (or power) and the airframe is utilized to return it.

But when a separate wire is used for the return and routed next to the first one, the area between the two is small and the familiar derivative voltage is greatly reduced. There remains, however, a high frequency component of short duration occurring immediately after t = o, as shown in (c). When extrapolated to full-scale levels, these high frequency voltages sometimes exceed 1,000 volts - a level that cannot be tolerated by many electronic components.

Some aircraft designers, in disbelief, have rationalized that these high frequency voltages are peculiar to the LTA test only and should not be extrapolated upward by the same factor as the familiar voltages are. Other designers have incorporated shielded cables or surge suppressors to deal with these voltages on the assumption that they are authentic. Such measures, of course, add to the cost and weight of the aircraft. Thus a better understanding of the origin of the high frequency voltages that occur when test current first enters the airframe is required.

Since the frequencies of some of the oscillatory voltages appeared related to the length of the airframe, it has been thought that traveling wave currents in the airframe may be the source of the high frequency voltages.

Traveling wave currents may be expected to reflect back and forth in the airframe at the speed of light if, for example, a mismatch exists between the surge impedances of the lightning channel and the airframe, as illustrated in Figure 3.

i_L $i_{A/C}$ i_L

$Z_L = 450\ \Omega$ $Z_{A/C} = 50\ \Omega$ $Z_L = 450\ \Omega$

REFRACTED CURRENT $= \dfrac{2Z_L}{Z_{A/C} + Z_L} = 1.8\ i_L$ $= \dfrac{2Z_{A/C}}{Z_{A/C} + Z_L} = 0.2\ i_L$

REFLECTED CURRENT $= \dfrac{Z_L - Z_{A/C}}{Z_{A/C} + Z_L} = 0.8\ i_L$ $= \dfrac{Z_{A/C} - Z_L}{Z_{A/C} + Z_L} = -0.8\ i_L$

i_L

$\tau = 0$ $1.8\ i_L$

$0.8\ i_L$

$-1.44\ i_L$ $\tau = T/2$

$\tau = T$ $0.36\ i_L$

$-0.288\ i_L$ $1.152\ i_L$ ETC

THESE REFLECTIONS CAUSE AN OSCILLATING CURRENT IN THE AIRFRAME:

$i_{A/C}$

1.8 1.5 1.3 1.2 1.1
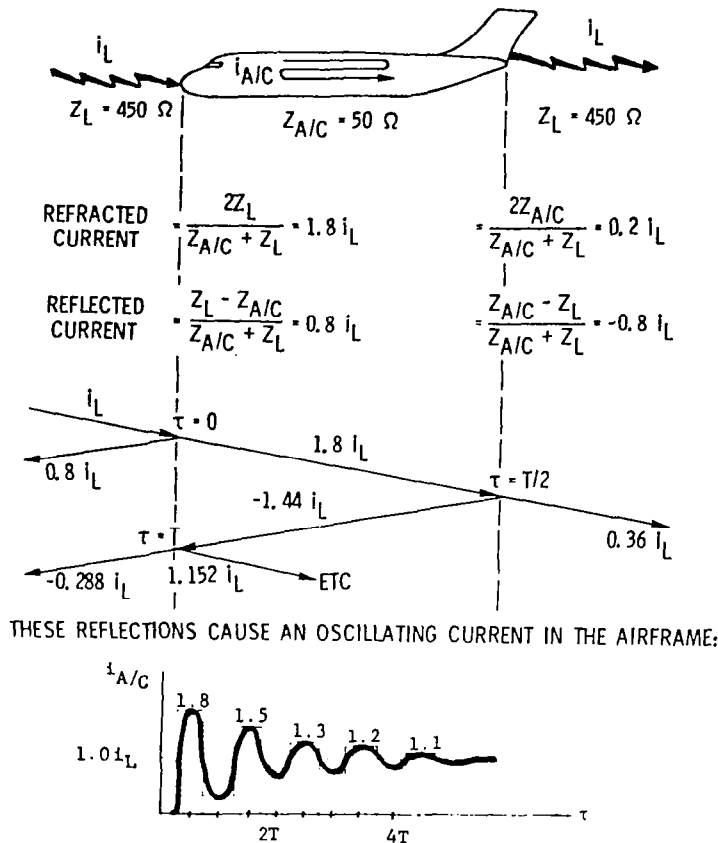
$1.0\ i_L$

$2T$ $4T$ τ

Figure 3 - Traveling Wave Currents.

The surge impedance of any conducting path is defined (ref. 10) as the ratio of the instantaneous surge voltage to the instantaneous surge current at a single point along the conducting path, as follows:

$$Z_o = \frac{e}{i} \tag{1}$$

where,

     e = conductor voltage with respect to its return path, V

     i = conductor current, A

It will be a constant for each conductor and return path. It can be shown that the surge impedance may also be expressed as:

$$Z_o = \sqrt{\frac{L}{C}} \tag{2}$$

7

where,

   L = inductance per unit length of conductor, H

   C = capacitance per unit length of conductor, C

If the surge impedances of the lightning channel and the airframe are not the same (that is, if the ratios of voltage to current are not the same), some of the energy in the lightning channel may be reflected back into the channel and may not immediately enter the aircraft. Similarly, energy that has been deposited on or in the airframe may not leave it at once, but may instead reflect back and forth as shown on Figure 3.

In Figure 3, the surge impedances of the lightning channel (Z_L) and the aircraft ($Z_{A/C}$) are assumed to be 450 ohms and 50 ohms, respectively. If the lightning channel and aircraft can be represented as transmission lines, and if the reflection and refraction coefficients (ref. 10) for a lossless line are applicable, then the traveling wave current in the aircraft would appear as shown in Figure 3. The velocity, (v) of the traveling waves in the aircraft would be that of light, 3×10^8 meters per second, and the period (t) of oscillation would be proportional to the length (ℓ) of the aircraft, or

$$T = \frac{2\ell}{v} \qquad (3)$$

and the frequency (f) would be

$$f = \frac{1}{T} \text{ hertz} \qquad (4)$$

and voltages induced by such traveling wave currents should be of the same frequency. In LTA tests to date, some voltages of these frequencies have appeared, but they are so cluttered with components of other frequencies as to make positive identification difficult.

This experimental investigation focused on the transmission-line aspects of the LTA test setup. These were aspects that had not been addressed thoroughly enough in any of the previous LTA programs, and included return conductor effects, aircraft surge impedance, transit time and ringing frequency, and transmission-line aspects of the test current generators. To enable a large number of variations to be made in test circuit parameters, a simple, geometric scale model of the F-8 airframe and return conductors was constructed. The geometric model technique has been utilized successfully in related work (ref. 11) and enables variations in test circuit and return conductor configurations to be made far more quickly than if done on a full scale setup.

8

The following paragraphs describe the basic full scale and model test arrangements, and present the results obtained.

EXPERIMENTAL INVESTIGATION

Full Scale F-8 Test Setup

F-8 DFBW airplane.- The NASA F-8 DFBW airplane was utilized as the test aircraft in this program. The aircraft is a single engine, all metal fighter-type aircraft with a high wing that can be raised a few degrees to obtain a higher angle of attack during landing and takeoff maneuvers. The NASA F-8, the dimensions of which are shown in Figure 4, has been utilized by NASA as a test bed aircraft to evaluate various aspects of digital flight control technology.

Whereas the ultimate goal of this work is to enable a better understanding of flight-control systems vulnerability in the lightning environment, this particular program was directed toward test technology development rather than assessment of the NASA F-8 DFBW system vulnerability. Thus, the DFBW system was not operating during this program. In fact, the flight control computer package was removed from the aircraft to provide room for a battery operated oscilloscope.

Aircraft instrumentation. - Induced voltages were measured in one flight control circuit only, so that the effects of many variations in test parameters could be studied on a common basis. The circuit chosen was a twisted two-wire pair that extended aft from plug AP3 in the flight control computer pallet area a distance of about 8 meters to plug P100 at the base of the vertical fin as shown in Figure 5.

The circuit was part of a multi-conductor bundle of DFBW circuits, and is typical of circuits that extend between the computer and secondary actuators located near control surfaces. It was basically unshielded, except that portions of it passed through several sections of metal conduit in this exposed area.

Both wires of the twisted pair were grounded to the airframe at P100, and terminated to ground with 50 ohms in the pallet area. The induced voltages were recorded during the first full-scale test series by a battery-powered 200 MHz oscilloscope and during the second full-scale series with a 100 MHz oscilloscope with a wide-band differential preamplifier, also powered from a battery. Most of the oscillograms reproduced in this report were produced by the 100 MHz oscilloscope. The pallet area where the oscilloscopes were located is pictured in Figure 6, and the location of the aft terminal of the instrumented circuits is shown in Figure 7.
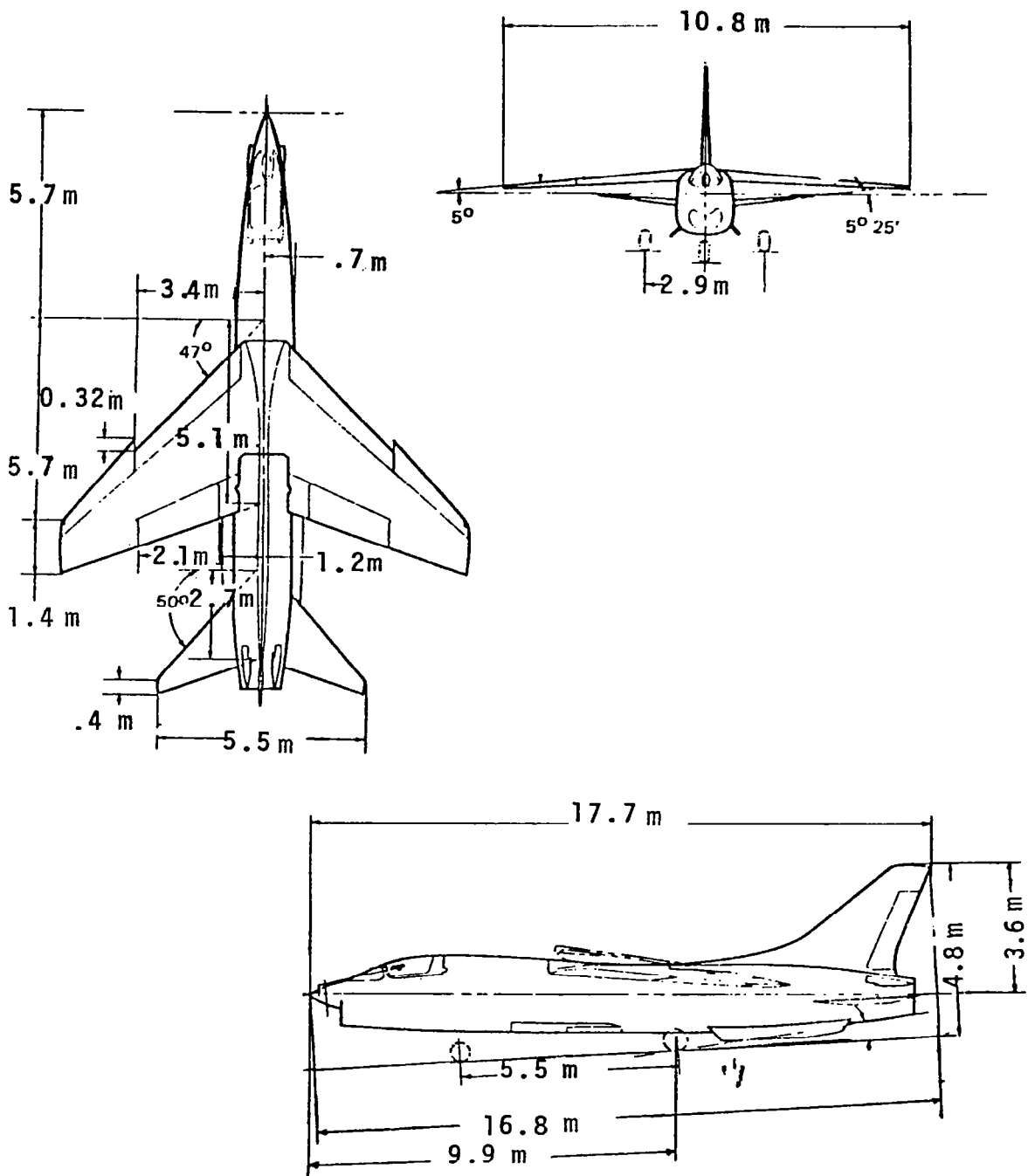
Figure 4 - Overall Dimensions of the NASA
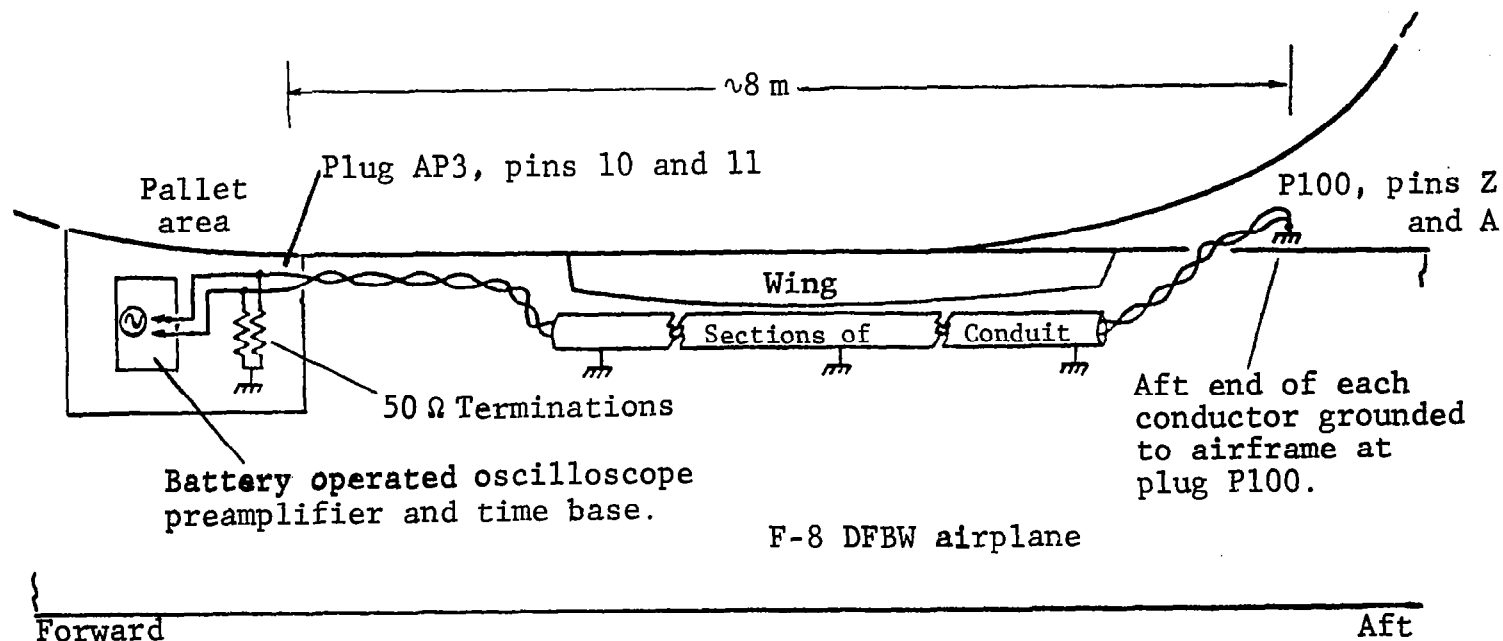F-8 Digital Fly-by-Wire Airplane.

Figure 5 - Instrumented Twisted-pair Circuit in NASA F-8
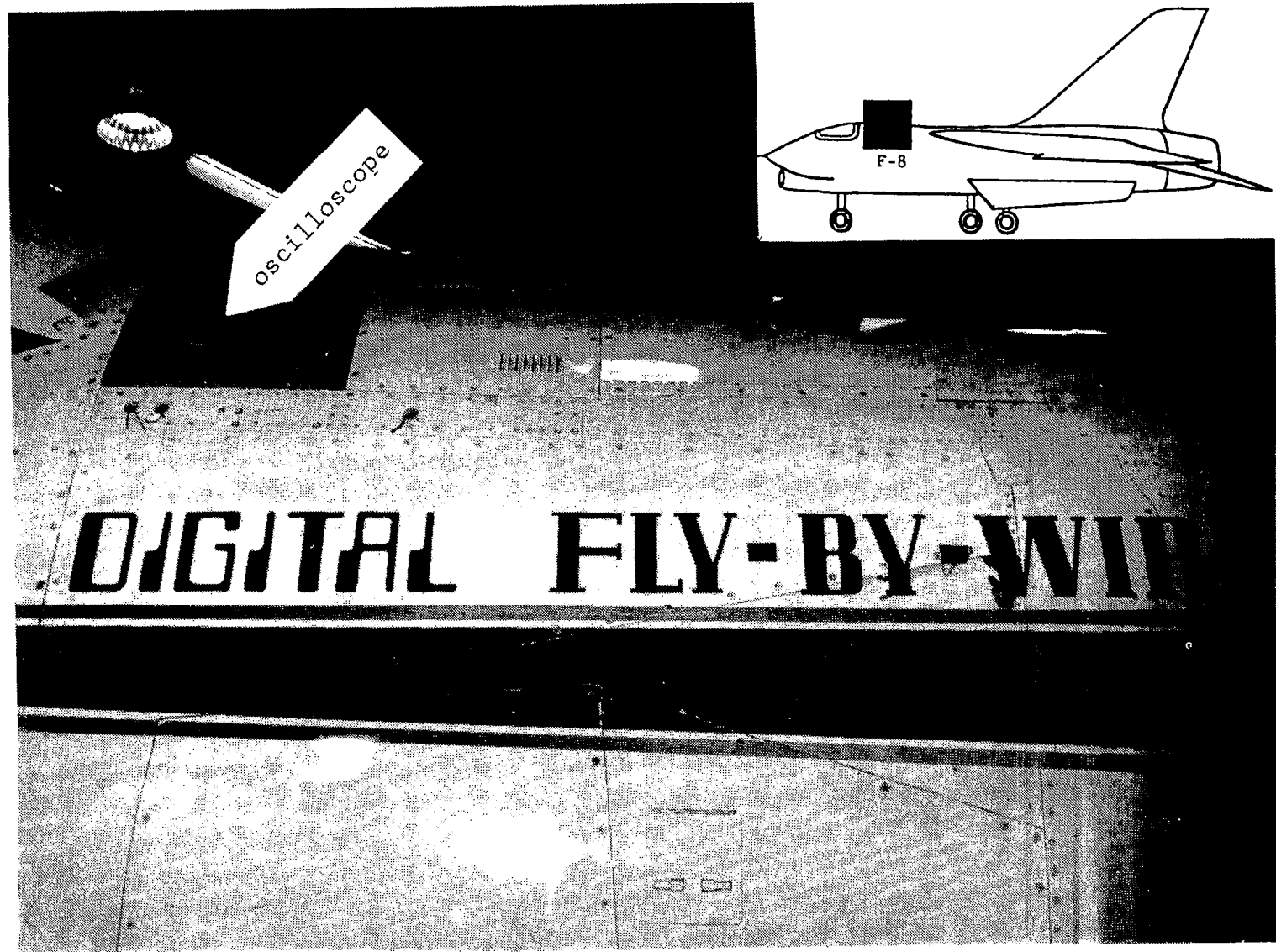Digital Fly-By-Wire Airplane.

Figure 6 - Location of Battery-Powered Oscilloscope
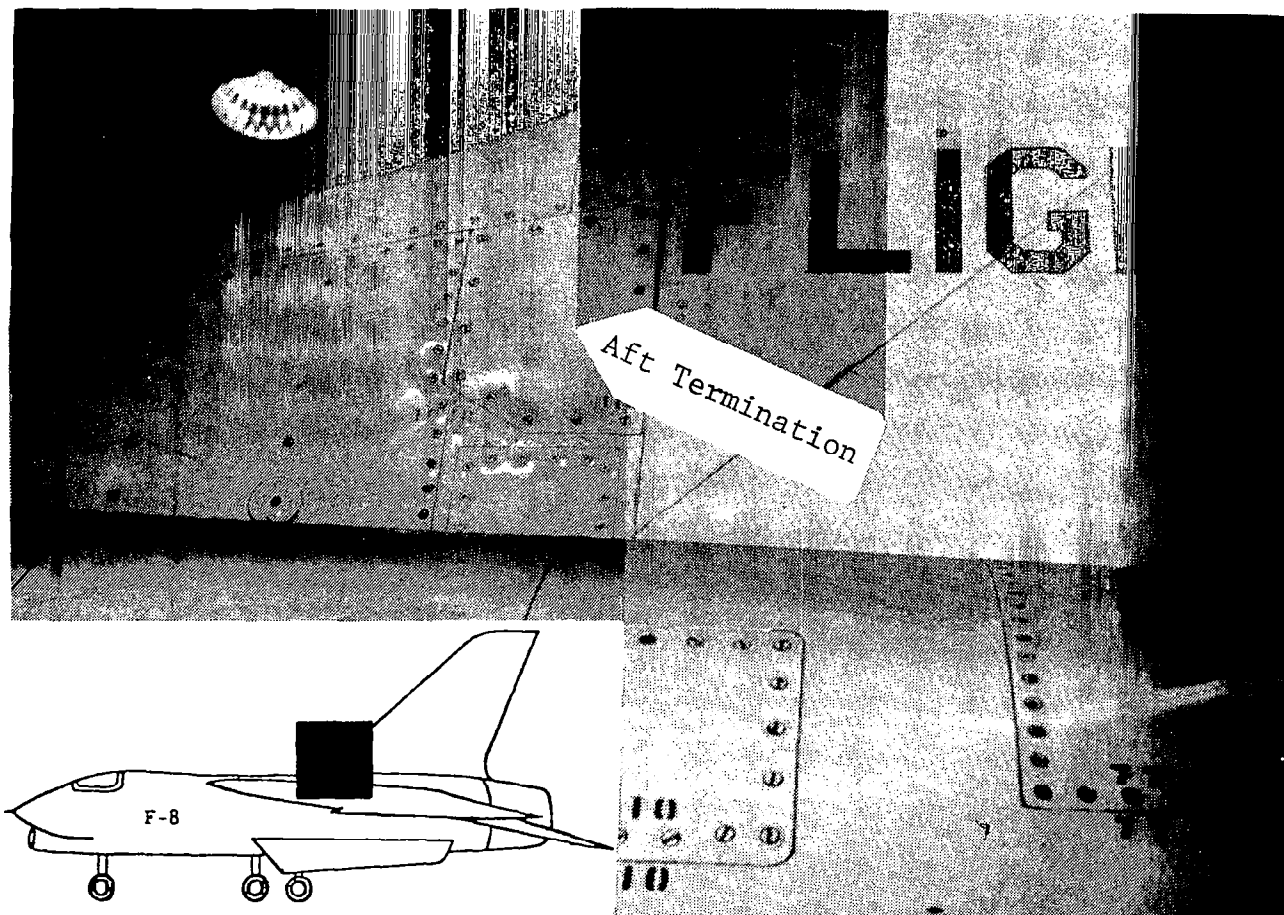to Measure Induced Voltages.

Figure 7 - Location of Aft Termination of Instrumented Circuit.

For most of the tests, the aircraft oscilloscope was trig-
gered by the voltage induced in a Rogowski coil around the nose
boom as shown on Figure 8. A coaxial cable conducted this voltage
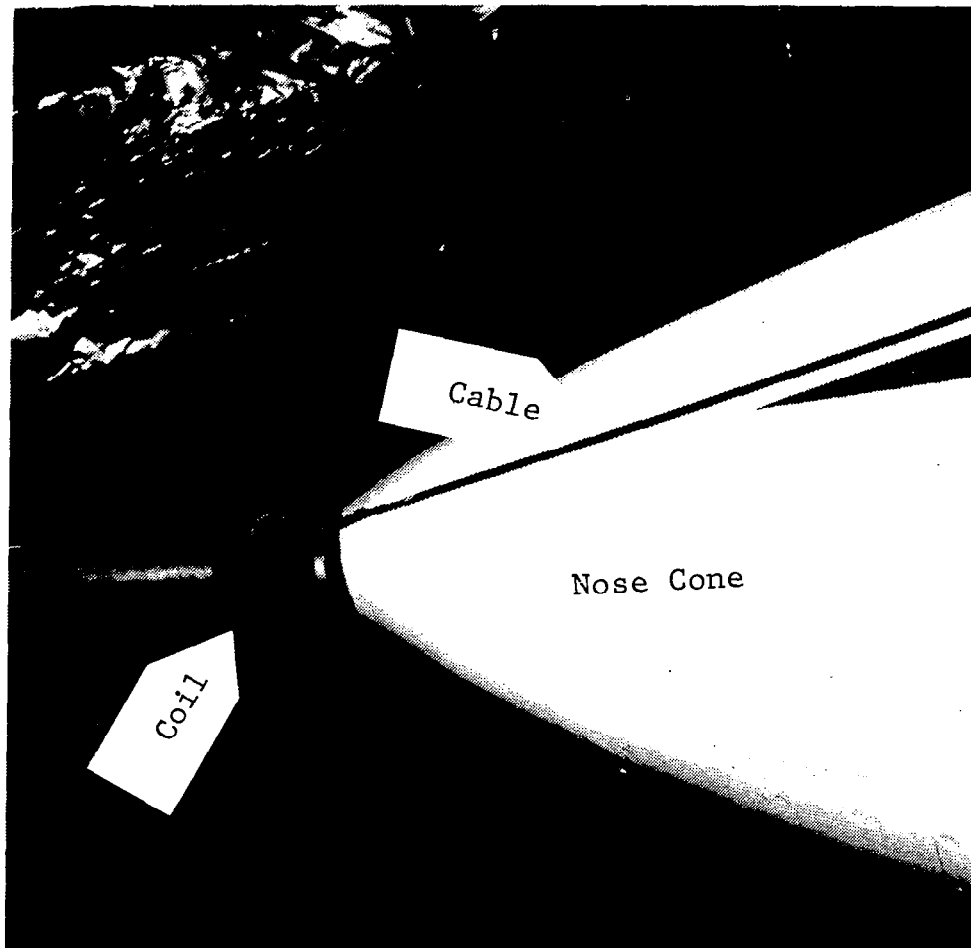to the oscilloscope trigger input.

Figure 8 - Rogowski Coil to Provide Aircraft
Oscilloscope Trigger Signal.

The aircraft oscilloscope had a differential preamplifier so
that the line-to-line voltage between conductors could be meas-
ured, as well as the voltage between either conductor and airframe
ground. The oscilloscope was connected to the circuit conductors
via a pair of short coaxial cables fitted with alligator clip
leads. 50 ohm line-to-ground terminations were used to terminate
each conductor. The alligator clip leads were short and twisted,
and the oscilloscope was grounded to a shelf within the pallet
area to minimize extraneous noise in the measurement system.

At intervals throughout the tests, measurements were made of the noise that appeared in the oscilloscope and the alligator clip leads when test current was applied to the aircraft. A typical noise measurement is shown on Figure 9.
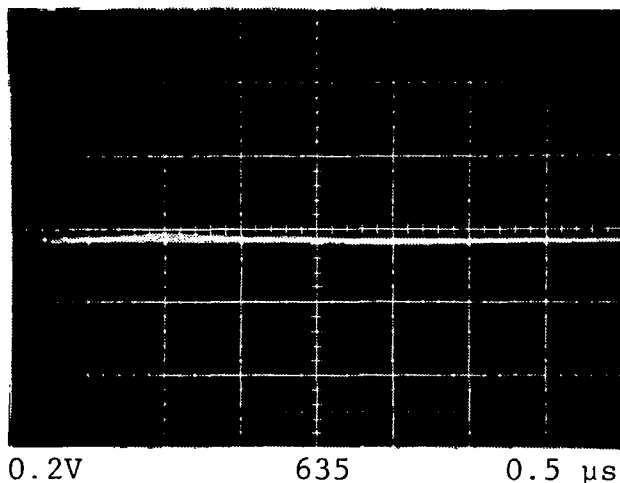

0.2V   635   0.5 μs

Figure 9 - Noise in Induced Voltage Measurement System
with Channels A and B Connected to Airframe
Ground in the Pallet Area. Voltage Shown Is
the Differential Voltage between Channel A
and Channel B.

Most of the line-to-line induced·voltage measurements were made with the same vertical sensitivity in Figure 9, and the signals ranged from one quarter of a centimeter to over one full centimeter of deflection, such that the noise level was nearly always less than 10% of the induced voltage signal.

Basic test configuration. - The aircraft was positioned in a metal-walled hangar with its main and nose gear wheels parked upon insulating sheets of clear polycarbonate resin, 6.1 m square and 9.5 mm thick. These insulating pads enabled the aircraft to be electrically charged up to 50,000 volts (50 kV) with respect to building grounds.

Since many of the tests would require return conductors, an array of four conductors, supported by wooden stanchions, was erected along the aircraft. In the first series of full scale tests, each conductor consisted of a group of three steel wires spaced approximately 0.4 m apart. The wires were covered with aluminum foil to see if this made any significant difference in test results (it did not). Figure 10 illustrates the location of the four return foils or groups of wires.
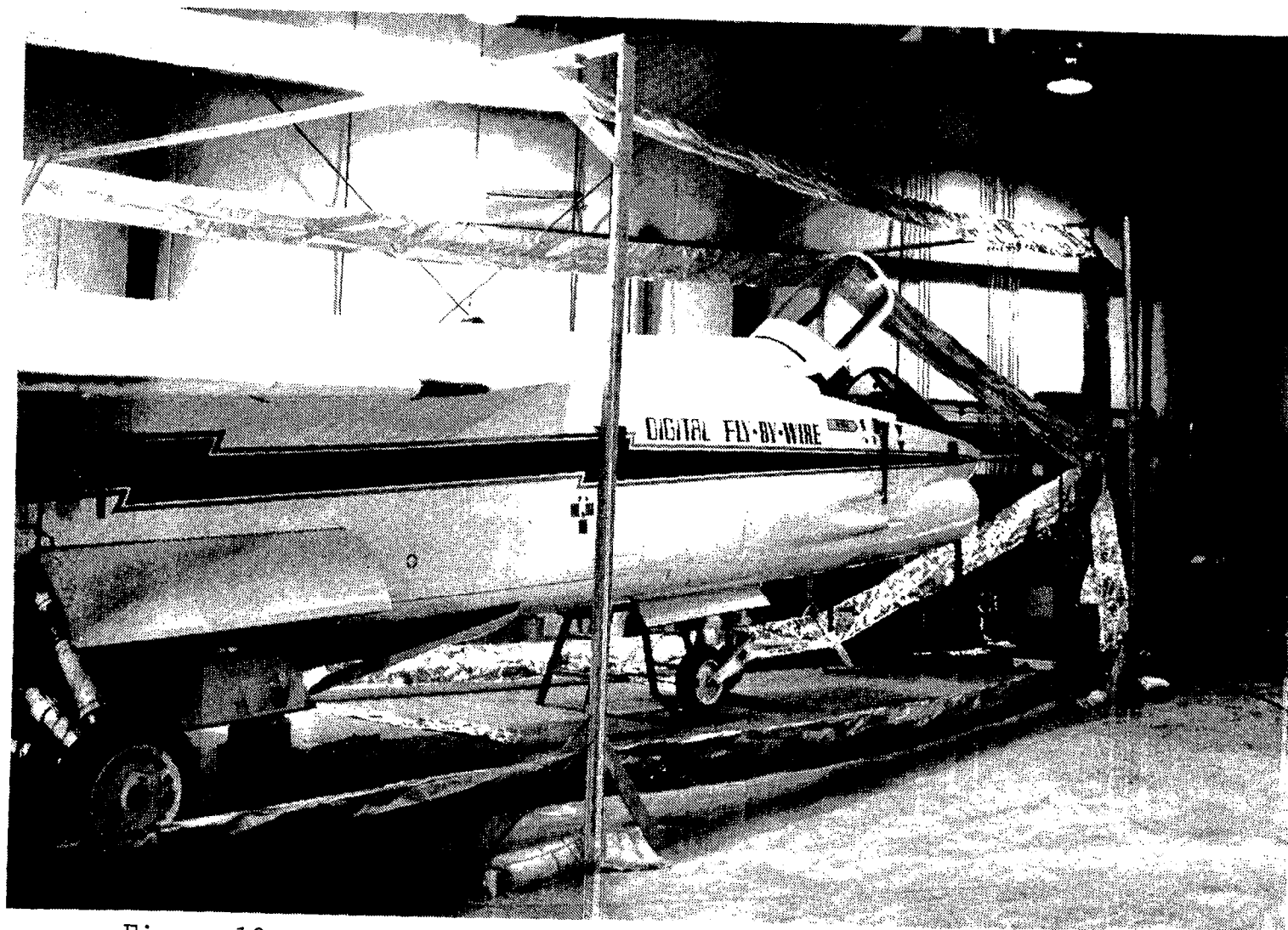
15

Figure 10 - Four Aluminum Foil Return Conductors Supported by Wooden Stanchions. Four Groups of Three Wires Were also Used in the Same Locations.

The four conductors were positioned approximately 2 meters from the aircraft in upper and lower and left and right quadrants to encourage cancellation of return current proximity effects of the aircraft.

The stanchions supporting the return conductors were made of wood with spacings and dimensions as shown on Figure 11. The four foils or groups of wires were brought together to facilitate a common connection point at each end of the aircraft.

Tests were begun using an "original" LTA test circuit in which electric charge is stored in a single generator capacitor (C). A waveshaping resistor (R) and inductor (L) are connected in series between this capacitor and the aircraft to provide a unidirectional current pulse which rises to its peak in 2 microseconds decays to 50% of its peak value in 50 microseconds. This is the familiar 2 x 50 μs waveform.

The capacitance consisted of one or more 0.5 μF, 50 kV capacitors connected in the manner necessary to provide the desired capacitance. The resistance was a bi-filar wound noninductive card-type resistor, and the inductor was a coil of AWG No. 10 insulated wire, wound on a 5 cm diameter plastic tube. Values of each element were varied during the tests and are given in individual circuit diagrams that follow throughout this report.

The generator capacitors and waveshaping elements were positioned between the nose of the aircraft and the forward ends of the return conductors. It was determined early in the program that each end of the return conductor array should be grounded to the building ground through terminating resistors. The terminating resistors were suspended at the apexes of the return conductor arrays and grounded to the building via aluminum conductors as shown in Figure 12.

The capacitors were charged from a 50 kV DC power supply located on a table outside of the return conductor array. The capacitors were discharged into the waveshaping circuitry and aircraft by means of a flapper switch mounted on one of the capacitor bushings, as shown on Figure 13.

Test circuit instrumentation. - The electrical parameters measured during the program were the current entering or leaving the aircraft, or at other places in the test circuit, and the voltage between the airplane and the adjacent external return conductors at the nose and tail of the aircraft, and occasionally at other points in the circuit.
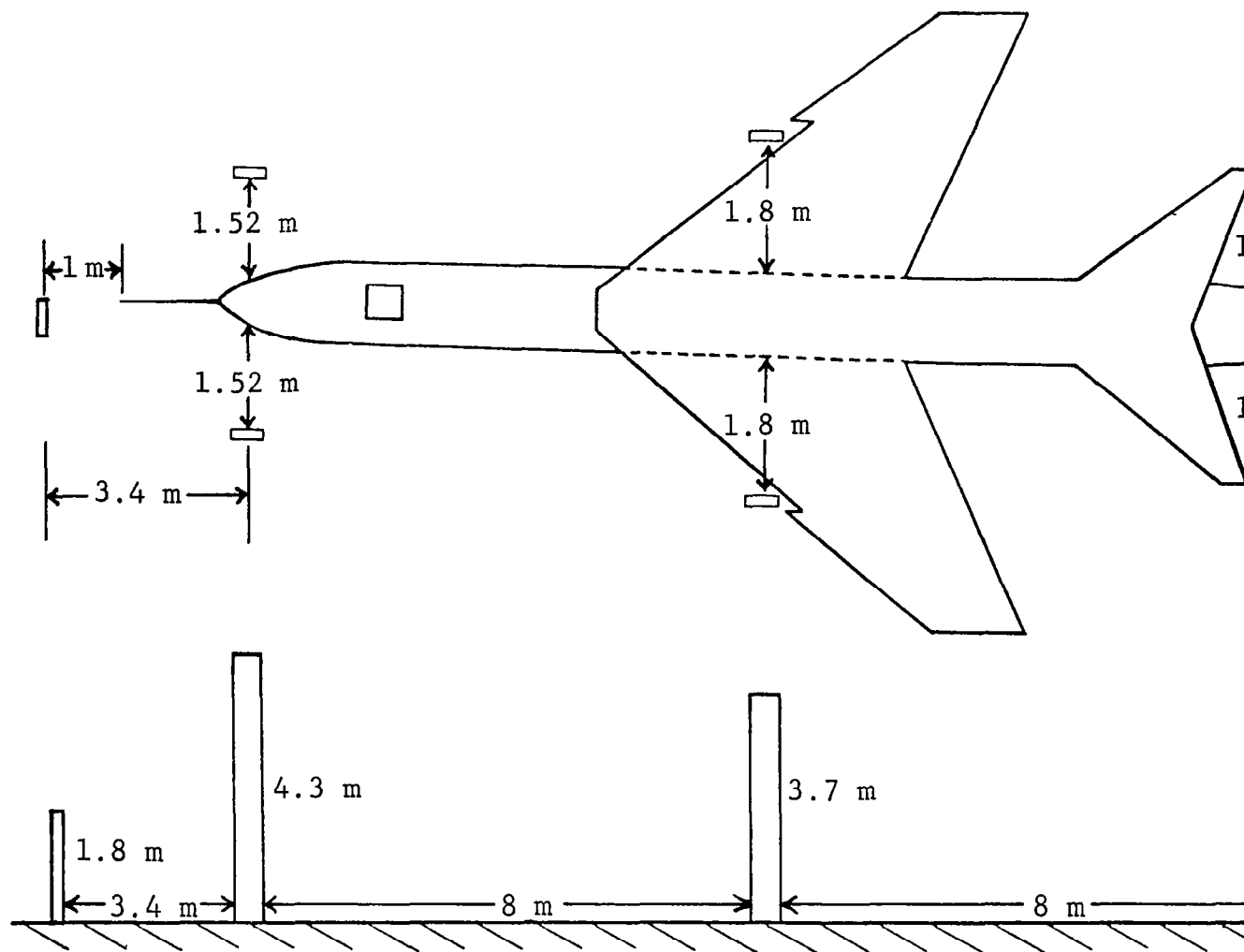
1.52 m

1 m

1.52 m

3.4 m

1.8 m

1.8 m

4.3 m

3.7 m

1.8 m

3.4 m

8 m

8 m

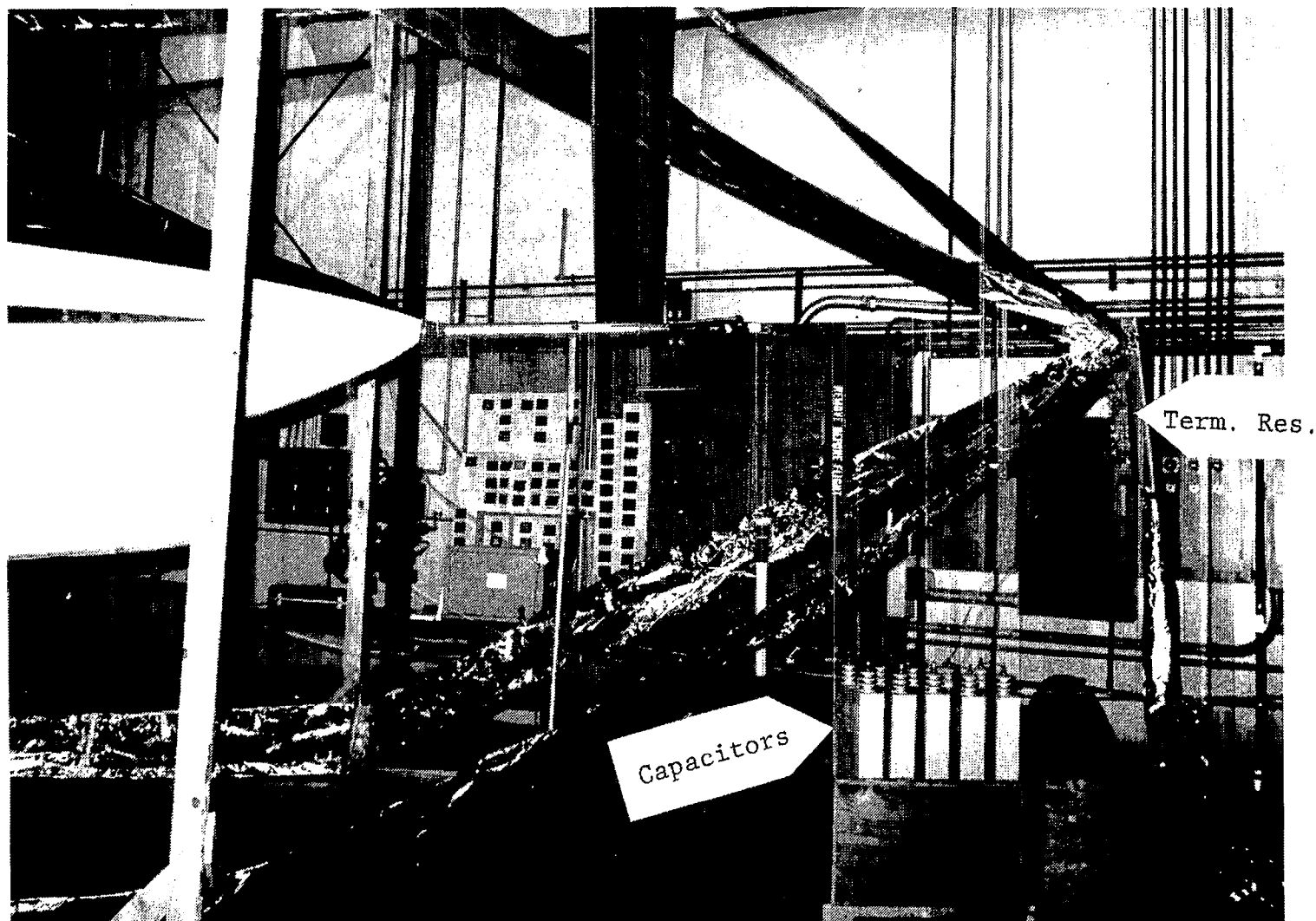Figure 11 - Dimensions and Location of Wooden Return Conductor

Figure 12 - Location of Generator Capacitors and Return Conductor
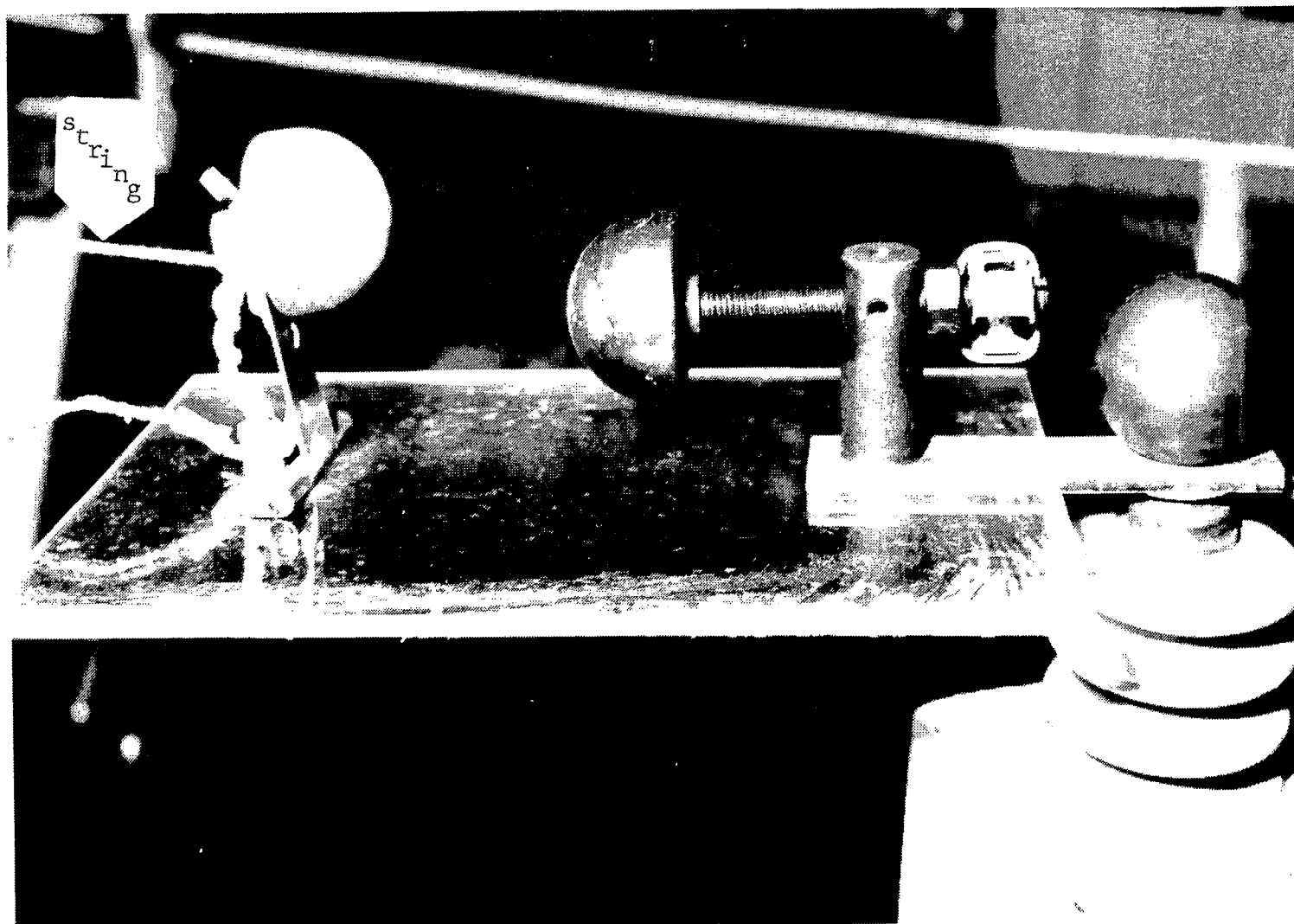Terminating Resistor at Forward End of Aircraft.

Figure 13 - Flapper Switch to Discharge Capacitors
into Aircraft Test Circuit.

The test current was measured with a 100:1 impulse current transformer (CT) loaded with a 0.1 ohm burden resistor, so that the ratio between test current and signal voltage at the oscilloscope was as follows:

$$e_{scope} = \frac{i_{test}}{100} \, (0.1\Omega) \qquad (5)$$

$$= \frac{i_{test}}{1000}$$

A test current of 250 amperes produced 0.25 volt at the oscilloscope - a level easily measurable. The CT was built and calibrated at the General Electric Corporate Research and Development Center and has a frequency response of 1 Hz to 100 MHz. It is shown at the aft end of the aircraft termination resistor in Figure 14. The CT output voltage was transmitted to a measurement oscilloscope located outside of the return conductor array via a 33 meter RG-58U coaxial cable. To minimize noise induced in this cable, it was enclosed within a braided shield and laid upon a 0.5 m wide aluminum foil strip that extended between the return line termination resistor and the oscilloscope enclosure.

Voltages were measured between the aircraft and return lines with a 100:1 resistance voltage divider comprised of two legs of five 1000 ohm carbon resistors arranged side-by-side in a plastic enclosure. The two 5000 ohm resistors were each connected to conductors of a 33 m, RG-22 twinaxial cable, which was terminated with 50 ohm line to ground resistors at the oscilloscope. To obtain higher voltage divider ratios, 5x or 10x terminations were added at the oscilloscope. For example, to measure traveling wave voltages between the aircraft and the return conductors when the generator capacitors were charged to 25 kV, the 10x termination was utilized so that:

$$e_{scope} = \frac{e_{test}}{(100)(10)} = \frac{e_{test}}{1000} \qquad (6)$$

or, if the test voltage was 25 kV, the oscilloscope voltage was

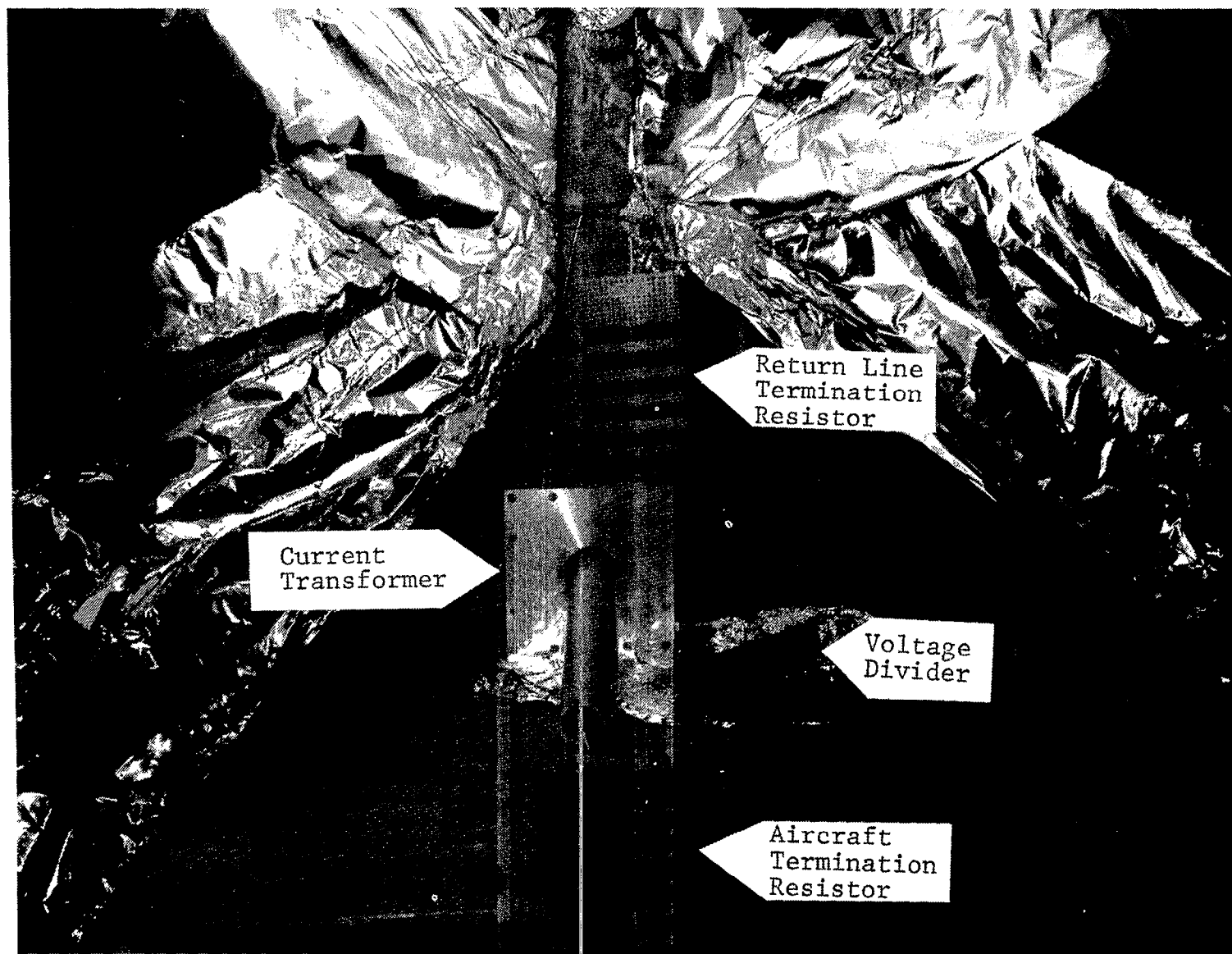$$e_{scope} = \frac{25 \times 10^3 V}{1000} = 25 \text{ volts}$$

Figure 14 - Impulse Current Transformers at Aft Termination, Showing Aircraft and Return Line Termination Resistors.

Test circuit current and voltage were recorded by a 400 megahertz dual beam oscilloscope with two wide band differential preamplifiers. This oscilloscope was powered from 115 VAC building power and housed within a five-sided aluminum box to minimize electromagnetic field coupling between the return conductors and the oscilloscope. This oscilloscope is shown in Figure 15.

Most of the time, this oscilloscope was also triggered externally by a voltage induced in a Rogowski coil located at the nose boom or other location close to the generator discharge flapper switch. This was done so that voltage and current measurements could be made at various locations along the test circuit and related time-wise to a common zero time reference. A Rogowski coil was chosen to provide the trigger voltage because it responds to the derivative of the test current and thus rises faster than the test current. The length of the trigger voltage, test current and test voltage measurement cables were made the same (33 m) to eliminate signal arrival time differences at the oscilloscope.

The response characteristics of the test circuit and current measurement systems was evaluated by applying square wave voltage and current signals to the CT and voltage divider and observing the response at the oscilloscope, which was separated from the sensors by the 33 m signal cables. The results of these evaluations are shown on Figure 16.

Occasionally, several measurements were made of radiated fields or other parameters also associated with the test circuit. These are described at appropriate points in the following text.

One-Tenth Scale Model F-8 Test Setup

As outlined in Objectives, a major purpose of this program was the evaluation of the relationships between various test aircraft. Since alteration of the test circuit and return conductor arrangement surrounding the F-8 airplane is a time-consuming operation, it was decided to use a relative geometric scale model to enable the large number of test circuit changes to be made and evaluated within the program. The following paragraphs describe the basic geometric scale model technique and the F-8 model test setup employed in this program.

Relative geometric scale models. - When studying the electromagnetic response of a system to lightning, it is often difficult to visualize and express mathematically all of the factors affecting the response. This is especially true when the system is physically large and the distributed nature of the electromagnetic fields produced by lightning conduction in the structure must
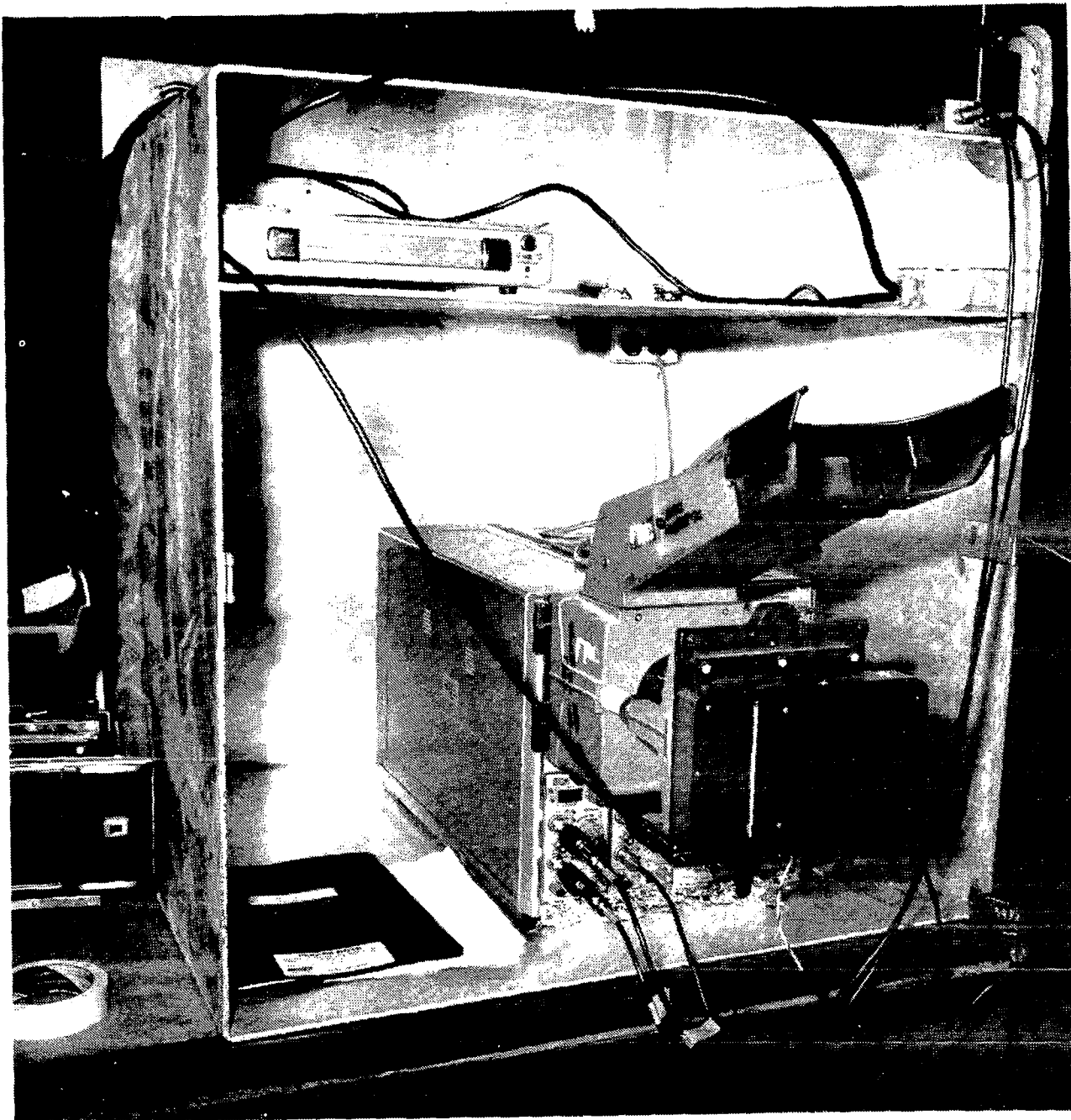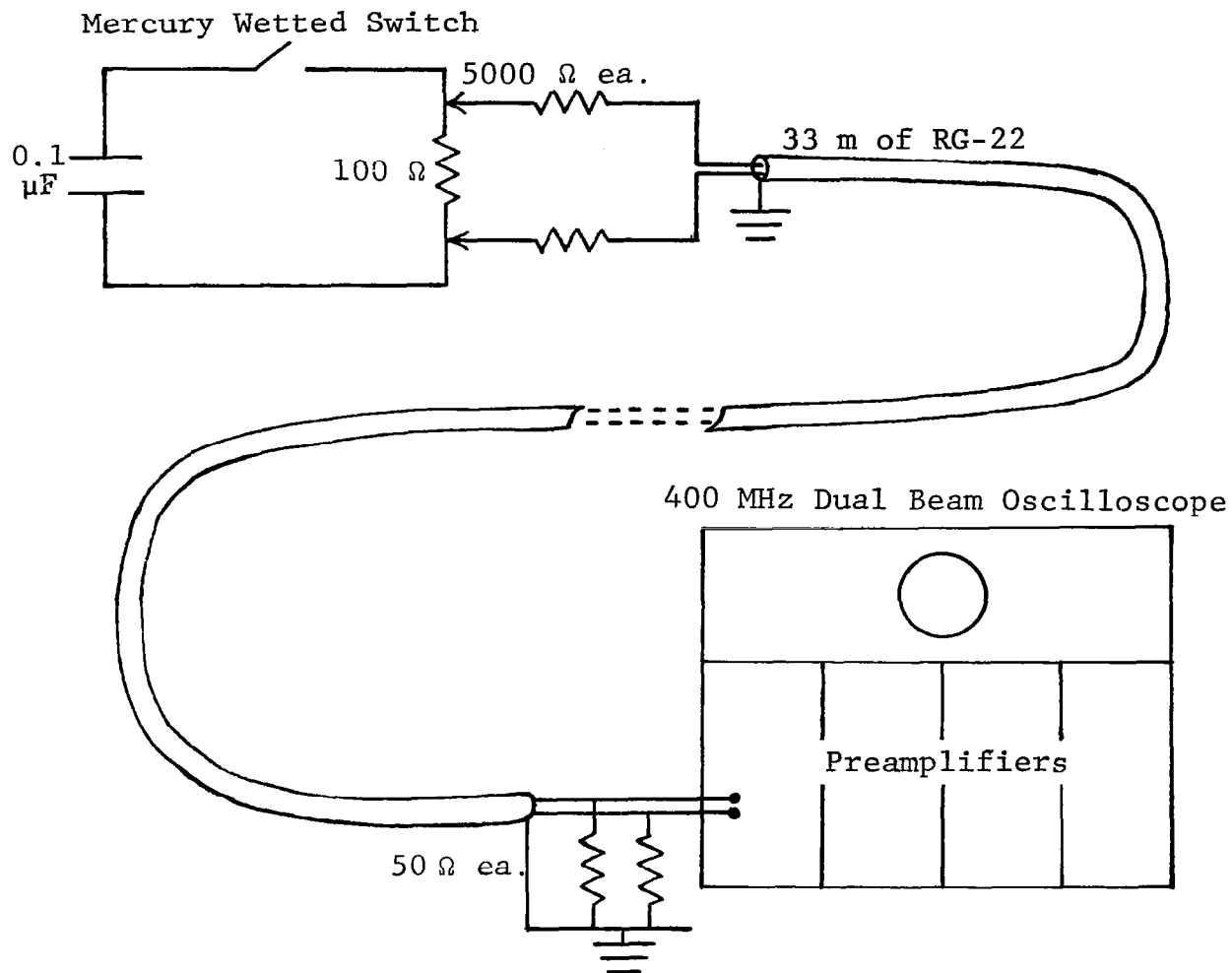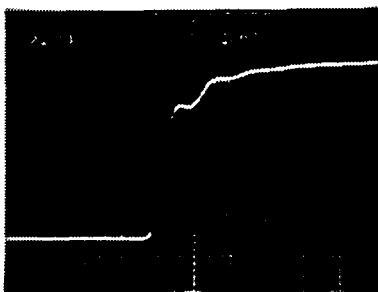
23

Figure 15 - 400 MHz, Dual Beam Oscilloscope within Shielded
         Enclosure for Measurement of Test Circuit Current
         and Voltages.

Mercury Wetted Switch

5000 Ω ea.

0.1 μF

100 Ω

33 m of RG-22

400 MHz Dual Beam Oscilloscope

Preamplifiers

50 Ω ea.

Measurement Circuit

12 ns Response

>100 mV/div 10 ns/div

Figure 16 - Response Measurement of Differential Voltage Divider.

be considered as well as the distributed nature of the electrical circuits of interest that are contained within the airframe. Often the mathematical expressions which describe these distributed fields are quite complex, and the data necessary to define the expressions are not readily available. In such cases, it may be easier to measure directly the desired system response than to derive and employ mathematical expressions.

If the system of interest is physically large, as, for example, a Boeing 747 aircraft or an Apollo launching tower, the injection of currents approaching the characteristics of natural lightning strokes in either pulse rise time or amplitude is not possible with laboratory facilities available today or in the foreseeable future. Instead, a geometric scale model of the system can often be tested to obtain some, at least, of the desired data. Sometimes the characteristics of the geometric scale model are such that quantitative measurements can be made.

The geometric scale model technique is not to be confused with computer models, about which much activity has recently centered. A digital computer model involves a digital computer providing numerical solutions for a mathematical model of a system. Other common models are electrical circuit models such as used in analog computers where lumped electrical parameters of inductance, capacitance and resistance are used to represent distributed parameters or other physical quantities which obey analogous laws of behavior. Neither of these models, of course, bears any physical resemblance to the system it represents. A geometric scale model, on the other hand, looks like and has a dimensional relationship to the full scale system of interest. The use of geometric scale models is much more prevalent in the fields of civil, mechanical and aerodynamic engineering than in electrical engineering, where geometric model techniques have only been used for antenna radiation pattern studies.

In a relative geometric model, the impedance, voltage between points, current distributions and magnetic and electric fields in the region around the model are simulated.

Relative geometric models are described in terms of scale factor, which is the relationship between the model property and the full scale property. Scale factor involves the fundamental physical dimensions of length, mass, time and charge. Only some of these factors can be chosen independently, usually three. Table II gives scaling relationships that apply in terms of the length (ℓ), time (t) and impedance (Z) parameters. The scale factors of all other quantities are derived in terms of these three. Any three parameters in Table II can be chosen arbitrarily and the rest of the parameters defined in terms of those three.

26

TABLE II - Scale Factors in a Relative Geometric Model

Quantity	Scale Factor (S) in Terms of length (ℓ), time (t) and Impedance (Z) of Full Scale (F) and Model (M) Systems
length (ℓ)	$S_\ell = \dfrac{\ell_M}{\ell_F}$
time (t)	$S_t = \dfrac{t_M}{t_F}$
resistance (R)	$S_R = S_Z$
capacitance (C)	$S_C = \dfrac{S_t}{S_Z}$
inductance (L)	$S_L = S_t S_Z$
impedance (Z)	$S_Z = \dfrac{Z_M}{Z_F}$
conductivity (σ)	$S_\sigma = \dfrac{1}{S_\ell S_Z}$
permittivity (ε)	$S_\varepsilon = \dfrac{S_t}{S_\ell S_Z}$
permeability (μ)	$S_\mu = \dfrac{S_t}{S_\ell S_Z}$
frequency (f)	$S_f = \dfrac{1}{S_t}$

Relative geometric models were first used to study lightning effects on power system transmission lines (ref. 12). In those studies, the scale factors were chosen such that the impedances of the model were equal to the impedances of the full scale lines. Thus, the impedance scale factor was set equal to unity. Since the model work was to be done in the air, the scale factor for permittivity (ε) was also set equal to unity. Since only one more scale factor could be chosen arbitrarily, length (ℓ) was selected to reduce the model to a manageable physical size. The three arbitrarily selected scale factors were then:

$$S_Z = 1$$

$$S_\varepsilon = 1$$

$$S_\ell = 1/10$$

These choices result in length and time scale factors being the same. If the scale factor (S_ℓ) for length is chosen to be

1/10, then the time scale factor (S_ℓ) is also 1/10, from Table II. With a length scale factor chosen to be 1/10, all other scale factors will be as shown in Table III.

TABLE III - Scale Factors for a One-
Tenth Scale F-8 Model

Quantity	Scale Factor
S_R	1
S_L	$\frac{1}{10}$
S_c	$\frac{1}{10}$
S_Z	1
S_σ	10
S_ε	1
S_μ	1
S_f	10

All of the requirements of Table III were met in the F-8 model except the requirement that the material conductivity of the model should be 10 times that of the full scale airplane. Materials with conductivity 10 times that of aluminum or copper do not exist.

Material conductivity requirements set one of the important dividing lines between what a practical relative geometric scale model can and cannot be used for. If, in general, the effects under study are influenced mainly by the electromagnetic fields outside of the model materials, then the model may be used for quantitative studies. In the 1/10 relative scale model of the F-8 aircraft which was tested in this program, the peak of the oscillatory current through the model with a 200 volt capacitive generator was about 5 amperes. The model circuit resistance was less than 0.5 ohms so it seems obvious that an electromagnetic property (inductance) was controlling the circuit response and the material resistance was of very little importance. Therefore, the model can yield quantitative data on the response of the F-8 to lightning-like current pulses.

Studies involving electromagnetic fields internal to a conductor enclosure that were produced by currents diffusing through the wall of that structure are quite another matter. The diffusion and shielding properties of materials are quite heavily dependent on the electrical conductivity. Therefore, the response of systems contained within the structure to fields that penetrate the structure material cannot yield quantitative results. However, the qualitative measurements are still useful and give insights into the trends that will occur in the full size system. Of course, aperture coupling, in which fields are admitted to the interior through holes, is not affected by material conductivity and will, therefore, be accurately represented in the model.

The above discussions present some of the practical background necessary to understand the concepts and practices involved in the application of relative geometric scale models. For a more rigorous derivation of the laws of similitude as applied to models, the reader is referred to reference 12, where the original work of P.A. Abetti is reproduced. Examples of the application of relative geometric scale models to aerospace lightning studies can be found in references 13, 14 and 15.

Model construction. - The model was constructed of 0.41 mm (0.016") aluminum sheet riveted together. The fuselage was formed as a simple cylinder 14.6 cm (5 3/4") in diameter, and the wing, elevators, and rudder were formed as flat surfaces. The nose of the aircraft was simulated with a funnel. A dimensional drawing of model is given on Figure 17 and a photo of the model in a typical test configuration is shown on Figure 18. A twisted pair of wires was installed inside the model fuselage and two major apertures (the tail opening and a 7.6 cm x 10.2 cm (3" x 4") opening to represent the cockpit) were placed in the model. Numerous incidental apertures remained between the rivets and seams.

Model test circuit. - The test circuit utilized for the model included scaled versions of those used during the full scale tests of the F-8. The same return conductor configurations were utilized as were present in the full scale test setup, as shown in Figure 19. The test voltages and currents applied to the model were much lower than those applied in the full scale tests to allow use of a mercury wetted relay switch in place of the spark gap used in the full scale tests. Repetitive switching at repetition rates low compared to the duration of the signals being measured will produce a steady display on the measurement oscilloscope and will produce a very clear trace even at fast sweep rates. The mercury relay was driven from a 60 Hz source, providing sixty operations per second. The time between switch closings was 17 milliseconds, and the duration of the applied pulses did not exceed 20 microseconds. A schematic diagram of the model generator circuit is given in Figure 19.

1.65 m

54.3 cm

7.6 cm

10.2 cm

7.3 cm

47°

49.5 cm

50°

27 cm

34.3 cm

3.2 cm

57.8 cm

57.2 cm

14.3 cm

Figure 17 - Design Drawing of 1/10 Scale Model of the F-8 Ai
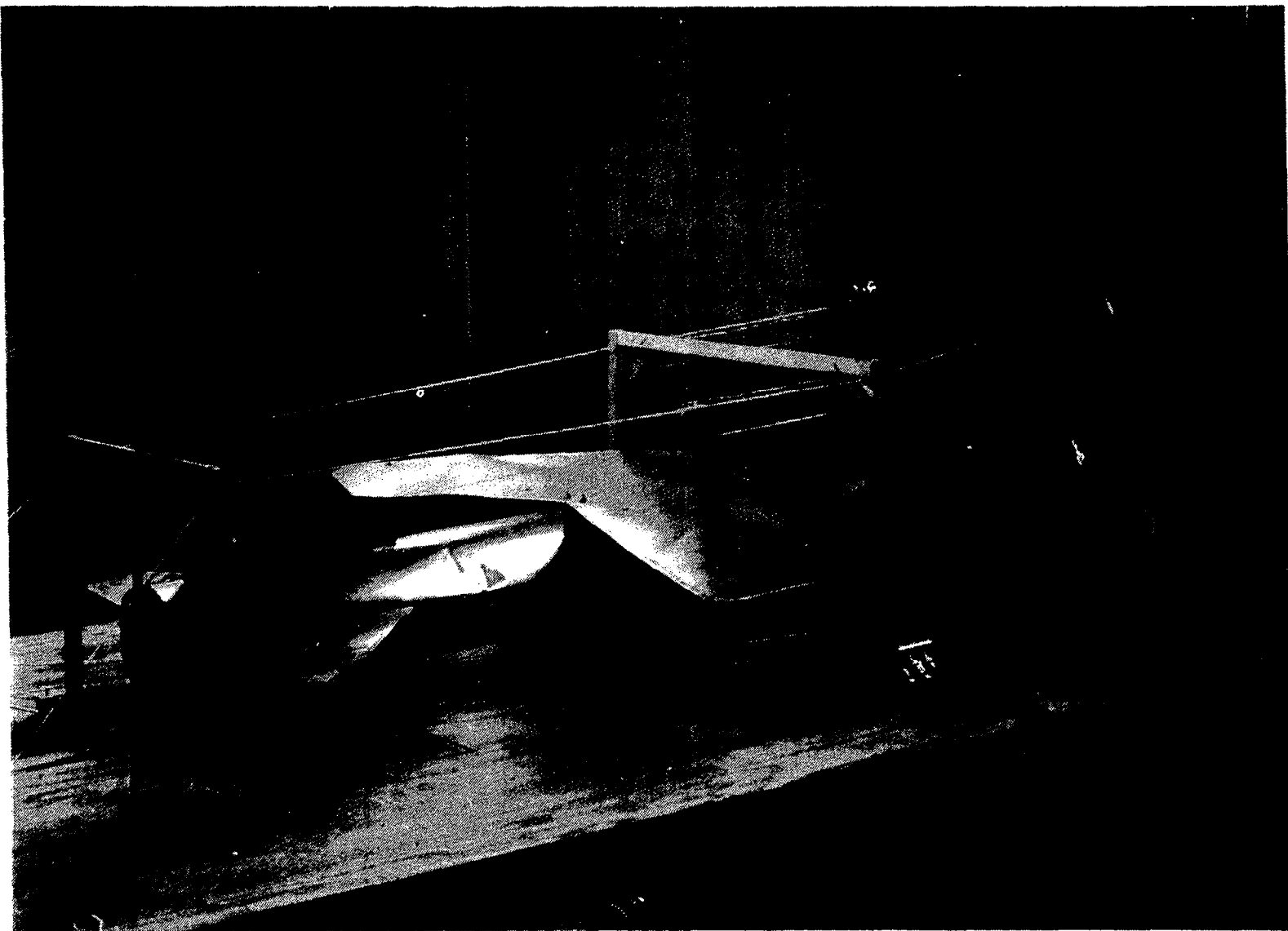
Figure 18 - One-Tenth Scale Model of F-8 DFBW
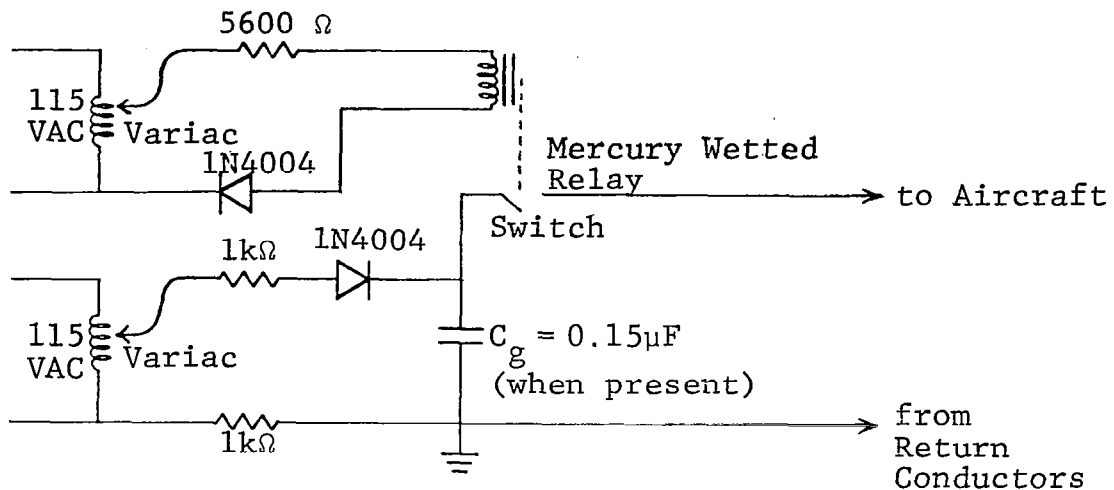Airplane and Test Circuit.

Figure 19 - Model Generator Capacitor Charging
and Switching Circuit.

During the full scale LTA tests, the aircraft and return con-
ductors were shown to have a loop inductance of 18 μH. According
to the inductance scale factor of Table III, the model test cir-
cuit should have had an inductance one tenth as great, or 1.8 μH;
whereas the actual inductance, as determined from ringing-fre-
quency tests, was 1.7 μH. This is an average difference of less
than 6%, a phenomenal similarity considering the simplicity of
the F-8 model.

To simulate the conductive structural steel in the floor of
the hangar where the full scale F-8 was tested, an aluminum foil
ground plane was placed under the model. Traveling wave oscilla-
tions were found to exist between the return conductors on the
model, just as they had in the full scale test setup. Thus, they
were resistively terminated with 115 Ω resistances. This return-
line traveling wave phenomenon also correlated very closely with
the response observed on the full scale F-8.

Measurements of the surge impedance of the transmission line
formed by the aircraft and the return conductors yielded a value
of 100 ohms on the model as compared to 124 ohms for the full-
scale F-8. These and other comparisons indicated that it was
possible to obtain useful quantitative data about the response of
the F-8 aircraft to various lightning current generator and test
circuit configurations. Consequently, the model was used to
determine the generator configuration and waveshaping elements
required to produce the traditional 2 x 50 μs current waveshape
with and without the aircraft terminated in a resistance equal to
its surge impedance. Evaluations of the test circuit response to
a lumped parameter ladder network as a means of simulating a
lightning channel were also first carried out on the model and

the design was established for a 6-segment ladder network to be evaluated on the full-scale F-8 aircraft. In the test results that are described in the following paragraphs both model and full scale results are presented.

Test Technique Evaluations

Return conductors. - When an aircraft in free space (flight) is struck by lightning, it becomes part of the stroke channel and conducts the lightning currents carried in that portion of the channel. The lightning current circuit is very large and the return paths of the lightning current are very diffuse. In most cases, the lightning current return path for that portion of the channel containing the aircraft is far enough removed that it has no effect on the aircraft.

Unfortunately, when tests are conducted on an aircraft using simulated lightning currents, two major differences are present. First, the aircraft is not in free space. It will be on the ground, and usually in a building which greatly alters its electromagnetic environment. These mediums of high conductivity (moist soils, concrete, building steel) are relatively close to the aircraft. Second, copper or aluminum conductors will normally be used to return the test currents to the current generator. Practical circuit limitations require that these return conductors be relatively close to the aircraft.

The first measurements of lightning induced voltages using laboratory simulated lightning currents (ref. 1) were conducted using single conductor return paths which were usually laid upon the floor beneath the aircraft.

Consideration was given to the influence of the return conductor during later testing (ref. 5) where two or more return lines were laid on the floor beneath the aircraft and routed around its perimeter. It was generally felt that these arrangements resulted in fuselage current distributions closer to actual inflight conditions, but no tests to verify this were performed. In almost all of the tests, the aircraft was maintained at building ground potential while the return conductors and generator were electrically insulated from ground. Also, the test generators employed were generally configured to provide a unidirectional simulated lightning current pulse and no consideration was given to the distributed transmission line represented by the aircraft and the adjacent return conductors.

More recently, investigators have begun to consider this distributed nature and have configured the return lines to be coaxially distributed around the aircraft in an attempt to get a fuselage current distribution the same as the free space situation (ref. 16). Each improvement in return conductor positioning around the fuselage has improved the current distribution in the aircraft which in turn has brought the magnetic fields surrounding the aircraft closer to the actual free space situation. However these changes have also affected the capacitive and electric field environment by increasing the distributed capacitance of the aircraft.

When the aircraft is charged to some voltage level, an electric field exists around the aircraft and electric flux lines are established. Basically, the flux lines can be thought of as lines drawn between units (electrons or protons) of charge on the aircraft to charges of opposite polarity in the area surrounding the aircraft. If the return conductor is solid and completely encircles the aircraft then all electric flux lines will terminate on the return. In this case when a traveling wave is introduced on to the aircraft, the wave will propagate between the aircraft and the return conductors and will be contained within them.

However, in most situations, it is not possible to build a solid coaxial return around the aircraft and a portion of the electric flux lines will terminate on other conductors outside of the return path. Basically, this represents the capacitance between the aircraft and the building floor or wall. When a traveling wave is introduced into this system, propagation will occur between the aircraft and the return conductors as well as the other conductors. The traveling wave currents that propagate between the aircraft and return conductors are returned to the source (generator capacitor) along the return conductors, but the waves propagating between the aircraft and the other conductors must find conductive paths back to the generator. When the aircraft and its return lines are isolated from building ground, the currents must be capacitively carried back to the return conductors, so traveling waves will exist between the airframe and the return conductors, the airframe and the building, and between the building and return conductors.

Similarly, if the aircraft is grounded, as has been the case in previous LTA tests, the return conductors rise in voltage, with respect to surrounding ground. So now waves propagate between the return conductors and aircraft, between the return conductors and building ground, and to complete the return path a wave must propagate between the building ground and the fuselage. How the electromagnetic waves which are propagating between the aircraft and building and between the return lines and building behave depends on how the transmission line that is formed between these

elements is terminated. If these lines are shorted or open cir-
cuited, reflected waves will occur.

During the first test series on the full scale F-8 aircraft,
measurements of the voltages between the return conductors and
the hangar grounds verified the existence of these traveling
waves. Initially, the return conductors were connected directly
to the building ground at the nose end, and the tail end was left
floating. Later, both ends of the return conductor configuration
were connected to building ground through resistors of approxi-
mately 100 ohms. Figure 20 shows examples of the voltages meas-
ured between the aircraft return conductors and the building
ground. By adding termination resistors to the ends of the
transmission line formed between the return conductors and the
building grounds, the duration of the oscillations was limited to
one cycle and the magnitude was reduced by a factor of about 5.

Various schemes were tried in an attempt to completely elim-
inate the remaining single cycle pulse that appeared between the
return conductors and the building ground. The lowest voltage
was obtained by laying a wide aluminum foil on the floor beneath
the aircraft and connecting it to each end of the return conductor
array. Unfortunately, this scheme diverted about 50% of the re-
turn currents to the foil and thus defeated the purpose of the
coaxial return conductor arrangement.

The arrangement and type of return conductors utilized during
the LTA tests was shown to have an effect on the induced voltage
results, as indicated by tests on the full scale aircraft in which
induced voltages in the aircraft electrical circuit were measured
to compare a return array of four groups of three parallel wires
in place of the four 0.5 m wide aluminum foils shown in Figure 10,
and to compare a return conductor array of four positions around
the aircraft with only two on the lower sides of the aircraft.
The results of these comparisons are shown in Figures 21 and 22.

Essentially, no difference in induced voltage response was
detected when parallel wire returns were utilized in place of the
aluminum foils, as indicated by the induced voltage comparison of
Figure 21. This was an important point since it is much simpler
to install and support an array of wires than the wide aluminum
foils. At various times during the full scale tests, both copper
and steel wires were used, with no discernible difference in in-
duced voltage response. The steel wires added approximately 2 ohms
of resistance to the circuit, which was of no consequence since
much higher resistances are already necessary for waveshaping
purposes.

It should be noted, of course, that one wire cannot replace
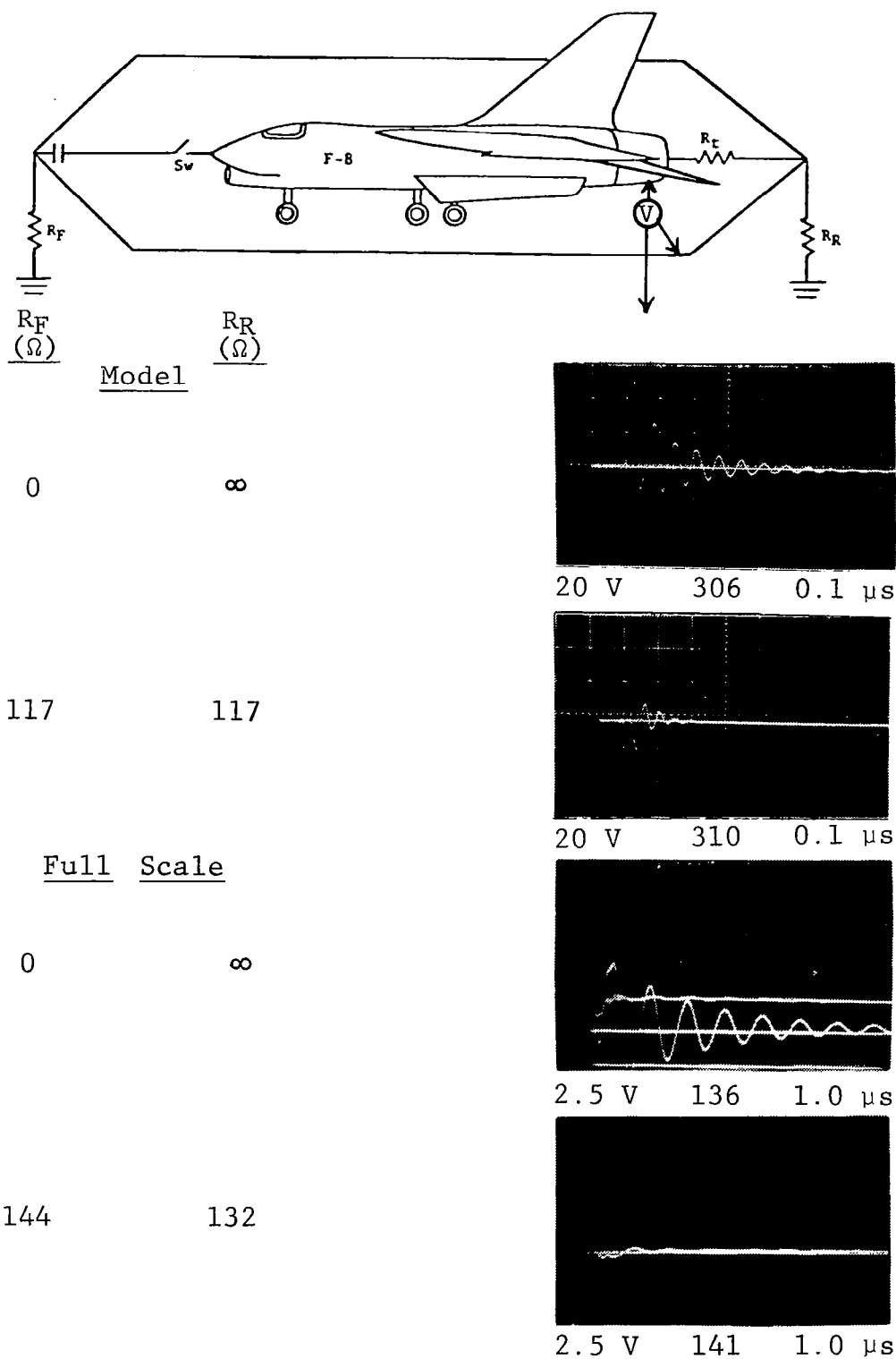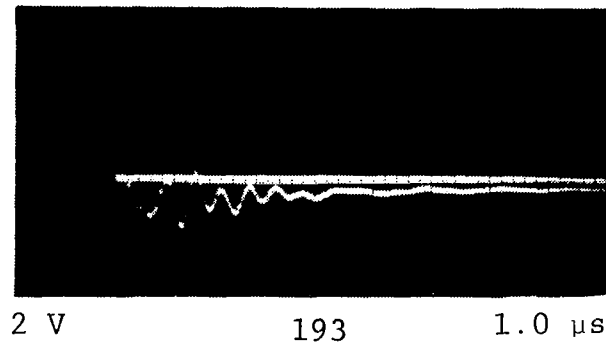one foil due to the differences in capacitance between the wire or

R_F (Ω)		R_R (Ω)	
	Model		
0		∞	
			20 V 306 0.1 μs
117		117	
			20 V 310 0.1 μs
	Full Scale		
0		∞	
			2.5 V 136 1.0 μs
144		132	
			2.5 V 141 1.0 μs

Figure 20 - Typical Return Line-to-Building Voltages
Before and After Termination.

Four Foil Returns

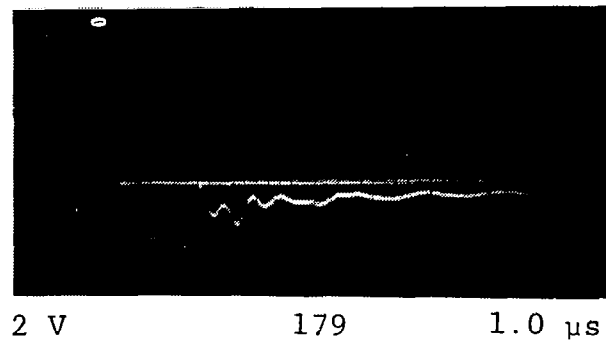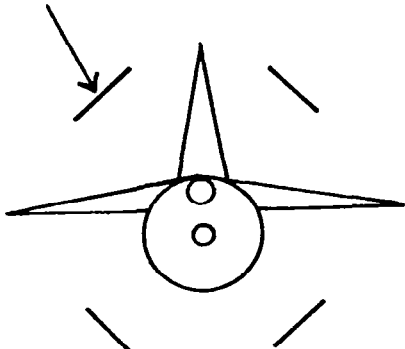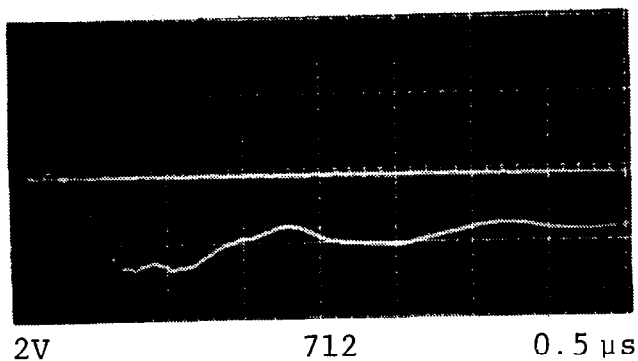2 V   193   1.0 μs

Four 3-wire Groups
in same locations as foils

2 V   179   1.0 μs

Figure 21 - Comparison of Induced Voltages with
Foil and Wire Return Conductors.

37

Return Conductors (4)

F-8

2V   712   0.5 μs

F-8

2V   713   0.5 μs
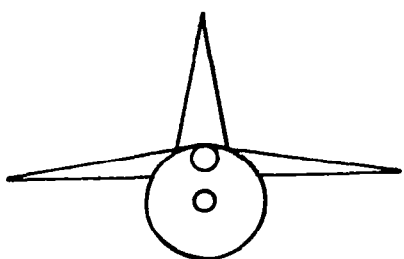
Return Conductors (2)
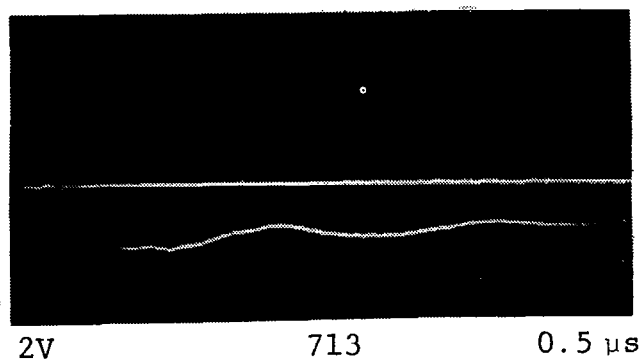
Figure 22 - Comparison of Induced Voltages
with a Balanced and Unbalanced
Return Conductor Arrangement.

foil and the aircraft. In the first full scale test series three wires spaced 0.25 m apart (0.5 m total width) effectively gave identical performance to the 0.5 m wide foils as shown in Figure 21. During the second test series, two wires spaced 18" apart were used, and no discernible difference was again noted.

Comparisons of induced voltages measured with all four return conductors in place versus only the lower returns are shown in Figure 22. Similar comparisons were conducted during the full scale test series, and in both cases, induced voltage levels were reduced by a factor of close to 27% when the top two conductors were removed. The reason for this is undoubtedly that the fuselage current becomes unbalanced and less dense on the upper portion of the fuselage when the upper return conductors are removed. The reduction in current density produces a corresponding reduction in magnetic flux density along the top of the fuselage, where the instrumented conductor is located.

Transmission lines. - As discussed previously, it is probable that during the first few microseconds after lightning contact with the aircraft, the airframe will behave as a short transmission line. That is, voltage and current waves will originate at the point of attachment and propagate along the airframe, possibly reflecting back and forth. The same phenomenon will occur during simulated lightning testing, although, as discussed earlier, the aircraft environment will differ considerably from the inflight condition.

In order to understand how these traveling waves relate to the aircraft induced voltage measurements, characteristics of these waves must be measured and identified. It was possible to measure the traveling wave currents entering and leaving the aircraft with the current transformer shown in Figure 14, but no such instrument exists with which to directly measure the current on the airframe. Attempts to measure the magnetic flux produced by the airframe current with $d\phi/dt$ coils were only partially successful, due to the difficulty of isolating the magnetically induced signal from that also capacitively coupled from the fuselage to the probe. Measurements of the voltage waves at various points along the fuselage were possible using the resistive voltage divider described earlier, and all data presented here are from those measurements.

As was shown in Figure 3, the surge impedance ($Z_{A/C}$) of an aircraft may be important in determining the magnitude of traveling waves that may occur along it when it is struck by lightning.

The surge impedance (Z_O) of any transmission line (also known as its characteristic impedance) was defined as:

$$Z_O = \sqrt{L/C} \quad \text{(ohms)} \tag{7}$$

where,

L = inductance per unit length (H/m)

C = capacitance per unit length (F/m)

and,

$$V_t = Z_o I_t \qquad\qquad (8)$$

where,

V_t = traveling wave voltage

I_t = traveling wave current

If a transmission line is terminated by a resistance equal to Z_o, then the traveling wave passes along it once and is fully absorbed by the termination resistance and no reflections occur. If the line is terminated in any other resistance or impedance, reflections or refractions occur and the transmission line will exhibit a damped oscillation. The rules for reflections and refractions on the transmission lines are illustrated in Figure 3 and described more fully in several texts (ref. 10). In general, voltage waves reflect positive at terminations with resistances higher than Z_o and negative at terminations with values lower than Z_o. In other words, terminating a transmission line in a resistance greater than Z_o will result in an increase in the total circuit voltage after a reflection, and terminating in a resistance less than Z_o will result in a reduction of the total circuit voltage after the reflection. Current waves behave in the opposite manner, reflecting negative at high termination impedances and positive at low impedances.

The surge impedance (Z_o) of the aircraft and its return conductors was determined by inserting various values of resistance between the aircraft tail and the return conductors and measuring the voltage appearing across this resistance when the generator capacitor is switched on to the other end of the line as shown in Figure 23. Current through this resistance was also measured most of the time. For the full scale tests, it was necessary that the termination resistors be capable of dissipating all of the energy stored in the generator capacitor. The maximum generator capacitance of 2.0 µF charged to 50 kV stores an energy of 2500 watt-seconds. Assuming that all of the energy is delivered and dissipated within less than one second, a resistor thermal capacity of about 2500 watt-seconds is required. 2500 watt noninductive resistors ranging in value from 30 ohms to 300 ohms (the probable range) were not readily available, so suitable resistors were assembled from 150 2-watt carbon resistors mounted on a fiberglass
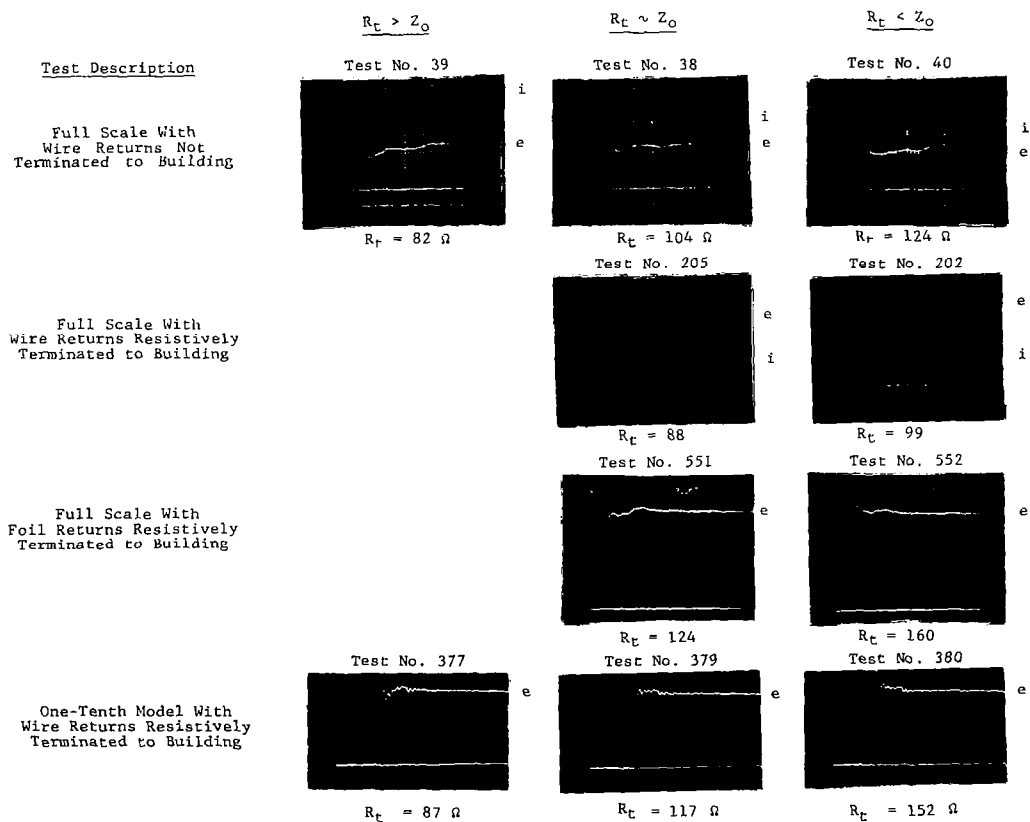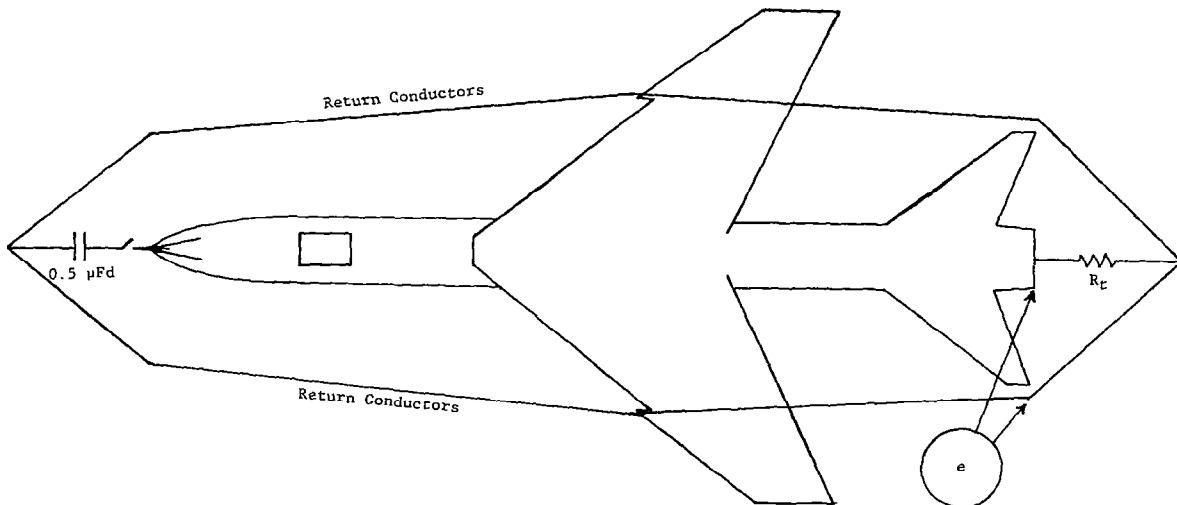
Test Description	$R_t > Z_o$	$R_t \sim Z_o$	$R_t < Z_o$
Full Scale With Wire Returns Not Terminated to Building	Test No. 39 $R_r = 82\ \Omega$	Test No. 38 $R_t = 104\ \Omega$	Test No. 40 $R_r = 124\ \Omega$
Full Scale With Wire Returns Resistively Terminated to Building		Test No. 205 $R_t = 88$	Test No. 202 $R_t = 99$
Full Scale With Foil Returns Resistively Terminated to Building		Test No. 551 $R_t = 124$	Test No. 552 $R_t = 160$
One-Tenth Model With Wire Returns Resistively Terminated to Building	Test No. 377 $R_t = 87\ \Omega$	Test No. 379 $R_t = 117\ \Omega$	Test No. 380 $R_t = 152\ \Omega$

Figure 23 - Voltage across Various Termination Resistances.

perforated board and wired 15 in parallel and 10 in series. Two
watt resistors have thermal ratings of approximately 20 watt-sec-
onds each, for a total of 3000 watt-seconds. Two of these resis-
tor boards can be seen in Figure 14.

Resistor values of 45, 54, 67, 82, 88, 104, 124, 132, 143,
160, 181, 212 and 226 ohms were installed successively in the R_t
position in the circuit of Figure 23 and the value of resistance
observed to give the least reflection was considered to be Z_o.
Unfortunately, since other transmission lines are present in the
system, aircraft to building and return conductors to building,
which each have different values of Z_o, it was not possible to
obtain an exact terminated wave and some oscillations were always
present.

Determinations of Z_o were made for the full scale F-8 test
circuit as well as the 1/10 scale model.

Figure 23 compares the results of four such tests. The first
tests were conducted prior to terminating the return conductors to
the building ground. The oscillations between the building ground
and airframe are apparent in these measurements. During a later
test series, the wire return conductors were replaced with alumi-
num foils. These foil returns were also resistively terminated to
the building with 140 ohm resistors at each end which removed most
of the return-to-building oscillations.

Changing from wire return conductors to aluminum foil lowered
the surge impedance by about 20% from over 100 ohms to about 90
ohms. This was no doubt due to the higher capacitance between the
airframe and the foils versus the wires. During the second full
scale test series, wire returns were again used and the surge im-
pedance was again over 100 ohms. The relative geometric scale
model which also utilized wire returns resistively terminated to
the buildings, compared very closely with the full scale tests of
the same arrangement.

It was suggested earlier that when an aircraft in flight is
struck by lightning, the airframe currents will be oscillatory
due to traveling wave reflections. The cause of this phenomenon
has been related to a surge impedance mismatch between the air-
craft and the lightning stroke channel. Estimates of the light-
ning channel surge impedance have ranged from 400 to 600 ohms
(ref. 10). The surge impedance determinations made on the air-
craft test circuits ranged from approximately 80 ohms to 125 ohms.
This would suggest a significant mismatch and the formation of
reflected traveling waves in the airframe as illustrated in
Figure 3. However, the aircraft surrounded by return conductors
is obviously not in "free space" as it is in flight.

42

To find out what the aircraft surge impedance might be if no return conductors were nearby, the one-tenth scale model was suspended in air and measurements of Z_O were made. Since connecting a termination resistor between the tail of the model and ground would compromise the set-up by moving ground close to the tail, a series resistor was inserted between the mercury-wetted switch and the nose of the aircraft. If this series resistor is equal to Z_O, then the voltage at the nose (e) will initially be one half of the capacitor charge voltage (E) and reach E after the reflection at the open tail returns to the nose. The test setup and results of these tests are shown in Figure 24. With the return conductors around the model, Z_O values of 88 to 105 ohms were measured as indicated in Figure 23. With the return conductors removed and the model suspended 0.7 m off the ground plane, a value of 250 ohms was determined. An elevation of 1.3 m increased the surge impedance to about 400 ohms, but further increases in elevation above ground made no difference because most of the coupling was between the front of the model and the vertical foil that was necessary to connect the low side of the capacitor to ground. All foils were then removed and the capacitor was grounded via a thin wire to the power system ground and earth. This time the final measurements indicated that the surge impedance had again risen and was about 730 ohms.

The main point of this experimental exercise was to illustrate that the transmission line surge impedance of an aircraft in flight is probably higher than the 88 to 124 ohm levels determined with the nearby return wires. If the aircraft in flight is treated as a classical transmission line problem, with the aircraft fuselage as one conductor and the earth as the other, a calculation of the characteristic impedance can be made. These calculations ignore the aircraft wings and consider the earth as a single return conductor while in fact it is a conducting plane. The inductance and capacitance of the aircraft are then given by:

$$L = \frac{\mu_o}{2\pi} \ln\left(\frac{h}{d}\right) \quad \text{(H/m)} \tag{9}$$

$$C = \frac{2\pi\varepsilon_o}{\ln\left(\frac{h}{d}\right)} \quad \text{(F/m)} \tag{10}$$

where:

μ_o = permeability of free space - $4\pi 10^{-7}$ (F/M)

ε_o = permittivity of free space = $\frac{1}{36\pi 10^9}$ (H/M)

h = distance between conductors
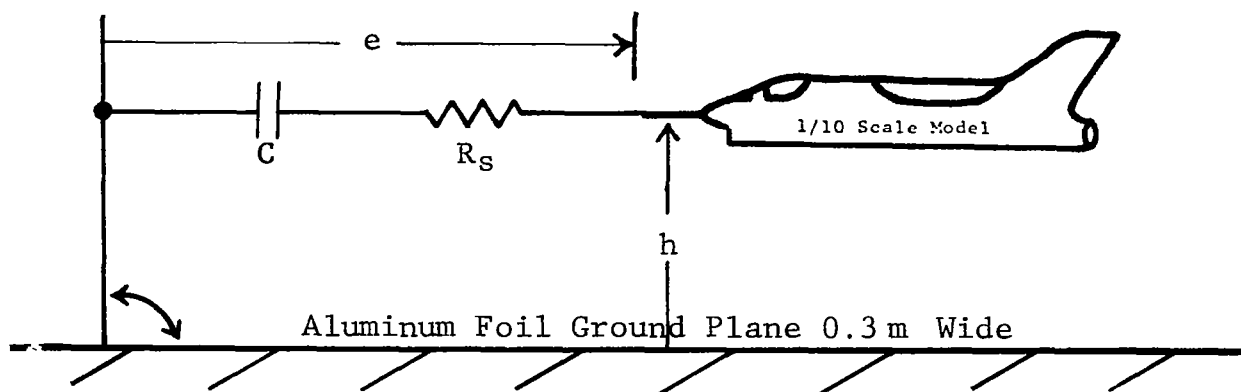
d = diameter of the fuselage
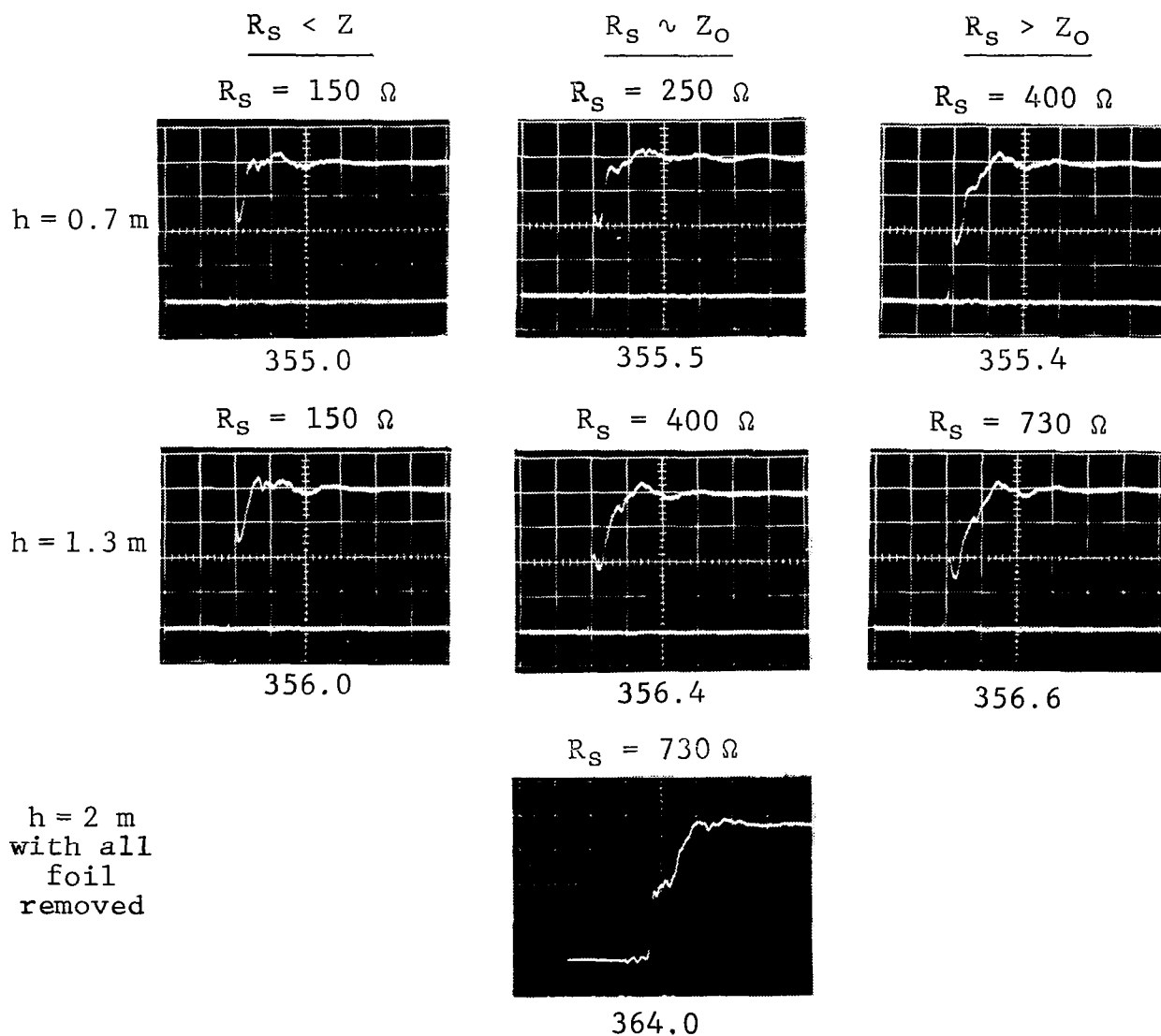
Figure 24 - Surge Impedance of the F-8 Model as
a Function of Distance Above Ground.

Since many aircraft lightning strikes occur at an altitude of about 3 km, h was chosen to be 3 km. The F-8 fuselage (d) is approximately 2 m. Using these numbers in equations (9) and (10) gives:

$$L = 1.5 \quad H/m$$

$$C = 7.6 \text{ pF/m}$$

Then, from eq. (2):

$$Z_o = \sqrt{L/C}$$

$$= 444\Omega$$

This is near the range of surge impedances often attributed to a lightning flash channel which is thought to be 400 to 600 ohms. It therefore seems quite probable that the field factors which determine the value of surge impedance of a lightning stroke channel are also controlling the surge impedance of the airframe in flight.

Traveling wave transit times. - If an aircraft fuselage supports traveling waves which are in fact reflected at each end of the aircraft, the frequency of oscillations will be related to the length of the aircraft and the velocity of wave propagation. The electromagnetic waves propagate in the air medium around the fuselage, and traveling wave currents flow on the fuselage itself. From Maxwell's equations, it can be shown that the velocity of propagation is a function of the medium in which these waves travel and can be calculated from:

$$v = \frac{1}{\sqrt{\mu\varepsilon}} \tag{11}$$

The permittivity (ε) and permeability (μ) of air is very close to that of free space so use of these values (μ_o and ε_o) will produce very small errors, thus:

$$v = \frac{1}{\sqrt{\mu_o\varepsilon_o}} = 3 \times 10^8 \text{ m/s} = c \tag{12}$$

where,

$$c = \text{velocity of light}$$

A traveling voltage wave introduced at the nose of an aircraft will require a transit time (τ) to reach the tail. Since the aircraft is in air, the transit time should be equal to:

$$\tau = \frac{\ell}{c} \quad (s) \tag{13}$$

where,

ℓ = length of the aircraft (m)

In the LTA test circuit, with the tail of the aircraft open circuited and the nose connected to the return conductors through the capacitor, applied voltage and current waves should reflect and oscillate as illustrated in Figure 26.

Every four transit times, the observed voltage waveform will repeat, giving an observed oscillation which has a period (t) which is equal to four transit times.

During the first full scale test series, traveling wave voltages were measured on the F-8 aircraft. A typical measurement is shown in Figure 25, triggered at the point of measurement so that the time between generator switching and arrival of the wave at the measurement point is not shown on the oscillogram. Stray electrical losses, as well as the non-uniform geometry of the aircraft eliminate the squareness of the traveling wave, but the basic frequency of the reflected wave is still very evident.

10kV

0

2.5 kV   162   0.2 µs
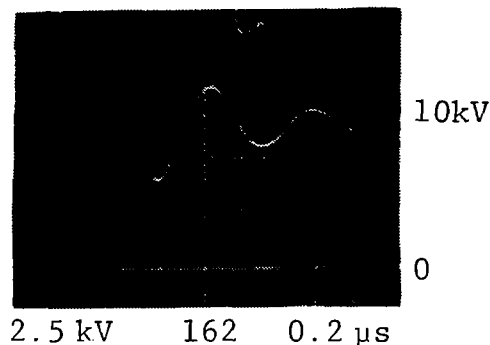
Figure 25 - Typical F-8 Ringing Frequency Oscillogram.
Voltage measured between aft end of aircraft and return conductors after 10 kV capacitor was switched onto aircraft.

This measurement gave a frequency of 1.74 MHz. Other measurements were slightly lower, so an average value of 1.7 MHz was obtained. This corresponds to a transit time of 145×10^{-9} seconds, assuming that four transit times elapse in the period of one cycle of voltage, as indicated on Figure 26.

At the speed of light, a distance of 43.5 m would be traveled in this time. The F-8 airframe is 17.1 m long and the distance from one apex of the return conductor array to the other was 22 m.
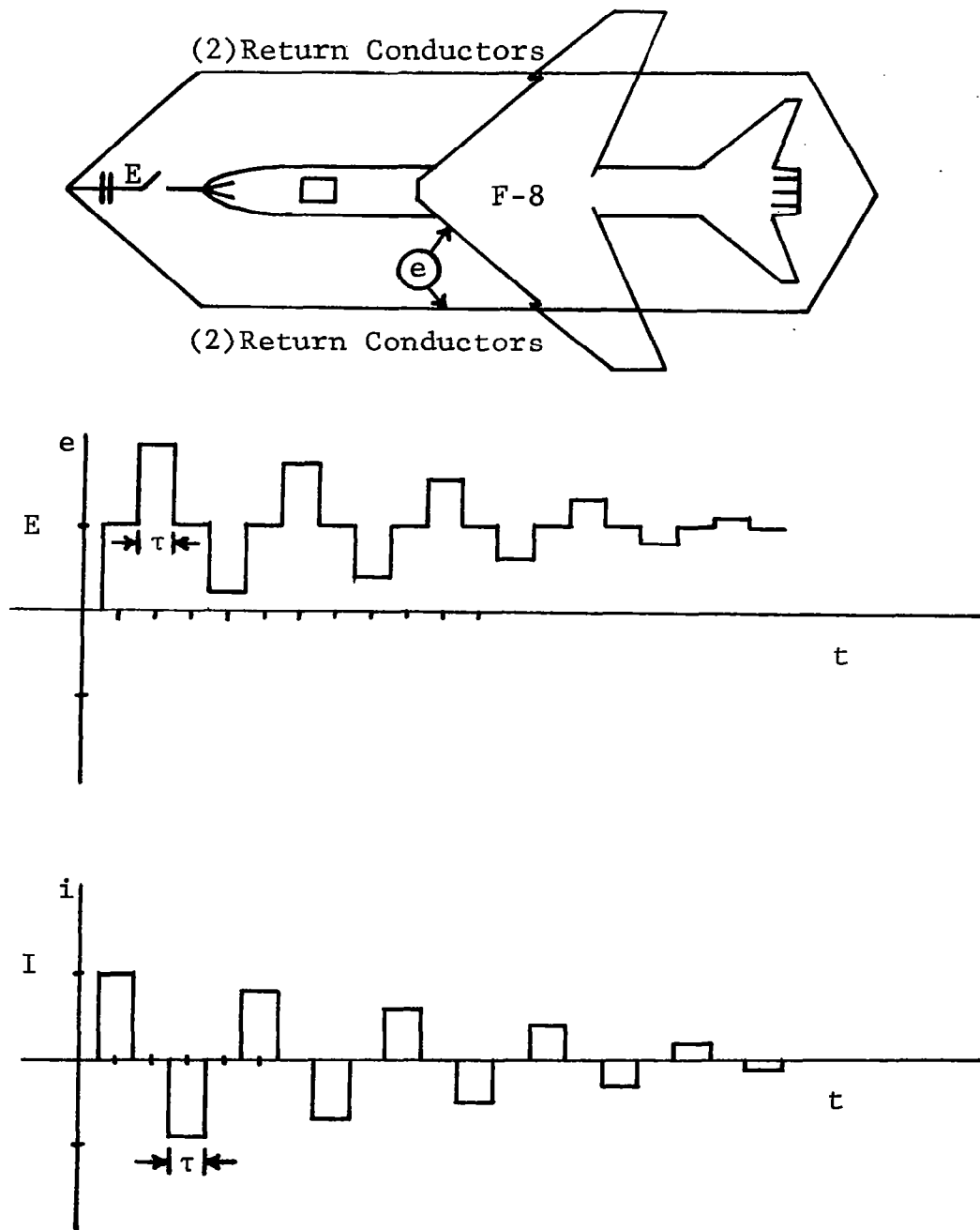
Figure 26 - Voltage and Current Traveling Waves on an
Idealized Test Circuit; as Observed at the
Center of the Fuselage.

Assuming that the larger apex-to-apex distance applies, the transit time determined from the measurement of Figure 25 is still twice as long as the actual distance would predict. The discrepancy between the measured transit time and calculated time is 2:1.

To verify these observations, tests were conducted on the 1/10 scale model of the F-8. The model test circuit from apex to apex of the return conductor was 2.25 m. In these tests, typical results of which are shown in Figure 27, average voltage waveform ringing frequencies of 15 to 18 MHz were measured.

5V/div   346 0.05μs/div
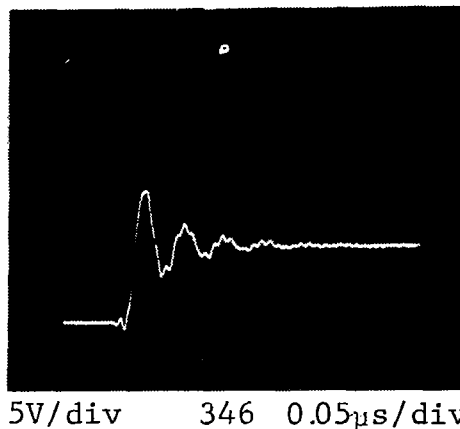
Figure 27 - Typical Relative Geometric Scale Model
Ringing Frequency Oscillogram.

In the oscillogram of Figure 27, an average frequency of 16.5 MHz was obtained which corresponds to a transit time of 15.2×10^{-9} s, or a distance of 4.55 m; again twice the length of the circuit.

To investigate the phenomena further, and to see if the wings, etc. on the model were somehow involved, the model was removed from the circuit and replaced first by a 13 cm diameter galvanized steel tube and then by a 1.3 cm copper pipe. The test results, shown by the data in Table IV indicate that the transit time was reduced as the conductor got smaller, but was still 23% longer than calculated.

Measurements of ringing frequency and transit time made during the second test series on the full scale F-8 yielded results essentially identical to those obtained during the first series.

In all of the above tests, the return conductors were not uniformly spaced around the center conductor. They start and end in conical fashion and spread at the fuselage center. The effects of the introduction of bends in the return path in this configuration on transit time is not known. Consequently, tests were

TABLE IV - Ringing Frequency and Transit Time
Measurements on Various Diameter
Cylindrical Conductors in Place on
Aircraft in One-tenth Scale Model
LTA Circuit

Conductor	Voltage Frequency	Transit Time	Z_o
1.3 cm tube	27.3 MHz	9.2 ns	280
13 cm tube	21.0 MHz	11.9 ns	120
1/10 scale F-8 Model	16.5 MHz	15.2 ns	82

Circuit Total Length = 2.25 m, τ = 7.5 ns

performed on a configuration which is shown in Figure 28. Here, return and center conductors are parallel and the ends are flat. Four configurations were tested with this fixture, as follows: (1) AWG no. 20 center conductor and a single AWG no. 20 return wire spaced 0.3 m apart; (2) same as (1) but eight AWG no. 20 return wires spaced in a 0.61 m circle around the center conductor; (3) same as (2) but a 0.13 m dia. tube used as a center conductor; and (4) same as (3) but the eight return conductors were moved closer to the center tube, forming a 0.15 m dia. circle around the 0.13 m dia. tube.

The test results from these four configurations are given in Table V. The total length of the configurations of Table V was 5.64 m, which corresponds to a transit time at the speed of light of 18.8 nanoseconds. As in the LTA circuit tests of Table IV the large tube transit time is longer than the thin wire transit time and both are longer than the calculated transit time. In these flat-ended tests the differences are smaller than in the previous tests. For example, the wire line transit time is 15% longer than the calculated time whereas in the LTA circuit test the thin tube transit time was 23% longer than the calculated time. Also, the large tube transit time is 15% longer than the wire for the flat ended-configuration while in the LTA circuit, the larger tube had a transit time 29% longer than the small tube.

It is also interesting to note that the surge impedance, determined by dividing the voltage traveling wave magnitude by the current traveling wave magnitude, for a two wire system of configuration (1) was the same for the semicoaxial system of configuration (2). Moving the return wires closer to the tube did reduce the surge impedance.

0.61 m

15.5 m

0.13 m
Dia.

e

i

AWG no. 20
Wires (8)

Sw

C
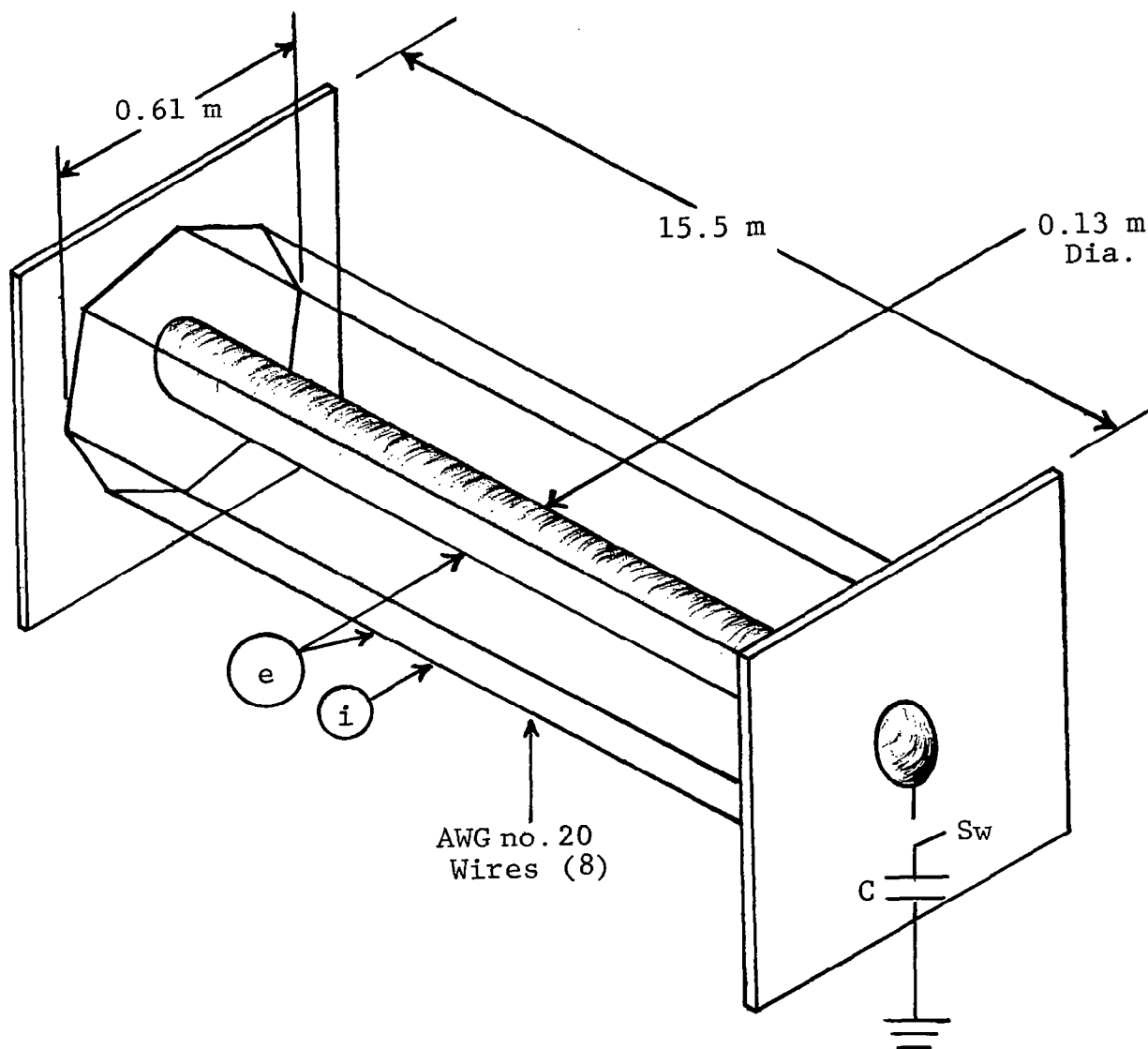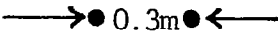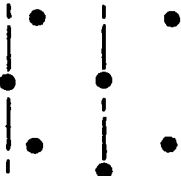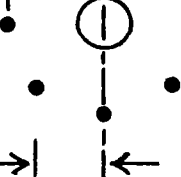
Figure 28 - Transit Time Test Circuit
Configurations.

TABLE V - Ringing Frequency and Transit Time
Determinations in 2 Coaxial Test
Configurations

	Frequency (MHz)	Transit Time (ns)	Z_o (Ω)
(1)	11.4	21.9	∿400
(2)	11.7	21.4	∿400
(3)	10.0	25.0	∿400
(4)	10.0	24.9	∿100

0.3m

0.15 m →

Using these same experimental techniques, measurements of traveling wave transit times were made on a length of RG58U co-axial cable, for which transit times have been established. The cable was 15.5 m long and has a published propagation velocity of 2×10^8 m/s due to the cable insulation dielectric. A measured transit time of 83 ns was determined as compared to a calculated value of 78 ns. The difference between these two values is less than 7%. Since the exact velocity of propagation is a function of the insulation dielectric constant which could vary slightly from one cable sample to another, the value obtained is sufficiently close to the calculated value to be considered identical for practical purposes. Thus, the transit time appears to be config-uration dependent and most closely approaches the speed of light when the center conductor in a coaxial arrangement is thin. This

transit time "discrepancy" was an area of continuing concern in this investigation and additional tests were made to help evaluate this phenomenon. The results of these additional tests are reported in later paragraphs of this report.

Grounded versus ungrounded aircraft. - In most LTA tests conducted prior to this program the aircraft has been grounded at the point on the fuselage where the induced voltage measurement is being made. This allows the signal to be conducted outside of the aircraft via a twinaxial cable and recorded with an external oscilloscope - a necessity in places where there is no room for an oscilloscope within the aircraft. Fiber-optic or other dielectric waveguide techniques offer a means of making this measurement while leaving the aircraft ungrounded. Thus, a comparison test was made to determine if a difference exists in the induced voltages measured within an ungrounded and a grounded airframe.

The original RLC LTA circuit was utilized for this evaluation, with the aft end of the aircraft shorted to the return conductors. In each case, the induced voltages were measured by the oscilloscope within the pallet area, even though the oscilloscope could have been placed outside of the aircraft and connected to the instrumented circuit via a cable in the grounded airframe test. The original 2 x 50 μs LTA test waveform was applied and the induced voltages with the aircraft ungrounded and grounded are shown in Figures 29 and 30, respectively. A comparison of the induced voltage oscillograms shows them to be nearly identical.

It should be noted that both ends of the return conductors were resistively terminated in this case, an improvement over the original circuits in which no attempt was made to dampen spurious oscillations existing between the return conductors and the "outside world".

Aircraft resistively terminated versus short circuited to return conductors. - The one-tenth scale model was utilized to determine the circuit element needed to pass a 2 x 50 μs current through the aircraft. Basically, this required that the total circuit inductance (L) be increased to accommodate an increase in the circuit resistance needed to terminate the aircraft to the return lines with its 124 ohm surge impedance while providing the same 2 μs rise time, since rise time is proportional to L/R. The value of the generator capacitance was also decreased to retain the fall time of 50 μs (to half peak value) with the higher circuit resistance, since this parameter is proportional to the RG product.
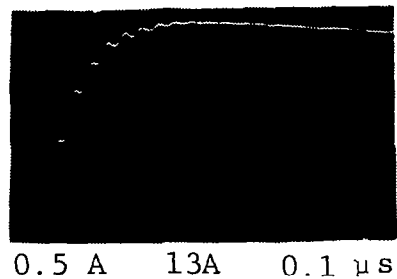
The resistivity terminated circuit is shown on Figure 31 together with the corresponding induced voltages. For the full scale generator charging voltage of 25 kV, the resistively
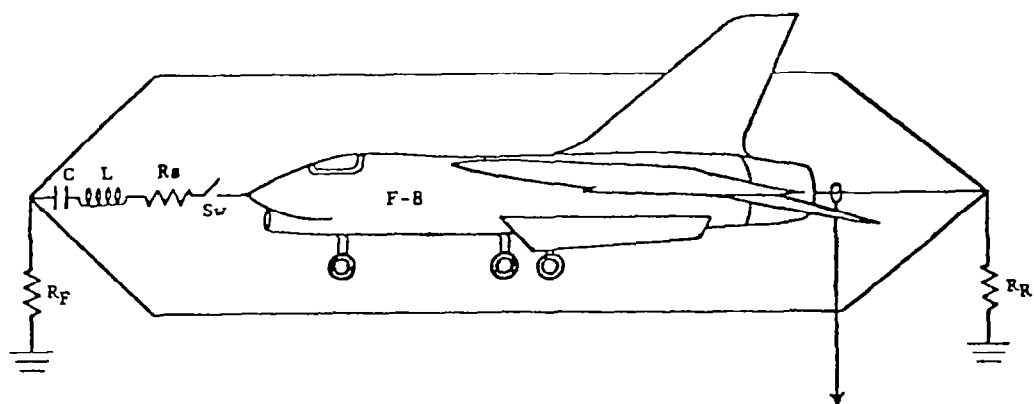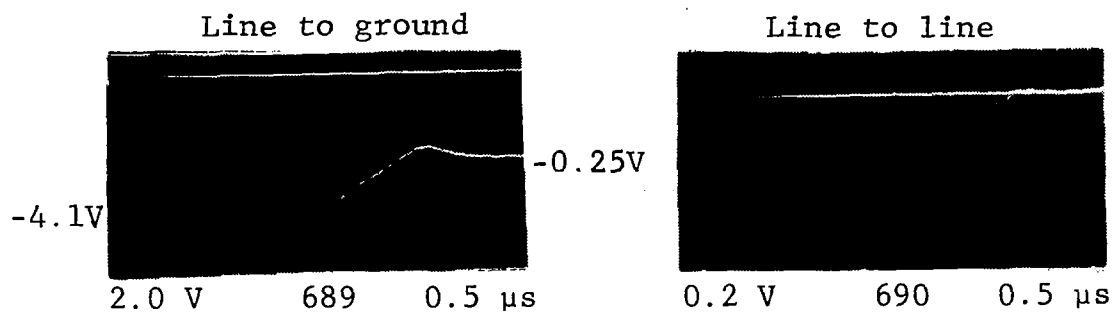
52

Line to ground   Line to line

-0.25V

-4.1V

2.0 V   689   0.5 μs   0.2 V   690   0.5 μs

Model

$L = 2.15$ μH
$C = 0.15$ μF
$R_s = 43$ Ω
$E \sim 130$ V

2.75 A

0.5 A   13A   0.1 μs

Full Scale

$L = 18$ μH
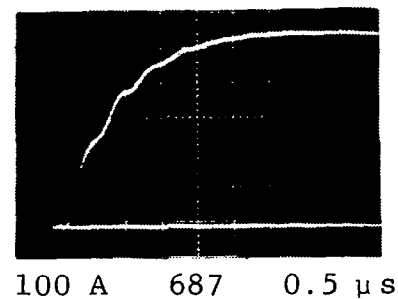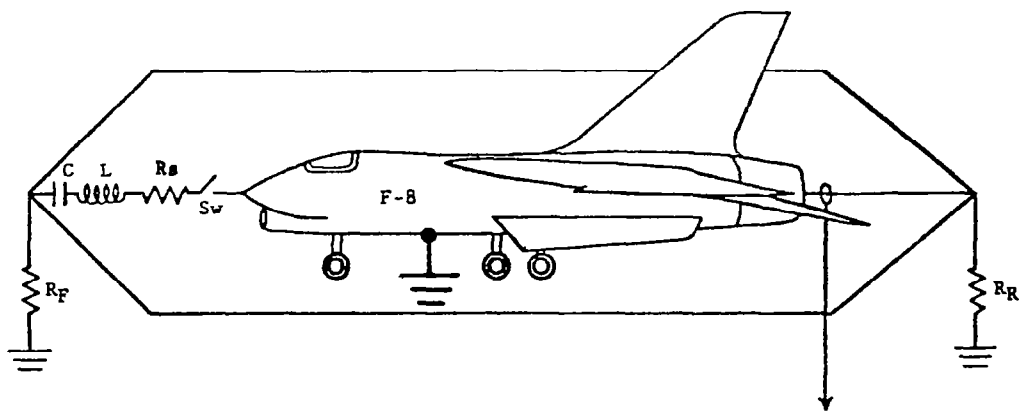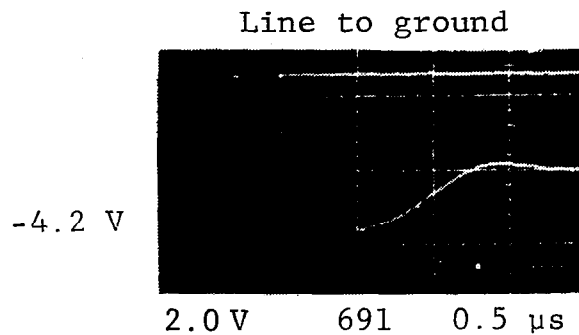$C = 1.5$ μF
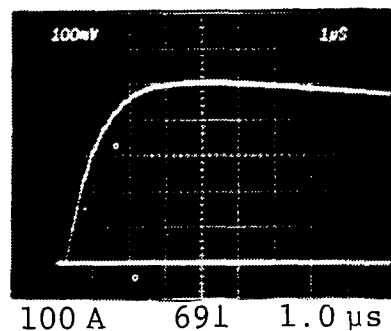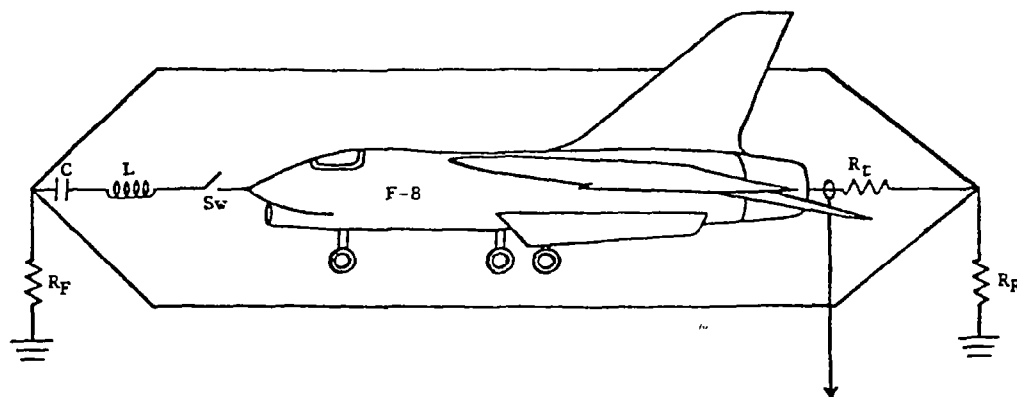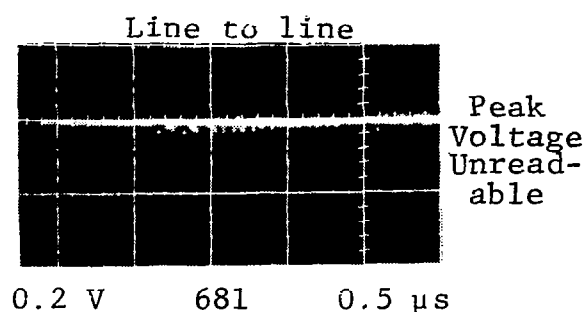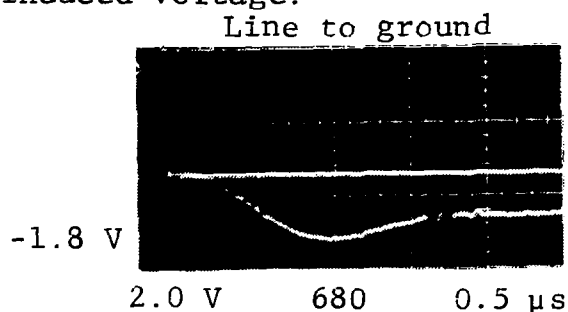$R_s = 45$ Ω
$E = 25$ kV

540 A —

100 A   687   0.5 μs

Figure 29 - 2 x 50 μs Return Stroke into Aircraft
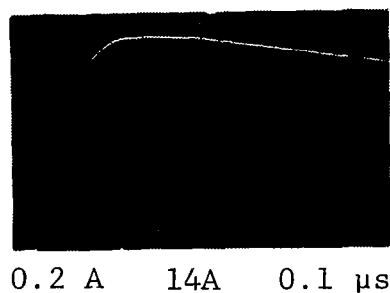Terminated with Short Circuit with
Aircraft Ungrounded.

53

Induced Voltage:

Line to ground

-4.2 V

2.0 V   691   0.5 µs

No model tests were made of this configuration.

Full Scale

L   18 µH
C   = 1.5 µF
R_S = 45 Ω
E   = 25 kV

100 A   691   1.0 µs

Figure 30 - 2 x 50 µs Return Stroke into Aircraft
          Terminated with Short Circuit with
          Aircraft Ungrounded.

54

Induced Voltage:

Line to ground   Line to line

                                          Peak
                                          Voltage
                                          Unread-
                                          able

-1.8 V

  2.0 V   680   0.5 µs   0.2 V   681   0.5 µs

Model   1.08 A —

L = 7.1 µH
C = 0.04 µF
R_t = 100 Ω
E = ~ 110 V

                                  0.2 A   14A   0.1 µs

Full   198 A   —
Scale

L = 90 µH
C = 0.5 µF
R_t = 124 Ω
E = 25 kV

                                  40A   680   1.0 µs
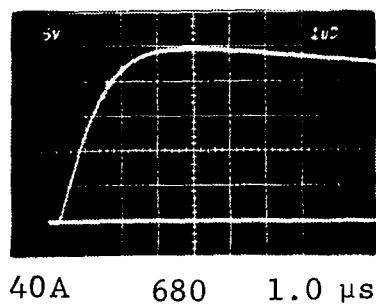
Figure 31 - 2 x 50 µs Return Stroke into Aircraft
        Terminated with $R_t = Z_o$.

55

terminated circuit provided only half the current provided by the short-circuited circuit of Figures 29 and 30. Taking this into account, it is seen that the line-to-ground induced voltage is about the same in either case (that is, about 2 volts per 250 amperes of peak current) but the line-to-line voltage is much lower with the aircraft terminated. This is probably because the higher frequency traveling wave oscillations that appear on the current wavefront are eliminated in the resistively terminated case. This result suggests that the line-to-ground voltage is more nearly proportional to the peak amplitude of the test current, whereas the line-to-ground voltages appear more closely related to the fast rate of rise and/or high frequency components of the test current. Further comments on these relationships will appear later in this report.

<p align="center">Improved Test Circuit Evaluations</p>

One of the objectives of this program was the evaluation of possible improvements in the LTA test circuits. Selection of candidate circuits was to be based on the results of cause-effect studies conducted during the first part of the program. During the investigations reported thus far, several important cause-effect relationships were identified. Among these are the following:

1. It is necessary to have return conductors to enable the return-stroke portion of the lightning flash to be simulated and these conductors must be distributed around the aircraft in order to minimize proximity effects on the distribution of current in the aircraft.

2. The airframe and its return conductors behave like a transmission line, although the velocity of traveling wave propagation in this transmission line is somewhat slower than that of waves in a "pure" air-insulated transmission line with a narrow center conductor. As with other transmission lines, the magnitude of the traveling voltage and current surges are related by the surge impedance of the line, and the surge impedance, in turn, is determined by the geometry of the line. In other words, it is determined by the size of the aircraft and its return conductors, and by their spacing.

3. The surge impedance of the F-8 aircraft and four aluminum foil or wire return conductors is about 100 ohms.

4. The surge impedance of an aircraft in flight is greater than this, perhaps between 400 and 800 ohms, and therefore may not be appreciably different than that of the lightning flash channel itself.

5. Reflected traveling waves may be eliminated by terminating the aircraft to its return conductors in a resistance equal to the transmission line surge impedance (in the F-8, 100 ohms) but an initial wave propagating once from the generator end of the aircraft to the opposite end will nearly always occur in the test, and very likely occurs in flight.

It therefore appears necessary that improved test circuits be capable of generating both the traveling wave phenomenon and the return stroke current. Since little is presently known about the magnitude of traveling waves produced on aircraft in flight, it may not be possible to accurately simulate these phenomena. It is necessary, however, that the traveling wave phenomenon be controllable.

In actuality, the traveling wave phenomenon would probably occur first, when the lightning leader first approaches or contacts the aircraft. A period of relative quiet then probably ensues, until the leader has propagated to the earth (or another opposite charge center) and the return stroke has been initiated. The return stroke is formed by the rapid discharge of the leader into the earth, from the ground up.

It may require a few milliseconds for the leader to reach the earth, and then the return stroke will propagate up from the earth at about 1×10^8 m/s (about 1/3 the speed of light). These two different phenomena are illustrated in Figure 32.

Thus, the basic phenomena that should probably be simulated are leader currents and return stroke currents. When each of these currents reaches the aircraft, traveling wave currents are also likely to be present.

Since traveling wave phenomena are involved in the return stroke as well as the leader attachment phase, it seems most appropriate to simulate the lightning channel as a transmission line rather than with lumped RLC components as in the original LTA configuration. Clearly, natural variations in lightning phenomena and aircraft size imply that a range of lightning channel and aircraft surge impedances are possible, so the test technique should enable these parameters to be known and controlled, and changes in them to be made. Configuration of the lightning generator to approximate a transmission line was therefore decided upon for evaluation.
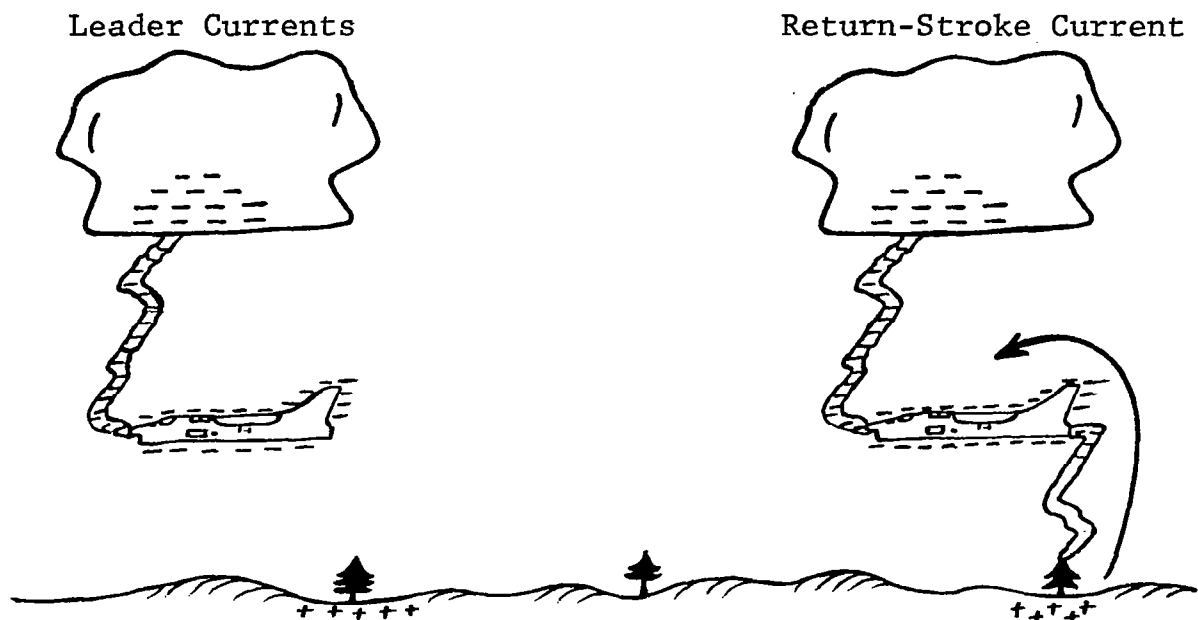
Leader Currents   Return-Stroke Current

Figure 32 - Lightning Strike Phases to be
Simulated in the LTA test.

Lumped parameter ladder network. - A transmission-line repre-
sentation of the lightning channel has long been considered appro-
priate (ref. 10), and mathematical analyses of such models have
recently been accomplished by Kim, DuBro and Tessler (ref. 17),
Little (ref. 18) and Strawe (ref. 19). In each case the lightning
channel has been represented as a lumped parameter ladder network
as shown in Figure 33.
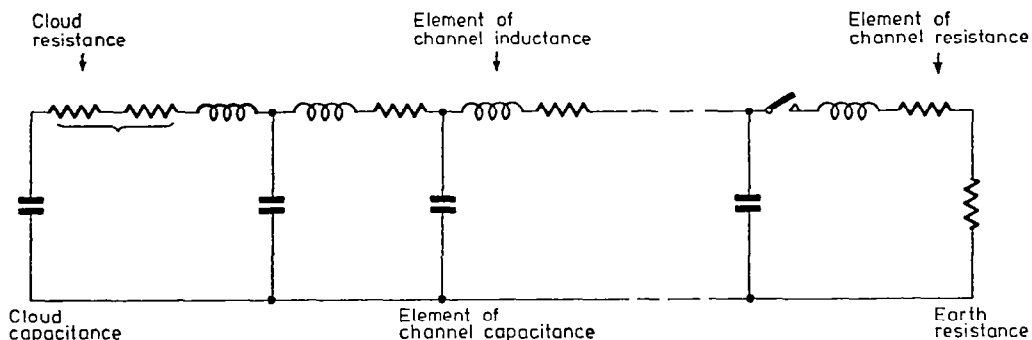
Figure 33 - Lightning Channel Represented as a Lumped
Parameter Ladder Network (from ref. 18).

Each of the referenced analyses utilized different numbers
of ladder elements and different values of R, L and C in each
element. Values of inductance ranged from 1400 to 6100 pF per
meter of channel length. The results of these analyses are

58

reported completely in the references and will not be repeated here, but in each case they show that:

1. The amplitude and rise time of the return stroke diminish as it propagates upward from the earth.

2. The wavefront of the return stroke currents is concave, and reaches its maximum rate of rise shortly before it reaches its peak amplitude, rather than at the beginning of current flow as in the double-exponential current produced by the original LTA circuit.

Inductance and capacitance selection. - For the test circuits to be evaluated in this program, it was necessary to select appropriate values of L and C. The rationale for this selection was as follows:

The surge impedance (Z_L) of a lightning channel has been estimated by Bewley (ref. 10) to range between 400 and 600 ohms, and most other researchers appear in agreement with this. As reported earlier, the surge impedance $(Z_{A/C})$, of the aircraft with respect to the return lines is about 100 ohms. It will be important to have the surge impedance of the lightning channel match that of the aircraft and return line configuration on some occasions, so a value of 100 ohms was selected for initial evaluations of the ladder network and the first test circuit evaluations were made using the 1/10 scale model.

Assuming that the return stroke travels through the channel with a velocity one-third the speed of light, then equations (14) and (15) should be satisfied as follows:

$$Z_L = \sqrt{\frac{L}{C}} = 100 \text{ ohms} \tag{14}$$

and

$$v = \sqrt{\frac{1}{LC}} = 1 \times 10^8 \text{ m/s} \tag{15}$$

combining (14) and (15):

$$L = \frac{L}{v} + \frac{100\Omega}{1 \times 10^8 \text{m/s}} = 1 \text{ } \mu H/m \tag{16}$$

and

$$C = \frac{1}{vZ} = \frac{1}{(1 \times 10^8)(100)} = 1 \times 10^{-10} \text{ F/m} \tag{17}$$

$$= 100 \text{ pF/m}$$

Simulation of a lightning channel 3000 m long would thus require capacitors totaling:

$$C_{total} = (3000m)(100 \times 10^{-12} \text{ F/m}) \tag{18}$$

$$= 0.3 \text{ }\mu F$$

and a total inductance of:

$$L_{total} = (3000m)(1 \times 10^{6} \text{ H/m}) \tag{19}$$

$$= 3 \text{ nH}$$

Number of segments.- The analysts referred to earlier utilized eight or more ladder segments to provide what was considered to be an adequate representation of a lightning stroke waveform, but it would be desirable to reduce the number of capacitors and inductors that must be assembled in a test circuit. At the same time, a closer approximation of an actual transmission line is achieved if each element is made to represent a smaller fraction of the total line. Therefore it was decided to represent a shorter portion of the total lightning channel with a lumped parameter ladder network representing six segments of 25 meters each. This would reduce the duration of the return stroke passing through the aircraft, but should not affect its rate of rise or peak amplitude; nor should such a reduction in length of channel simulated significantly affect the nature of the short-duration traveling waves in the aircraft.

For the full scale test circuit, this required that for each 25-meter segment,

$$L = (25m)(1\mu H/m) = 25 \text{ }\mu H \tag{20}$$

and,

$$C = (25m)(100pF/m) = .0025 \text{ }\mu F \tag{21}$$

For the 1/10 scale model evaluation, the values of L and C were divided by the scale factor of 10 in accordance with the rules of Table III.

A comparison of the lumped parameters selected for this program with those utilized in the analyses referred to earlier is presented in Figure 34. It will be noted that the surge impedance of the experimental line is considerably greater than that of either of the analyzed lines. Also, the capacitance per meter of the experimental line is considerably lower than that of either of the analytical models. Considering the remoteness of a typical lightning flash from earth or any other conductor, the 100 pF/m

Parameter	Kim, et al.	Little	F-8 Test in This Program
Length of Channel Being Represented	3000 m	3000 m	150 m
No. of Ladder Elements	8	8	6
Length of Each Element	375 m	375 m	25 m
Parameters			
R	0.01 Ω/m	1.0 Ω/m	0
L	0.04 μH/m	2.0 μH/m	1.0 μH/m
C	3000 pF/m	1400-6100 pF/m	100 pF/m
$Z_L = \sqrt{\dfrac{L}{C}}$	13 Ω	38-18 Ω	100 Ω

Figure 34 - Comparison of Lumped Parameters Utilized in This Program with Those Utilized in Analytical Models.

estimate seems more appropriate than the higher values utilized by Kim et al. and Little; however, no attempt was made in the analysis to confirm or disprove either of these values by calculation.

At first, the lumped parameter ladder network was tested in the one-tenth scale model configuration. A series resistance of one ohm per segment was included initially, but measured currents were indistinguishable from those occurring in the ladder circuit without the resistance present, so testing was continued without the series inductance.

Leader attachment simulation. - Figures 35 and 36 illustrate the model and full scale test results, with the lumped parameter ladder network used to represent a leader first attaching to the nose of the aircraft. These figures show the current entering the airframe (and in some cases, airframe voltages also) and the line-to-ground and line-to-line induced voltages in the instrumented circuit.

In Figure 35, only the approaching leader is simulated. The airframe currents produced in the model are very similar to those that entered the full scale F-8, and in each case, related to the line charging voltage and the 100 ohm surge impedance, as expected.

Since the aircraft was unterminated, the current was reflected back and forth in the airframe. The reflections, which can be seen in the current oscillograms of Figure 35, are lower in amplitude than the initial surge due to losses.

In the full scale tests, the voltage (e) between the nose of the aircraft and an adjacent return wire was also measured. During the first pulse the voltage oscillates in phase with the current, as expected, and is then out of phase. The fuselage remains at a DC voltage level determined by the redistribution of charge from the 75 m simulated leader.

The induced voltages shown on Figure 35 peak during the first half microsecond which is the time the airframe current is rising and changing most rapidly, indicating the voltages are induced by magnetic flux passing through apertures such as the wing-to-fuselage seam and the cooling air louvres in the pallet area covers. The line-to-ground voltage includes a lower amplitude oscillatory component which appears to be in phase with the successive current oscillations, indicating that it may be related to the structural resistive voltage along the length of the fuselage. This voltage would appear in the line-to-ground measurement but not in the line-to-line measurement which observes only the voltage in the loop between the two wires of the circuit.
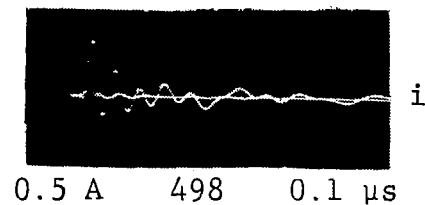
62

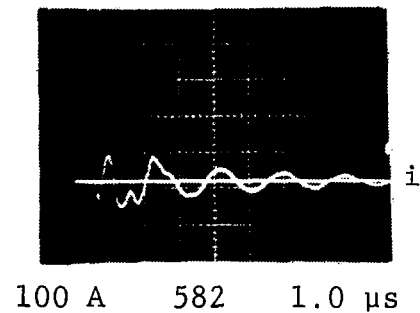Induced Voltage: Line to ground   Line to line

$-1.16\,\text{V}$

2.0 V   666   0.5 µs   0.5 V   665

Model

L = 2.5 µH
C = 220 pF
E = 80 V
I = 0.8 A

0.5 A   498   0.1 µs   e Nose-to-Re
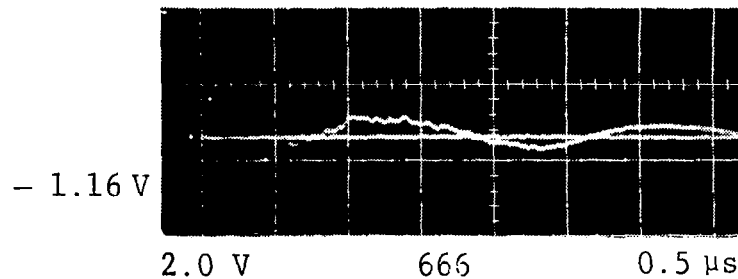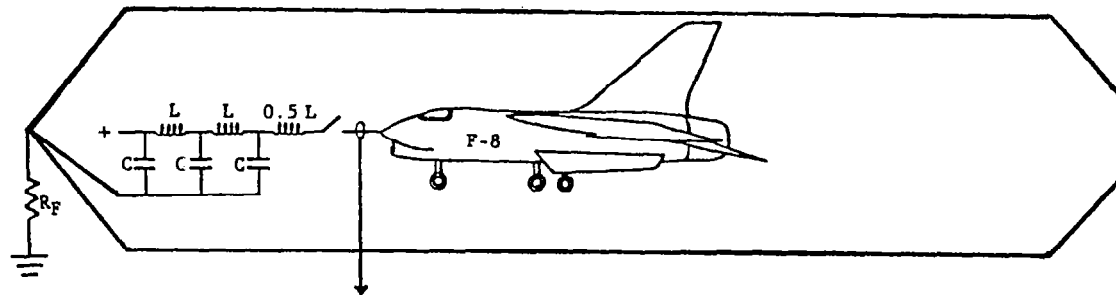
Full
Scale

L = 25 µH
C = 2000 pF
E = 25 kV
I = 250 A
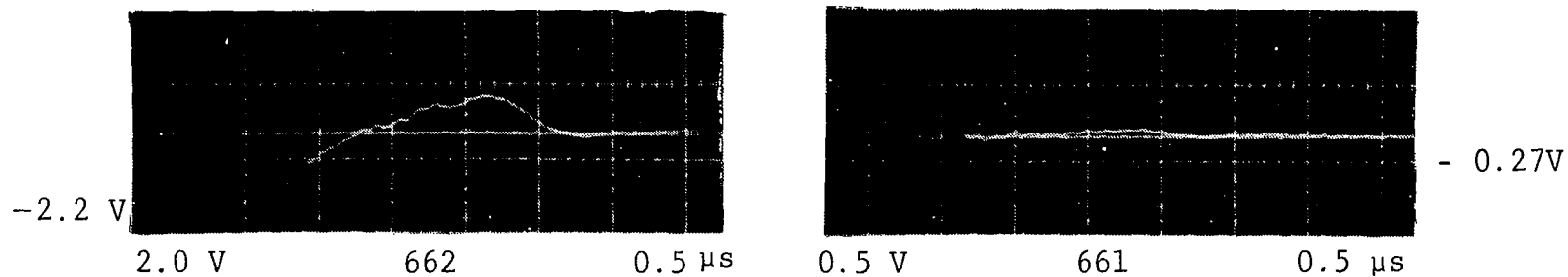
100 A   582   1.0 µs   5 kV   588
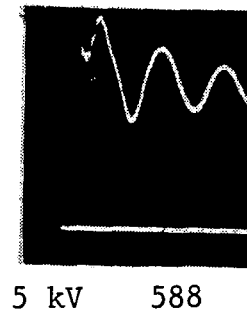
Figure 35 - Simulated Leader Attachment to Unterminated Aircra

Induced Voltage: Line to ground

Line to line

- 0.27V

−2.2 V

2.0 V   662   0.5 µs   0.5 V   661   0.5 µs

Model

L = 2.5 µH
C = 220 pF
E = 100 V
I = 1 A

0.5 A   510   0.1 µs   0.5 A   511   0.1 µs   0.5 A   512   0.1 µs

Full
Scale

L = 25 µH
C = 2000 pF
E = 25 kV
I = 260 A

100 A   601   1.0 µs   100 A   600   1.0 µs   100 A   617   1.0 µs
500 V   500 V   500 V
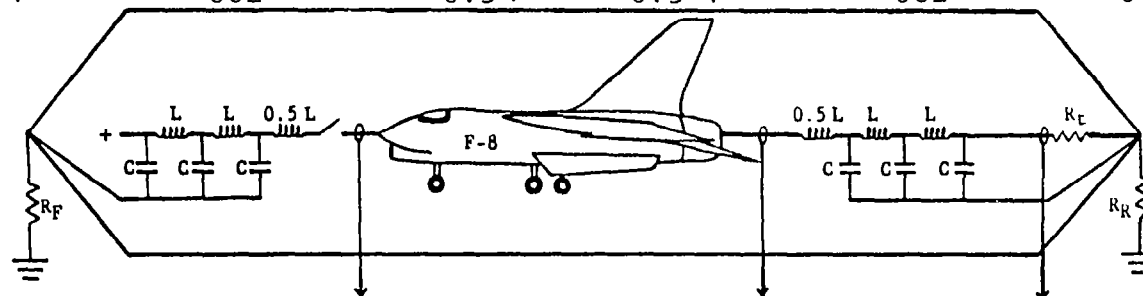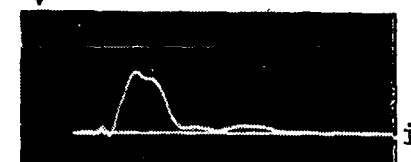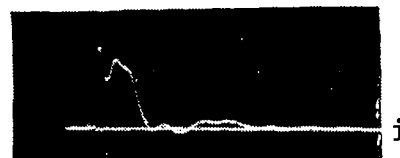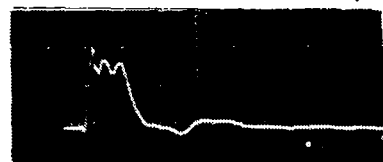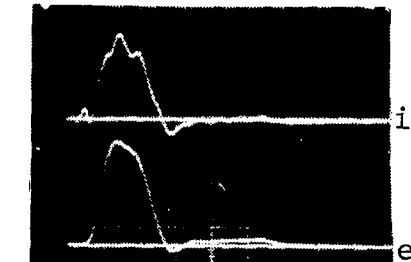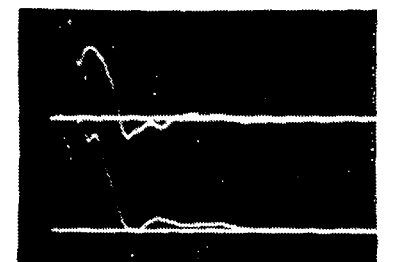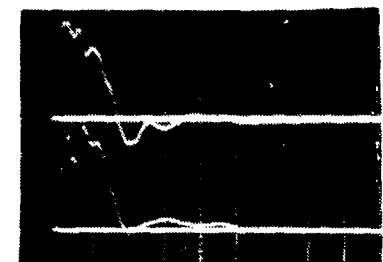
Figure 36 - Leader Attachment with Aircraft Terminated.

Figure 36 illustrates a similar case as that of Figure 35, except that an uncharged ladder network is attached to the tail of the aircraft. This has the effect of terminating the aircraft in its surge impedance of 100 ohms, and of providing a path for the leader to continue onward from the aircraft. Whether this is a better simulation of the actual leader attachment situation or not is not known. If an aircraft is intercepted by a leader, continued propagation of the leader will occur, but it takes place in a series of steps, with a pause of many microseconds between each step.

As shown in this figure, the peak amplitude of the airframe current is about the same as that of Figure 35 when the aircraft was unterminated, but the duration of the current surge is longer and reflections are essentially eliminated. This is due to the 100 ohm termination of the aft end of the aircraft. It will also be noted that the rate of rise of the airframe current is greatest at the nose of the aircraft where the switch is located. It is somewhat less at the tail, and even slower at the earth end of the simulated channel. The airframe voltage is very similar in waveform to the current, due to the absence of reflections, and there is excellent similarity between the model and full scale current waveforms.

In this circuit, line-to-ground induced voltage shows a greater IR component than was evident when only the attaching leader channel was present. This is because the current remained at its peak level for a longer period of time, permitting more current to diffuse to the interior of the aircraft skin and cause a more pronounced resistive voltage rise, which is superimposed on the magnetically induced component. Only the magnetically induced component appears in the line-to-line measurement, of course. The majority of the voltage still appears to be related to di/dt though.

Return stroke simulation. - By moving the switch to the ground end of the ladder network and beginning with the entire channel charged, the return stroke can be simulated. By closing the switch, the channel begins to discharge at the ground end first, creating a current wave that propagates up the channel in the manner of a return stroke. This situation is shown in Figure 37. This time, the current rate of rise is greatest at the ground end of the channel because the switch is located there. The amplitude remains approximately the same but the rate of rise diminishes as the wave progresses further up the channel.

Since the current rate of rise is now much slower at the aircraft than was the case in the leader attachment simulation of Figures 35 and 36, the magnetically induced voltage is also much lower than that measured during leader attachment. The resistive
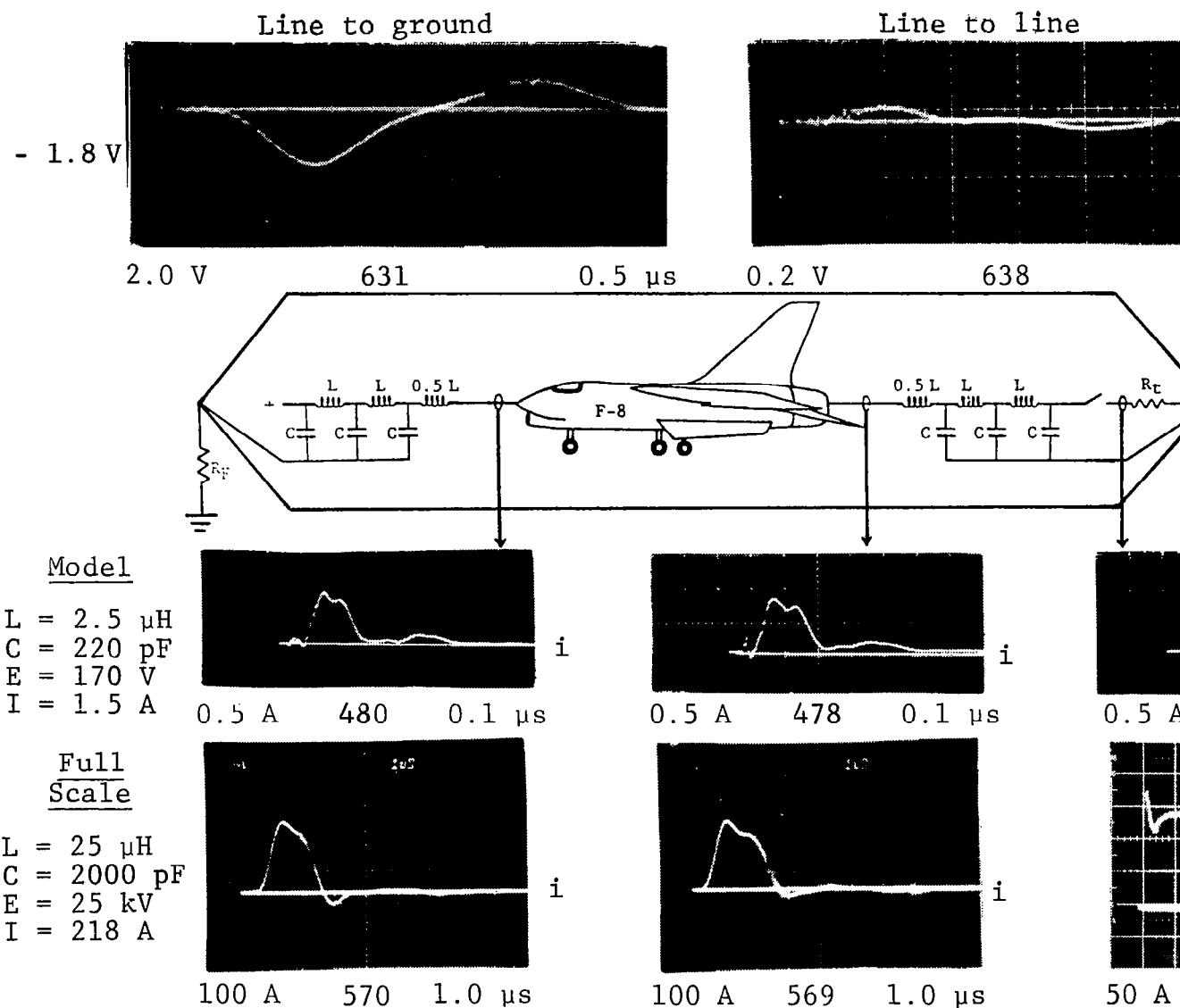
Induced Voltage:

Line to ground | Line to line

- 1.8 V

2.0 V 631 0.5 μs 0.2 V 638

F-8

Model

L = 2.5 μH
C = 220 pF
E = 170 V
I = 1.5 A

0.5 A   480   0.1 μs   0.5 A   478   0.1 μs   0.5 A

Full
Scale

L = 25 μH
C = 2000 pF
E = 25 kV
I = 218 A

100 A   570   1.0 μs   100 A   569   1.0 μs   50 A

Figure 37 - Return Stroke Through Aircraft.

voltage, which appears only in the line-to-ground measurement, is now higher than before but not more than 1/2 of the total line-to-ground induced voltage and is approximately the same amplitude as the resistive voltage induced by the leader current in the instrumented circuit of Figure 36. This is because the resistive voltage is directly proportional to the airframe current and the current in these circuits is, in turn, proportional to the charging voltage divided by the 100 ohm surge impedance, and the charging voltage and surge impedance were the same for all of these tests.

This is not to imply that the transmission line charging voltage should be the same for a leader simulation as for a return stroke simulation. Additional discussion of this matter appears in a later paragraph; and in any event, additional information is needed on leader and return stroke channel characteristics to clarify this aspect.

Study of the full-scale current oscillograms of Figure 37 shows that the duration of the current wave is proportional to the length of the charged transmission line and that the effective velocity of propagation is about one-half the speed of light.

At the ground end, the total time duration (T) of the return stroke current (until sharp drop-off begins) is, from oscillogram 638 of Figure 37:

$$T \sim 2.5 \ \mu s$$

This should be the time necessary for the current wave to propagate all the way up the channel and discharge the entire length. For a total simulated channel length (ℓ) of 150 m plus the aircraft length of 17 m, the effective velocity (v) was

$$v_{effective} = \frac{T}{\ell} \qquad (22)$$

$$= \frac{2.5 \times 10^{-6} \, s}{167 \, m}$$

$$= 1.5 \times 10^8 \ m/s$$

Considering the imperfections in the simulation, this result compares favorably with the goal of representing a channel with an effective velocity of 1×10^8 m/s.

The return stroke current duration in the model test was one tenth of that in the full scale test, producing an effective velocity along the one tenth scale channel of also about 1.5×10^8 m/s.

It should be remembered that the actual velocity of current flowing in the lumped parameter ladder network remains at (or very near) the speed of light. The lumped parameters in the network make the network appear physically longer than it actually is.

Induced voltage relationships. - As mentioned in the foregoing paragraphs, cause-effect relationships appear to exist between the induced voltages and the airframe currents, with line-to-ground voltages appearing to be a combination of structural resistive as well as magnetically induced voltages, and the line-to-line measurements indicating only induced effects. A closer comparison of these measurements for each of the conventional LTA and lumped parameter ladder circuits evaluated is presented in Table VI. In this table, oscillograms of the wavefronts of the airframe currents generated by each test circuit are shown, together with values of the peak current maximum rate of rise and peak induced voltages.

A comparison of the five results shown on Table VI indicates two important results:

1. Line-to-ground voltages appear to be related to peak current.

2. Line-to-line voltages appear to be related to current rate of rise.

For example, the line-to-ground voltages appearing in the instrumented aircraft circuit during the leader attachment in test 666 of Figure 35 are about the same as those measured in the return-stroke simulations of test 631 of Figure 37 and 680 of Figure 31, when the peak currents were approximately the same; even though the rate of rise in the return stroke simulations was much lower. Conversely, the line-to-line voltages were significant only during the fast rate-of-rise tests. The data of Table VI have been plotted on Figures 38 and 39 to further illustrate this result. In each graph, one of the test results is displaced significantly from the line approximating all of the others. The reason for this is unclear, and may simply be due to an experimental error. Unfortunately, the data were not compared in this manner until after the full scale test program was complete and the setup dismantled, so the test could not be repeated.
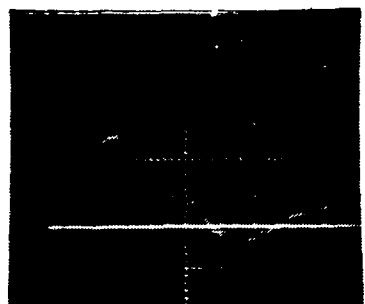
The relationships between induced voltages and simulated lightning current in the airframe are further illustrated in Figure 40, in which the oscilloscope traces of typical line-to-line and line-to-ground voltages measured in the instrumented circuit are shown together with the test current. Since the circuit voltages were recorded with an on-board oscilloscope it

Table VI - <u>Current Rate-of-Rise vs. Induced Voltage</u>

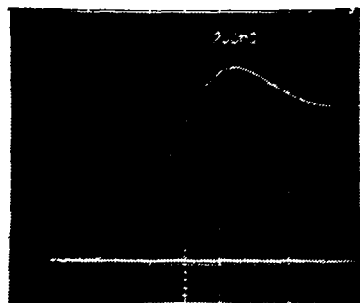| Test Config.	Current (i) and Voltage (e) Entering Aircraft		Peak Current (A)	Maximum di/dt (A/µs)	Peak Ind L-G (V)
Leader Attachment to Unterminated Aircraft	i	 100 A 583 0.1 µs	250	2055	-1.16 (Test 666
Return Stroke	i	 40 A 573 0.2 µs	218	393	-1.8 (Test 631
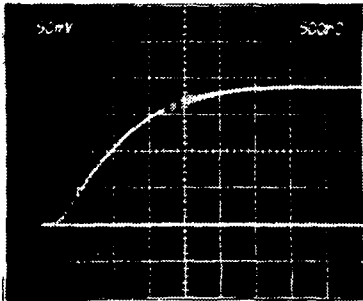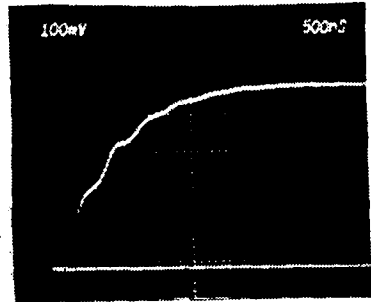
Table VI - Current Rate-of-Rise vs. Induced Voltage (continued)

Test Config.	Current (i) and Voltage (e) Entering Aircraft	Peak Current (A)	Maximum di/dt (A/μs)	Peak Induced Voltage L-G (V)	L-L (V)
	Lumped Circuits				
2 x 50 μs Return Stroke with Aircraft Terminated in Z_o	50A 679 0.5μs	190	140	-1.80 (Test 680)	Lost in noise (Test 681)
2 x 50 μs Return Stroke with Aircraft Short Circuited	100A 688 0.5μs	500	886	-4.10 (Test 689)	-0.24 (Test 690)
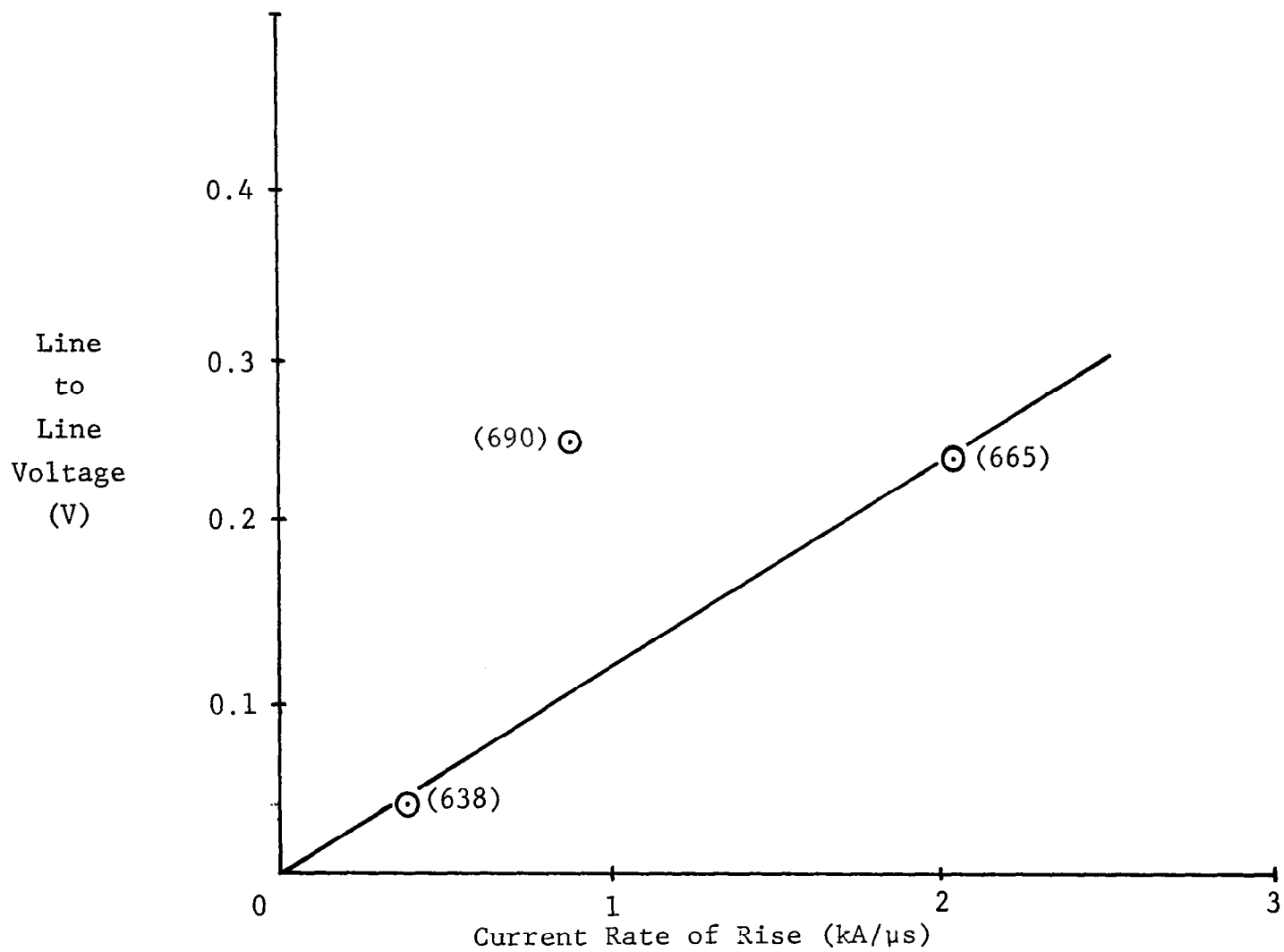
Figure 38 - Line-to-Line Voltage vs. Current Rate of Rise.
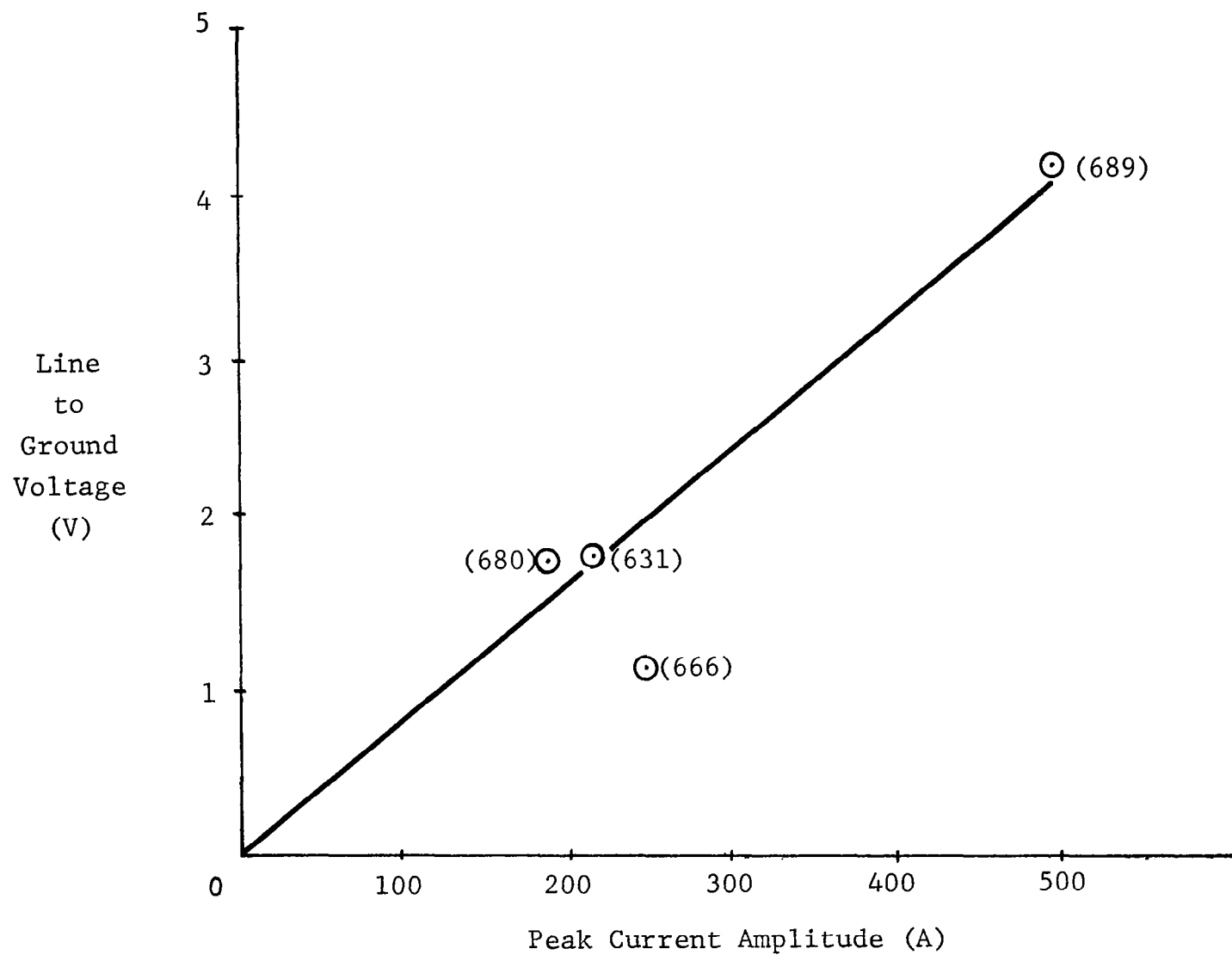
Figure 39 - Line-to-Ground Voltage vs. Peak Current Amplitude.

I_pk ≈250 A

Current

0   0.5   1.0   1.5   2.0   2.5 μs

≈0.2 V

Line-to-Line Voltage

Line-to-Ground Voltage

e_IR

≈ 2 V
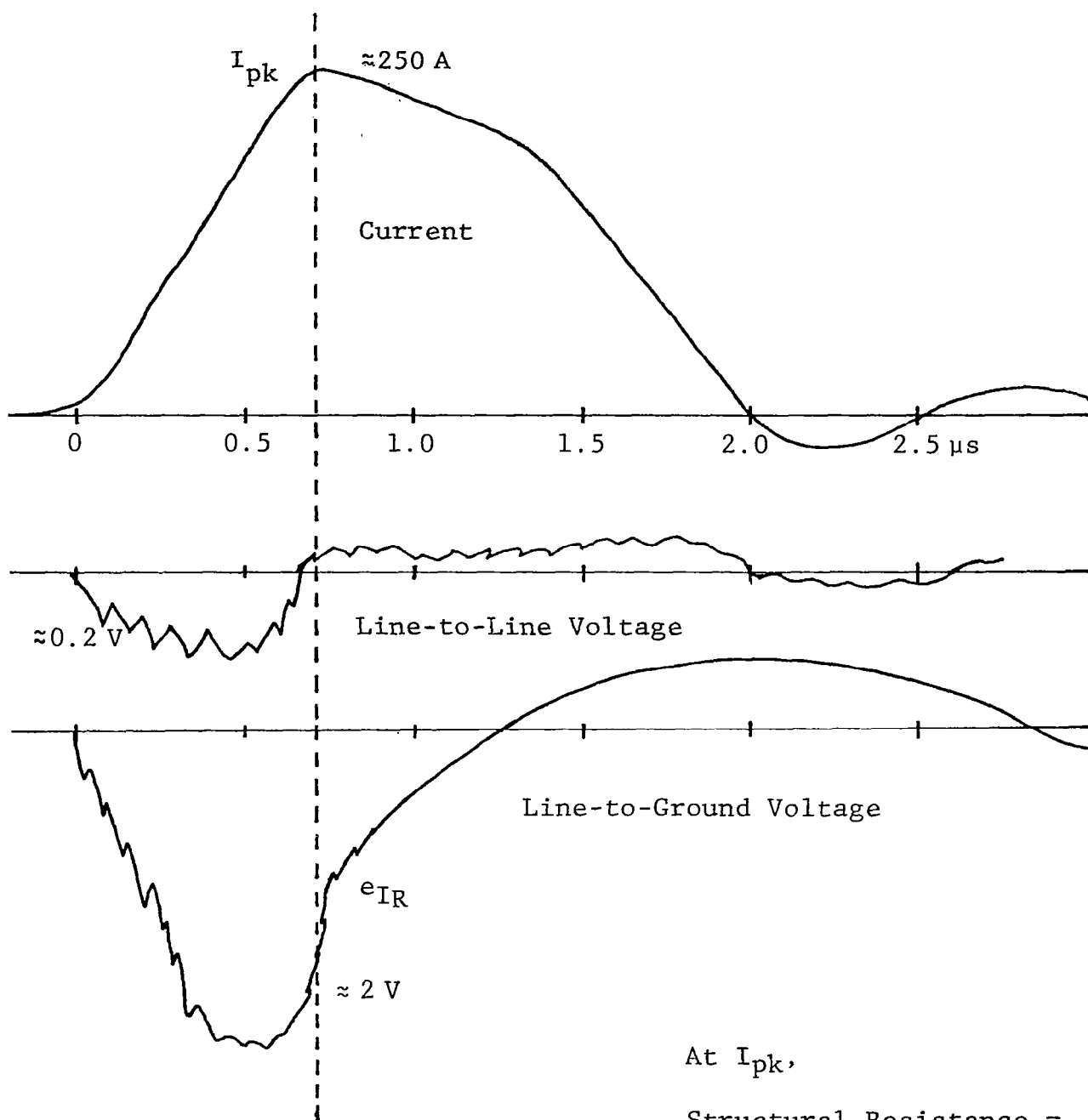
At I_{pk},

Structural Resistance =

$$R_s = \frac{IV}{250A} = 0.004 \ \Omega$$

Figure 40 - Relationship Between Induced Voltage
and Simulated Lightning Current.

was not possible to positively synchronize the measured voltages with the test current that was recorded by oscilloscopes outside of the aircraft. Thus, the time relationship indicated in Figure 40 by the dashed line is an estimate.

If this time relationship is correct, it is evident that the line-to-line voltages are maximum when the current is changing most rapidly, pass through zero when the current is maximum and unchanging, and become opposite in polarity when the current is changing again in the opposite (decreasing) direction. This is a derivative relationship that indicates the voltage is induced by the changing magnetic flux (ϕ) that accompanies the test current according to the familiar relationship:

$$e = -\frac{d\phi}{dt} \tag{23}$$

On the other hand, the voltage measured between either of the aircraft circuit conductors and the airframe (the line-to-ground voltage) appears to be a combination of magnetically induced and structural resistive voltages, as would be expected. This is indicated by the fact that the voltage reaches its peak during the time the di/dt is maximum, but stays positive until the time when the current is maximum when it is lower than for the line-to-line voltages, verifying the existence of an in-phase resistive component.

If the time relationship of Figure 40 is correct and if the line-to-ground voltage is in fact a simple combination of magnetically induced and structural resistive components, the voltage at peak current should be due to resistance only, and the structural resistance (R_S) responsible for this component can be estimated from the relation:

$$R_s = \frac{e}{i} \tag{24}$$

$$= \frac{1.0\,V}{250\,A} = 0.004 \text{ ohms}$$

At first glance, a resistance of 4 milliohms along 8 m of conventional aluminum fuselage appears somewhat high; but since most of this resistance is probably in the fastened joints and seams which are heavily treated with anticorrosion (and therefore non-conductive) coatings, this result may indeed be realistic.

To obtain another data point on the aircraft structural resistance, an ohmmeter measurement was made along the fuselage using a kelvin-type bridge. Several readings were made which yielded resistance values of 5 to 7 milliohms.

Streamer initiation effects. - A high frequency oscillation appearing as "hash" is superimposed on the induced oscillograms of Figures 35 and 36. It was suspected that this resulted from high voltage streamers that occur in the switch gap during the switching process or from airframe corona effects.

In an attempt to evaluate this, a segmented diverter was inserted in series with the switch in the leader attachment simulation of Figure 36. This device provides a longer path for streamers to develop prior to complete closure of the gap and current flow onto the airframe, thus forcing streamer development to begin a finite period of time prior to leader current flow from the ladder network onto the aircraft. The result of this test is shown on Figure 41, where it is evident that the high frequency oscillations now occur well in advance of the leader current. When separated from the high frequency oscillations, the leader current pulse appears quite smooth. A region of "hash" remaining on the decay of the leader current pulse may be due to an instability in the arc along the segmented diverter, but the smoothness of the front and peak of the leader pulse is unmistakable. This is apparent on oscillogram 620 as well as 622, in which the test was repeated with a slower oscillograph sweep to enable the entire leader current to be captured. The leader current and airframe voltage appearing at the aft end of the aircraft are also shown on Figure 41.

The 11.1 MHz frequency of the streamer initiation effects measured in the instrumented circuit was the highest frequency observed during any of the induced voltage measurements. It does not appear elevated to any of the other frequencies observed, and appears too high in frequency to be due to traveling waves in the airframe. These "streamer effects" were always considerably lower in amplitude than the voltages induced by simulated leader or return stroke currents in any of the test circuits evaluated, and time did not permit further evaluation of them in this program.

Extrapolation of induced voltages. - In the past, voltages induced during LTA tests have usually been extrapolated to correspond with full scale current amplitudes of 30 kA to represent an "average" lightning stroke and 200 kA to represent a severe stroke that is thought to be exceeded in amplitude only 1% of the time. The LTA tests have usually been performed with 2 x 50 µs current waveforms that provide an average rate of rise of 150 A/µs. Thus, linear extrapolation according to current amplitude has carried with it a linear extrapolation of rate of rise to 150 kA/µs.

The waveforms produced by the lumped parameter ladder networks have a higher maximum rate of rise than that produced by
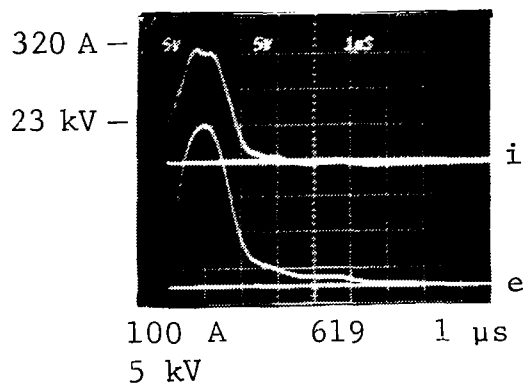
Induced Voltage L-G

0.5 V   620   0.5 µs   100 A   619   1 µs
                                      5 kV

320 A —
23 kV —

i

e
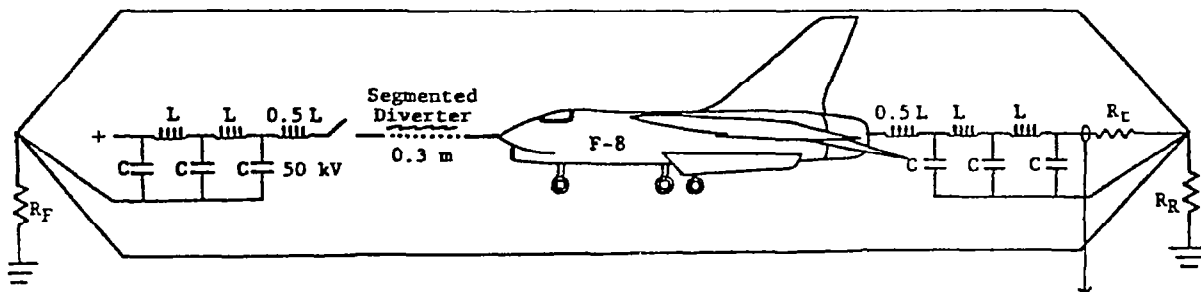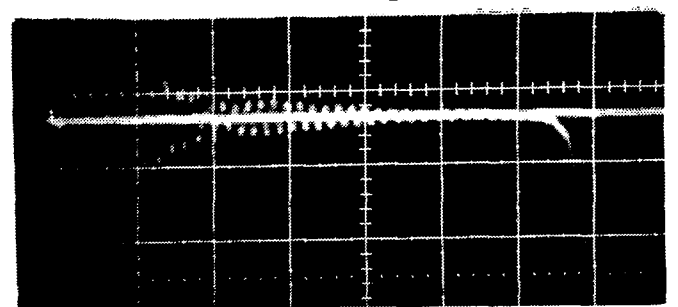
Voltage Induced by
Streamer Initiation

Period = 0.09 µs
     f = 11.1 MHz

Induced Voltage L-G

3.15 V —

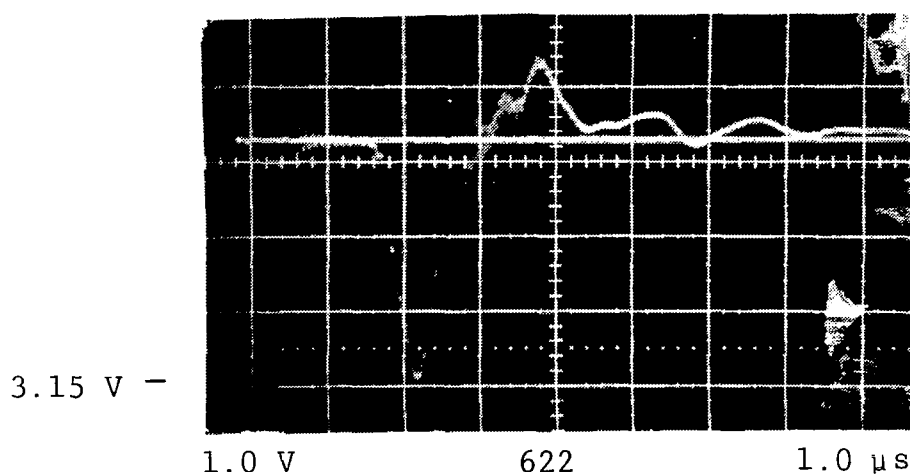1.0 V   622   1.0 µs

Figure 41 - Separation of Voltages Induced by Streamer
           Initiation and Leader Current Entry by
                  Use of Delayed Sparkover.

the original LTA circuit, for a given current amplitude, so extra-
polation of voltages induced by the ladder networks according to
current amplitude may predict unrealistically high voltages.
Since it has been found that some induced voltages appear to res-
pond to current rate of rise and others to current amplitude, it
appears proper to extrapolate induced voltages according to the
current parameter that they are related to. For example, in the
circuit instrumented in this program, the line-to-ground voltages
were related to peak current, and the line-to-line induced volt-
ages were related to current rate of rise. Examples of how these
extrapolation factors may be determined for voltages measured in
the original LTA circuit as well as the 100 ohm lumped parameter
ladder network are shown on Tables VII and VIII. In each case,
the extrapolations are to a severe current amplitude of 200 kA
and a severe rate of rise of 100 kA/μs. Several things are of
interest from the analyses of Tables VII and VIII.

1. The predicted line-to-ground voltage is consider-
    ably greater than the line-to-line voltage, indi-
    cating the protection afforded by independent
    return circuits.

2. The predicted voltages resulting from the 100 ohm
    ladder network test are quite close to those re-
    sulting from the original LTA test.

3. Predicted line-to-line voltages, which are of pri-
    mary concern to digital data transfer circuits in
    such systems as fly-by-wire flight controls, would
    be several times higher if they had been extrapola-
    ted according to amplitude along with the line-to-
    ground data, as was usually done in the past.

4. The need to apply the correct extrapolation factor
    is therefore apparent, and emphasizes the need, in
    turn, to correctly identify the dominant cause
    factors during the tests.

    Further investigation of transit times. - As described ear-
lier in this report, attempts to derive the traveling wave transit
time and velocity from the frequency of airframe voltage or cur-
rent oscillations resulted in indicated velocities lower than the
speed of light.

    Other attempts to determine the traveling wave transit time
were made by measuring the elapsed time between appearance of
the wavefront at the nose and tail of the aircraft. This was
done for both the current and voltage waves, and was accomplished
by triggering of the oscilloscope for all measurements with a
signal from the Rogowski coil on the nose boom. The cable

TABLE VII - Extrapolation Analysis Using the Original LTA Circuit
(using data from Tests 680/690 of Table VI and Figure 29)

1. <u>Line-to-Ground</u> Voltages were most closely related to <u>Peak Current</u>, so:

$$\text{L-G Extrapolation Factor} \sim \frac{200 \text{ kA}}{500 \text{ A}}$$

$$\sim \underline{\underline{400}}$$

2. <u>Line-to-Line Voltages</u> were most closely related to <u>Maximum di/dt</u>, so:

$$\text{L-L Extrapolation Factor} \sim \frac{100 \text{ kA/}\mu\text{s}}{0.89 \text{ kA/}\mu\text{s}}$$

$$\sim \underline{\underline{112}}$$

3. Thus, for the <u>Return Stroke</u> Phase:

	Test Data (V)	x	Ext. Factor	=	Predicted Voltage
Line to Ground	4.1		400		1640
Line to Line	0.24		112		27

78

TABLE VIII - Extrapolation Analysis Using the
100Ω Ladder Network
(using data from Tests 631/638 of
Table VI and Figure 37)

1. Line-to-Ground Voltages were most closely related to Peak Current, so:

$$\text{L-G Extrapolation Factor} \sim \frac{200 \text{ kA}}{218 \text{ A}}$$

$$\sim \underline{\underline{917}}$$

2. Line-to-Line Voltages were most closely related to Maximum di/dt, so:

$$\text{L-L Extrapolation Factor} \sim \frac{100 \text{ kA/}\mu\text{s}}{0.39 \text{ kA/}\mu\text{s}}$$

$$\sim \underline{\underline{256}}$$

3. Thus, for the Return Stroke Phase:

	Test Data (V)	x	Ext. Factor	=	Predicted Voltage
Line to Ground	1.66		917		1523
Line to Line	0.04		256		10

transmitting this signal to the oscilloscope was shorter than that bringing the traveling wave measurement from either the nose or tail, providing a short delay time that enabled the start of the waves always to be seen. The same instrument cable and probes were used to make the measurements at the nose and tail.

The current wave measurements are shown on Figure 42 and the voltage waves on Figure 43.

For the model, a velocity of 2.09×10^8 m/s was determined, but in the full scale test using the same circuit, a velocity of only 1.39×10^8 m/s is determined, as shown on Figure 42. Note that the oscillograph sweeps are the same for the model and full scale test currents in this figure. Thus, in the full scale situation the beginning of current rise is less abrupt. For the purpose of establishing more definite times of arrival, the intersect of the second graticule line above the zero line was selected. This should be valid if the waveforms are identical, which was verified by superimposing one upon the other. The reason for the apparently slower traveling wave velocity between the model and full scale tests is not clear.

In the tests of Figure 43 the traveling wave voltage waveform appearing at the nose and tail were measured and the difference in their times of arrival was determined to be 0.07 µs, which resulted in a velocity along the 17 m F-8 aircraft of 2.45×10^8 m/s. This was the highest velocity determined from any of the transit time measurements, and is about 80% of the velocity of light. The reason that the voltage waveform of this circuit apparently propagated along the aircraft faster than the current waves of Figure 42 is also unclear.

The influence of generator circuit elements on the frequency of airframe voltage oscillations was found to be significant in other tests in which the voltage between the unterminated tail of the aircraft and the adjacent return lines was measured when series inductance and resistance was inserted between the generator capacitor and the airframe, as shown in Figure 44. From these results, it is clear that the period of oscillation depends significantly upon the lumped test circuit elements as well as the length of the aircraft. In other words, the voltage observed at the open ended tail of the aircraft is dependent upon all elements in the circuit loop, not just the aircraft. The addition of a 20 µH inductor, for example, doubles the effective length of the circuit and produces a period twice as long as that when no lumped inductance is present. Finally, addition of a series resistance reduces the reflection magnitude the aircraft appears to become slowly charged to the capacitor voltage.
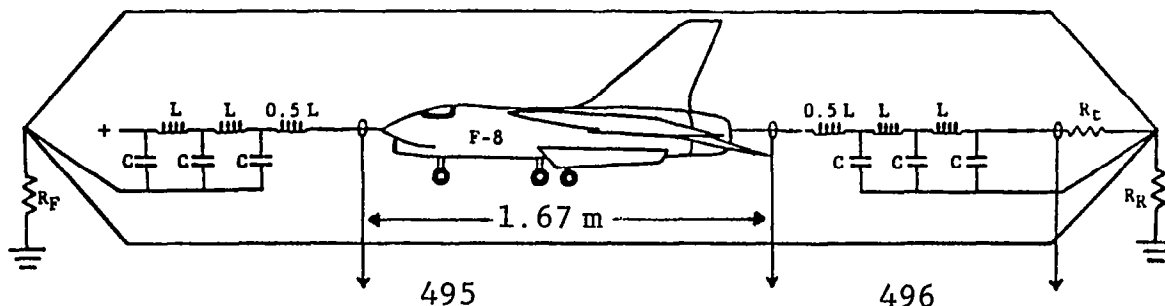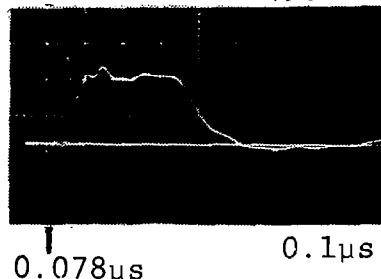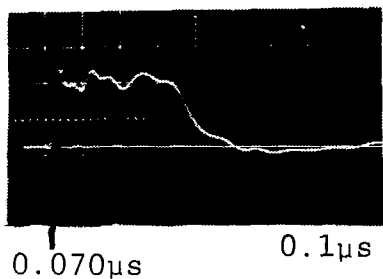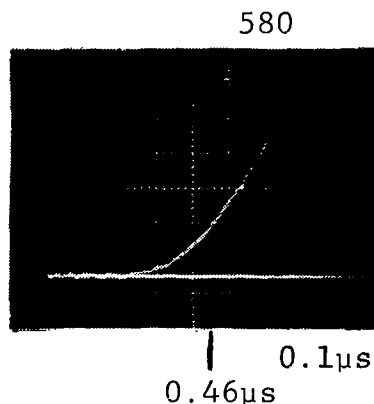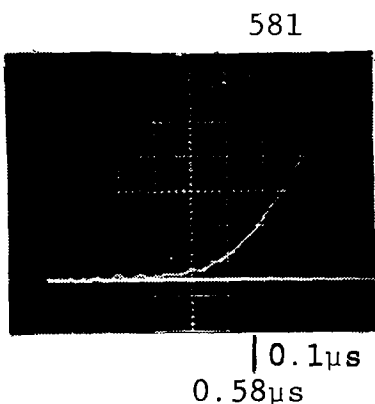
$$\tau = (0.078 - 0.070)\ \mu s\ = 0.008 \pm .002\ \mu s$$

$$v = \frac{d}{\tau} = \frac{1.67\ m}{0.008 \times 10^{-6}\ s}$$

$$= 2.1 \pm 0.7 \times 10^{8}\ m/s$$
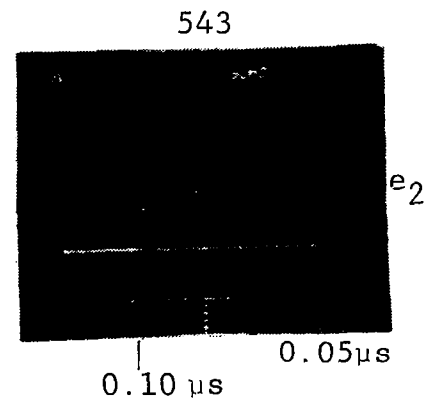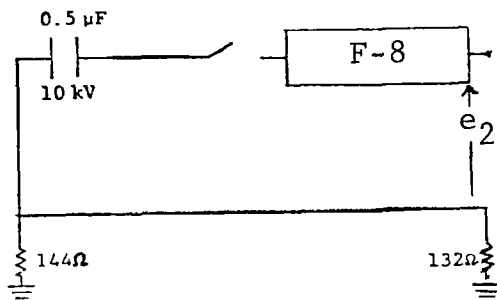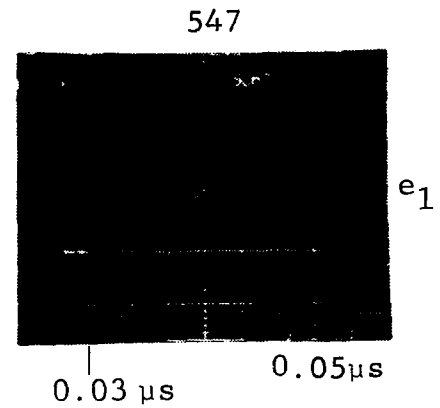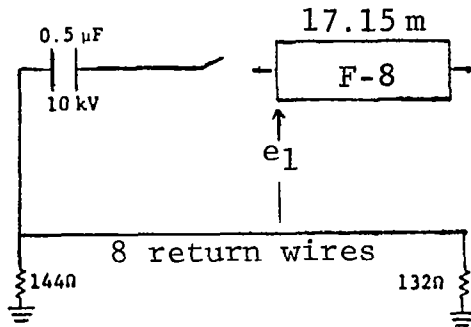
$$\tau = (0.58 - 0.46)\ \mu s = 0.12\ \mu s$$

$$v = \frac{d}{\tau} = \frac{1.67\ m}{0.12 \times 10^{-6}\ s}$$

$$= 1.39 \times 10^{8}\ m/s$$

Figure 42 - Transit Time Determined from Current
Wave Entry and Exit Times.

$$\tau = (0.10 - 0.03) \times 10^{-6} \, s$$
$$= 0.07 \times 10^{-6} \, s$$

from which

$$v = \frac{d}{\tau} = \frac{17.15 \, m}{0.07 \times 10^{-6} \, s}$$
$$= 2.45 \times 10^{8} \, m/s$$

Figure 43 – Transit Time Determined from Voltage Wave Entry and
Exit Times.
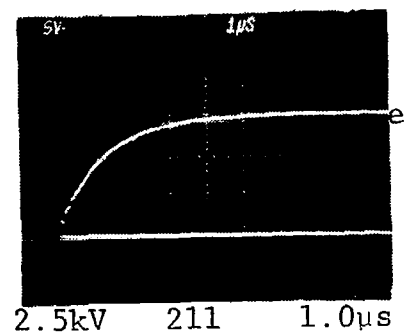   ● Closer to speed of light than when
     derived from the current waves.
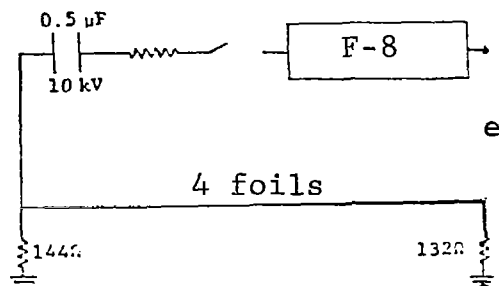
0.5 µF
10 kV

F-8

e

4 foils

144Ω   132Ω

de/dt
Antenna
next to
Wing

2.5kV   217   0.2µs

Period = 0.54 µs

$\tau = \dfrac{0.54}{4} = \underline{\underline{0.135\ \mu s}}$

0.5 µF
20 µH
10 kV

F-8

e

4 foils

144Ω   132Ω

f = 900 kHZ

2.5kV   213   1.0µs

Period = 1.1 µs

$\tau = \dfrac{1.1}{4} = 0.275\ \mu s$

0.5 µF
10 kV

F-8

e

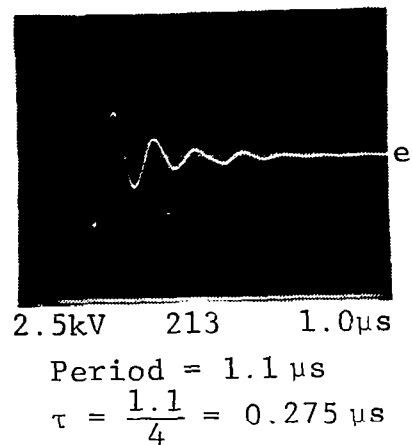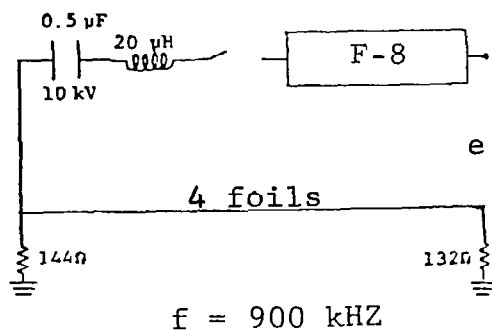4 foils

144Ω   132Ω

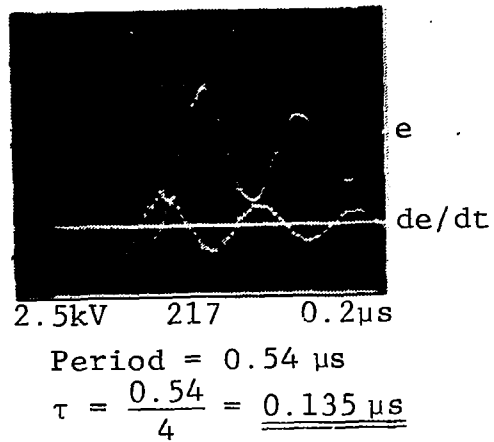5V   1µs
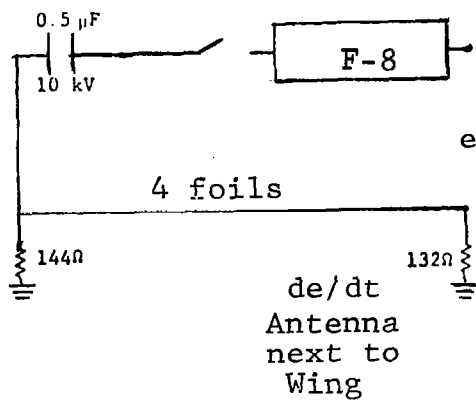
e

2.5kV   211   1.0µs

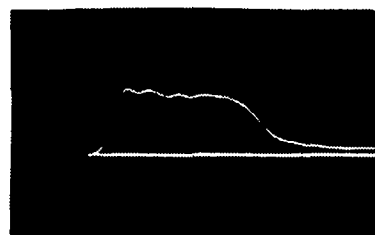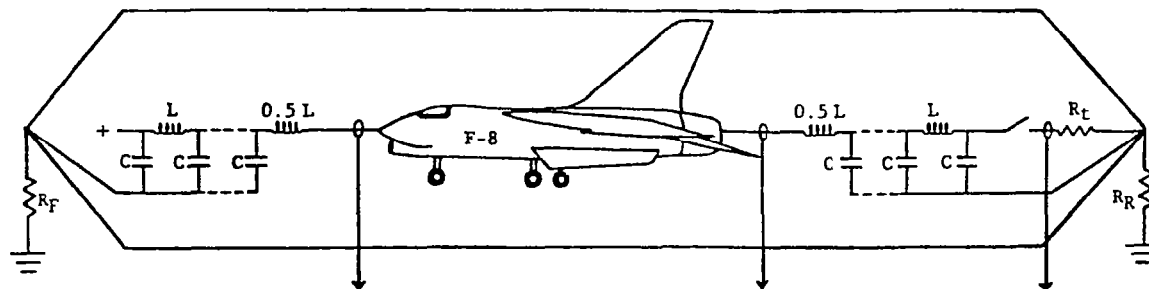Figure 44- Airframe Voltage Oscillations vs. Driving Circuit.

Review of all of the traveling wave transit time evaluations
conducted during this program indicates a trend toward the speed
of light as the diameter of the center conductor diminishes.
Parallel wires or coaxial arrangements of either wires or insula-
ted cables showed velocities closer to those expected, whereas
when an aircraft or large cylinder becomes the center conductor,
the velocity diminishes. Discussions with researchers familiar
with the theory of antennas and the interaction of solid conduc-
tors within an electromagnetic field have disclosed that this
phenomenon should, perhaps, have been expected. It has been shown,
for example (ref. 21) that the velocity of propagation of waves
on a thin wire in an electromagnetic pulse field can be less than
the speed of light, and that larger diameter conductors may expe-
rience slower velocities.

Notwithstanding this, the (supposed) transit time and velo-
city discrepancies were causes of concern in this investigation,
and indicate the need for further investigation aimed at determin-
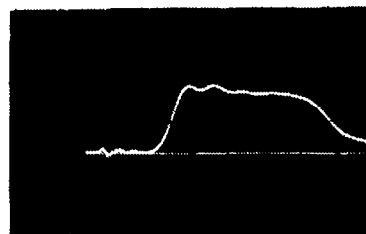ing a physical explanation for this phenomenon.

Simulation of longer lengths of leader channel. - As des-
cribed earlier, the lumped parameter ladder network simulated in
the full scale tests consisted of six 25 m segments which repre-
sented a total 150 m length of channel. Simulation of a longer
length would, of course, require additional capacitors and induc-
tors. In order to evaluate the test current produced by a longer
length of simulated channel, a 20-segment network representing
500 m of channel was evaluated on the scale model. Each segment
had the same length and circuit elements as in the previous model
tests. The resulting currents are shown in Figure 45.

In Figure 45, which represents a return-stroke, oscillograms
470, 468 and 469 show the current entering the nose, exiting the
tail, and at the ground end of the channel. The duration of the
current at the ground end is longer than at the aircraft, due to
the longer length of channel to be discharged. As before, the
fastest rate of change appears at the switch, which in this case
is located at the ground. Comparison with the same situation in
a shorter channel of Figure 37 illustrates that the rates of cur-
rent rise and decay are similar. The one difference is the dura-
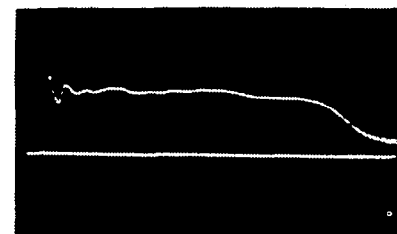tion of the current pulse.

Oscillogram 483 shows the current in each of the 20 segments,
from the earth to the cloud end. Here again it can be seen that
the stroke duration is longest at the ground end and shortest at
the cloud. It must be remembered, of course, that these simula-
tions represent channel discharge phenomena only and do not in-
clude simulation of the intermediate or continuing current dis-
charges that are caused by drainoff of the charge remaining in
the original cloud center. These are much slower and lower in
amplitude currents that do not significantly influence induced
voltages.

84

0.5 A   470   0.1 μs   0.5 A   468   0.1 μs   0.5 A   469   0.1 μs
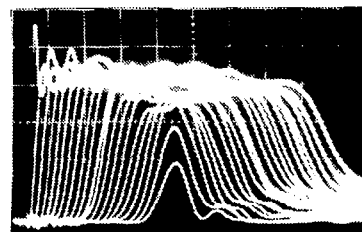
Current in each Segment

Model

L = 2.5 μH
C = 220 pF
R_t = 100 Ω

earth
cloud

0.2 A   483   0.1 μs

Figure 45 - Return Stroke Current in a 500 m, 20-Segment Network
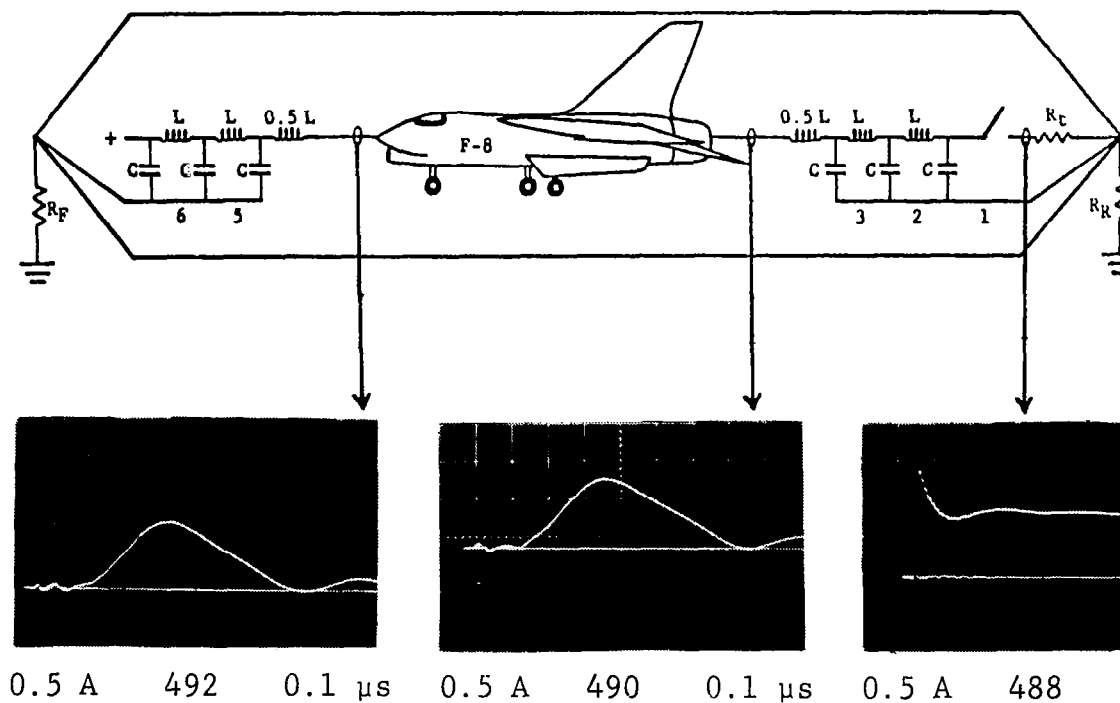(Each Segment Represents 25 m of Lightning Channel.)

Following the 20-element evaluation, a second test was made to see if the 500 m channel could be represented with fewer segments, each representing a longer length of channel. If this were satisfactory, a smaller number of components would be necessary. The results of this evaluation are shown on Figure 46. The lumped inductors and capacitors in this network are each four times larger than those of the 25 m segments. Thus, each segment now represented was 600 m. As shown in Figure 46, the amplitude of the stroke current waveforms was equivalent to that of the currents in the 25 m segments, but the rate of rise of the currents entering and leaving the aircraft is much less than that produced by the shorter segments. Clearly, the larger segments act less like a transmission line and are not appropriate for use in this test circuit.

Additional cause-effects evaluations using the model. - To obtain another look at the causes of the induced voltages, a series of tests was made on the one-tenth scale model with a single wire installed in approximately the same location as the instrumented circuit in the full-scale F-8. The wire was grounded to the model fuselage, so induced voltage measurement is representative of a line-to-ground situation.

According to the model scaling laws of Table III the conductivity of the model fuselage material should be ten times that of the full scale aircraft materials if structural IR rises are to be faithfully represented in the model. Such materials are not available so the model was made of aluminum with the same conductivity as the full scale F-8. The location and size of apertures in the model are also not good replicas of those in the F-8. Thus, the amplitude of the induced voltages measured in the model cannot be compared directly with those observed in the full scale aircraft, and no attempt was made to do this.

The model induced voltage waveforms should, however, be fairly representative. Measurements were made using the RLC test circuit with the aircraft terminated in an open circuit, resistor equal to its surge impedance, and short circuit to the return lines. The original LTA RLC circuit and a similar circuit modified to include a resistive termination were also studied. In addition to the induced voltages, measurements were made of the voltage surge appearing between the fuselage and an adjacent return line, and of the current exiting the tail of the aircraft. The test circuit and circuit elements for each test are shown together with the measurements in Figure 47.

The measurements shown in Figure 47 indicate the induced voltage is clearly related to the traveling waves on the model fuselage. The first case shown is with the aircraft terminated in an open circuit.

0.5 A   492   0.1 μs   0.5 A   490   0.1 μs   0.5 A   488

Current in each Segment
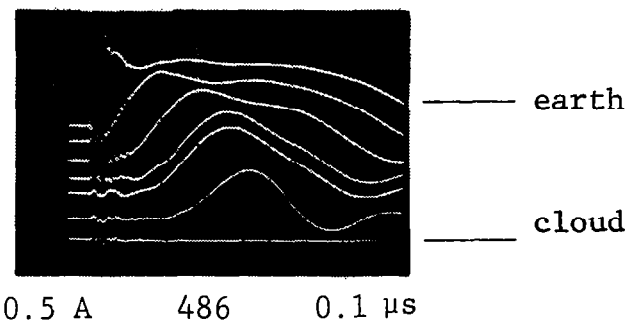
Model

L = 2.5 μH
C = 220 pF
R_t= 100 Ω

—— earth

—— cloud

0.5 A   486   0.1 μs

Figure 46 - Return Stroke in a 500 m, 6-Segment Network
(Each Segment Represents 100 m of Lightning Channel.)

Figure 47 - Geometric Scale Model Induced Voltage Measurements.

88 Test Condition

Open Circuit
$R_s = 0$
$L_s = 0$
$R_t = \infty$

0.5 V   2 V

Terminated
$R_s = 0$
$L_s = 0$
$R_t = 82\ \Omega$

0.5 V   2 V   0.5 A

Short Circuit
$R_s = 0$
$L_s = 0$
$R_t = 0$

0.5 V   1 V   0.5 A

STD 0.2 x 5.0 μs
$R_s = 43\ \Omega$
$L_s = 1.7\ \mu H$
$R_t = 0$

0.5 V   0.5 V   0.5 A

Terminated 0.2 x 5.0
$R_s = 0$
$L_s = 1.7\ \mu H$
$R_t = 83\ \Omega$

0.5 V   2 V   0.5 A
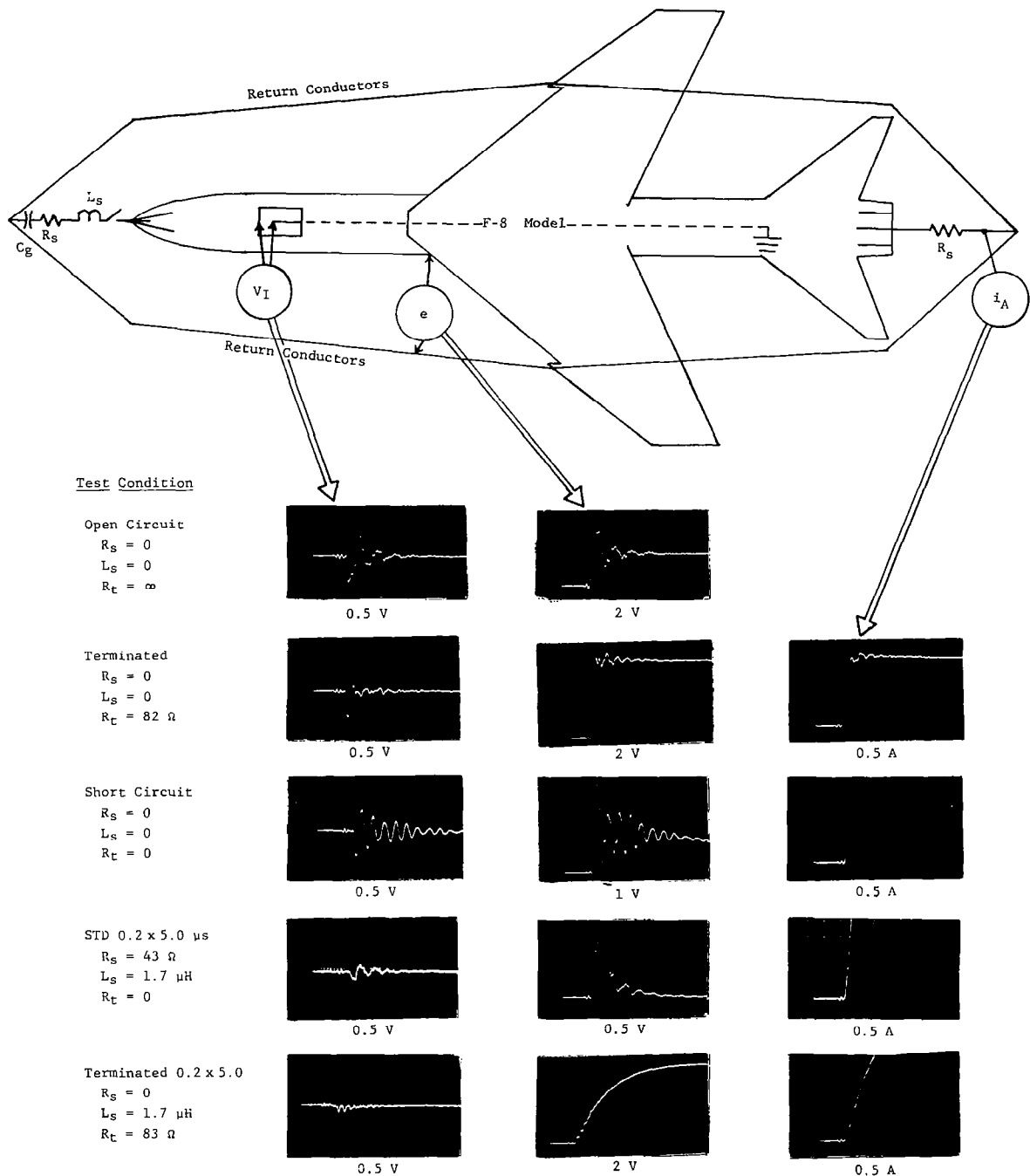
Note: 0.50 μs/div sweep for all oscillograms.

When the mercury wetted switch is closed, the capacitor voltage is immediately impressed on the front of the model. This voltage wave propagates down the fuselage on the transmission line formed by the model and the return lines. The surge impedance (Z_O) of this system was determined to be about 100 ohms. Therefore, associated with the voltage is a current wave of magnitude equal to the capacitor voltage divided by Z_O. The rise time of this wave will be fast, approximately equal to the voltage wave rise time. When the traveling voltage and current waves reach the open end of the fuselage, the voltage wave reflects back toward the nose. Ideally, this would occur at the same amplitude (E) as it began, and with the same polarity. Thus, it would return at double the original amplitude (E + E = 2E) while the current wave (I) reverses in polarity and returns, cancelling out the current (I - I = 0).

Back at the nose of the aircraft, the traveling waves encounter the capacitor. The capacitor acts as a short for the transmission line and causes the voltage wave to reverse. However, only the portion reflected at the open end (E) reverses, so the voltage on the line after the wave again reflects if 2E - E = E. At the capacitor, the traveling current wave (-I) is reflected without polarity change and returns. So the current on the line after this reflection is -I. When these reflections again reach the far end of the model fuselage, the voltage and current traveling waves (-E, -I) reflect as before with the voltage remaining the same polarity (-E) and current changing polarity (I). After these waves start back to the nose, the voltage and current on the line are both zero (E - E = 0, -I + I = 0). At the nose the waves reflect as before, with voltage reversing and current remaining the same polarity so the traveling waves (E, I) and the voltage and current levels on the line are the same as at the start. The cycle can then repeat and would do so forever if there were no losses on the line. Losses due to insulation resistance and stray capacitance and inductance remove energy from the line by absorbing it or diverting it into other systems. Thus the reflections shown in the fuselage voltage wave in the first case of Figure 47 are less than the original amplitude.

In the ideal case of a lossless transmission line, the traveling waves would be perfect square waves with durations equal to the wave transit times. However, the losses in the fuselage system are quite high and the waves never become the ideal square waves. Thus, visualization of the wave propagation described above is somewhat difficult. To help identify traveling wave phenomena in the other cases, traveling wave voltage and current measurements were made on a 50 ohm (Z_O) coaxial cable system where the losses were lower and the square waves more identifiable. The traveling voltage and current waves were measured in the cable at three points corresponding to the nose, mid-fuselage and tail for three of the termination conditions of Figure 47, and

the results are shown on Figure 48. One test was also conducted with a lumped inductor inserted in series with the input nose end, and it can be seen that the inductance changes the square waves to triangle-like waves. In this 50 ohm cable test, the center conductor represents the aircraft and the cable shield represents the return conductors.

By studying Figure 47 and 48, the model fuselage currents can be determined and from them the current changes (dI/dt) which should be related to the induced voltages in the model. For the first condition with the aircraft terminated in an open circuit, the current is continuously oscillating, so there should be an induced voltage that is the derivative of the current with the same basic frequency as the current. This derivative relationship is apparent in the induced voltage oscillograms of Figure 47, and it is also evident in the full scale test of Figure 35, for example.

In the third case, with the aft end of the model short circuited to the return lines, the voltage measured in Figure 47 shows that the traveling waves are reflecting back and forth along the fuselage similar to the behavior of the cable currents shown in Figure 48. A superimposed low frequency oscillation is responsible for the waves not returning to zero, and losses cause the distortion of the traveling waves. The oscillation frequency of the voltage is about twice that of the open circuit case, since now the current traveling wave frequency is twice the open circuit case, as shown in Figure 48.

In the final two cases (4 & 5 of Figure 47), inductors were inserted between the capacitor and the model. In the fourth case, the model tail remained shorted, and in the final case it was terminated on an 82-ohm resistor. The rate of rise of the traveling current waves is reduced in both cases by the inductor, which resulted in lower amplitude induced voltages, as evident in the final two induced voltage oscillograms (Figure 47).

It should also be noted, in comparing all of the induced voltages of Figure 47, that the first induced voltage peaks in the first three cases are nearly the same amplitude, since the wavefront of the first traveling wave was the same in each of these three cases.

RECOMMENDATIONS

A. Any of the circuits evaluated may be utilized for LTA testing, provided the driving cause-effects relationships are established, and accommodated during data analysis as described in Tables VII and VIII.
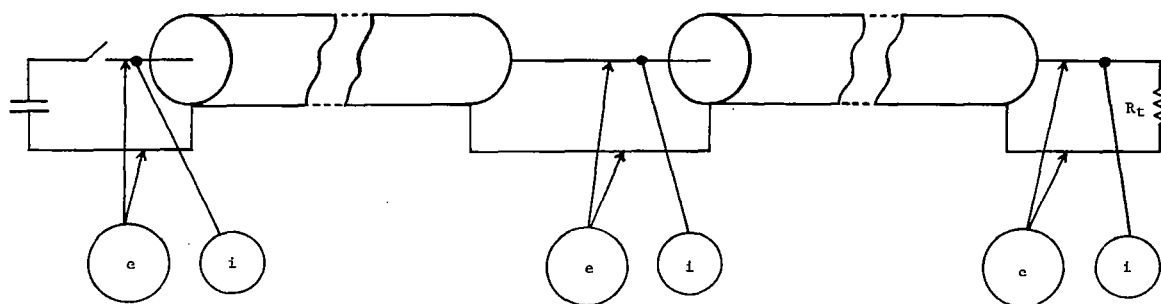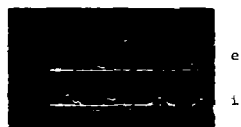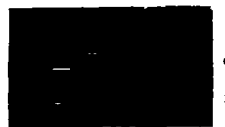
Test Conditions

Open Circuit
$R_t = \infty$
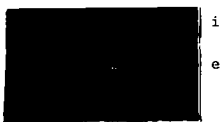
Inductive Input
2 μH

Terminated
$R_t = 50\ \Omega$

Shorted
R = 0

Note: All oscillograms taken at 0.1 μs/div, 5 V/div and 1 A/div.
Upper trace is voltage; Lower trace is current.

Figure 48 - 50 Ohm Cable Transmission Line Voltage
and Current Traveling Wave Measurements.

B. **The lumped parameter ladder network may be an improvement because:**

1. It is a better simulation of a lightning channel, because it represents the channel surge impedance as well as the charge per unit length of a typical lightning channel.

2. Lightning voltage and current may be controlled and related by the surge impedance of the simulated channel and of the aircraft with respect to its return conductors.

3. Impedance matching between the simulated lightning channels and the aircraft can be known and controlled.

4. Both leader attachment and return stroke phases can be represented.

5. The ladder network is efficient. Fast rates of rise and high currents can be obtained with reasonable DC charging voltages, as shown in Figure 49. This figure shows the maximum rate-of-rise and peak currents that can be obtained from the 100 ohm ladder network, the original lumped RLC LTA circuit, and the lumped RLC circuit with the aircraft terminated in its surge impedance (Z_o), as a function of generator capacitor charging voltage. Both of the lumped RLC circuits produce the basic 2 x 50 µs return stroke waveform, but the unterminated circuit produces reflections that act to increase its maximum rate of rise. A study of the figure shows that the ladder network produces the best combination of rate of rise and peak current.

6. It produces a return-stroke waveform with concave front more representative of lightning than the double exponential waveform, as shown in Figure 50. This results in the maximum rate of rise occurring closer in time to the peak current than is the case with the lumped RLC circuit, in which the maximum rate of rise is at t = 0+. A study of return-stroke waveforms recorded in the literature (ref. 22) shows that many lightning return strokes have concave fronts, as shown on Figure 51.

C. **Whichever test circuit is used:**

1. The relationship between induced voltages and airframe currents or their rates of change. should be determined and appropriate extrapolation factors calculated. In particular:

Figure 49 - Performance of Various Test Circuits.

93
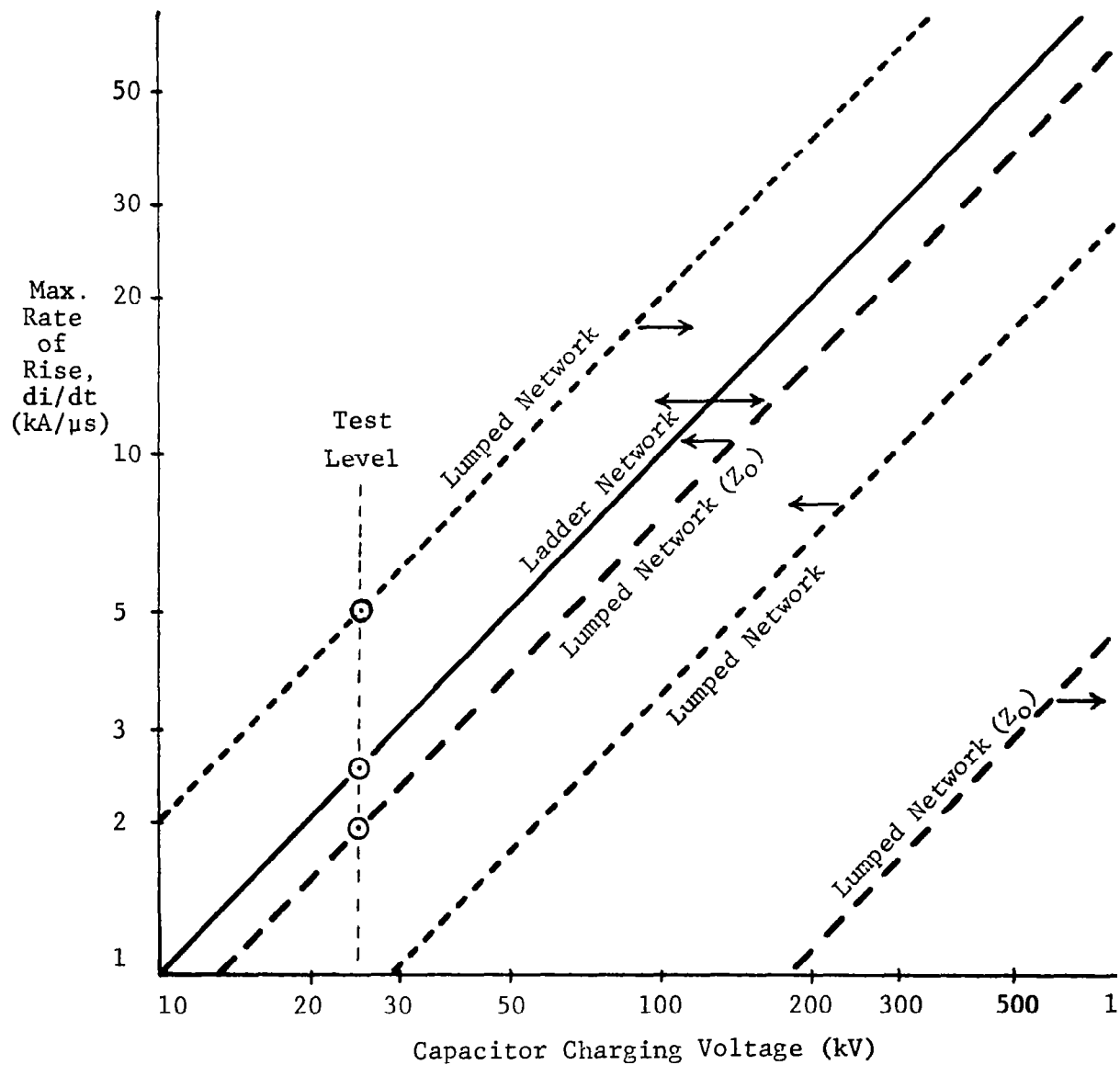
Original RLC Circuit

100A   622   0.5µs
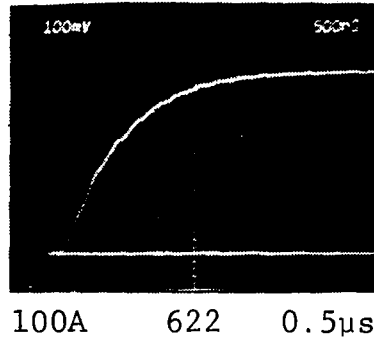
Convex Front

di/dt is
max. at
t = 0

Lumped Element Ladder Network

40A   572   0.2µs
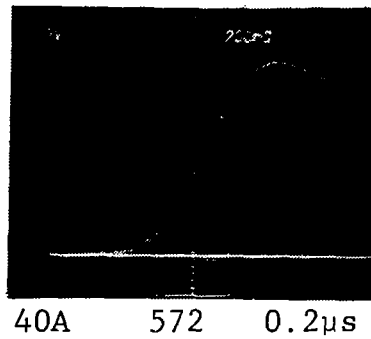
Concave Front

di/dt is
max. at
t = 0.4 µs

Figure 50 - Wavefront Comparison.

Figure 51 - Front Waveshapes of Lightning Currents as
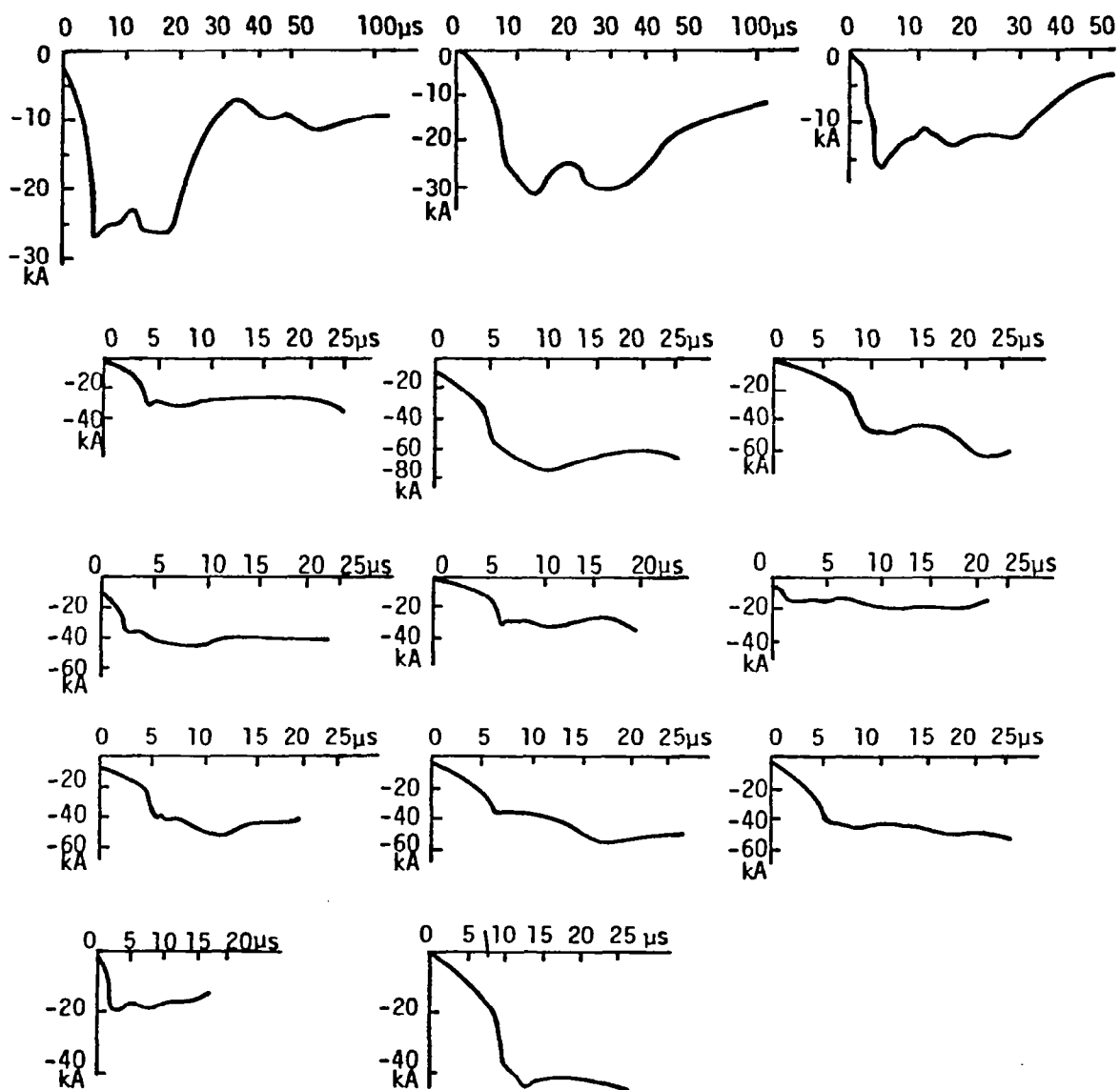Measured by Berger.

A. Voltages dependent on amplitude should be extrapolated by a factor:

$$\frac{200 \text{ kA}}{I_{Test}}$$

B. Voltages dependent on rate of rise should be extrapolated by a factor:

$$\frac{100 \text{ kA/}\mu s}{di/dt_{test}}$$

C. The above factors may be the same if the test current has a waveform that is a proportional replica of the lightning current waveform that is desired to be simulated.

2. Traveling waves between return conductors and the surrounding building may affect the test results. These effects may be reduced by terminating each end of the aircraft return conductor array to building ground with a resistance equal to their surge impedance with respect to the building. This will be approximately 150 ohms in many cases.

3. At least 4 return conductors should be used, spaced symmetrically around the aircraft. Either wires or foils may be utilized.

D. The geometric scale model technique is a powerful tool for evaluating test circuits needed to obtain desired current and voltage waveforms and generator requirements.

CONCLUSIONS

This investigation resulted in an improved understanding of the cause-effect relationships inherent in the induced voltage process taking place in aircraft electrical circuits when the aircraft is subjected to lightning-like current pulses. It also enabled some evaluations to be made of several modified LTA test circuits, with the objective of identifying one(s) that might be improvements. While this investigation did not answer all of the questions surrounding the LTA process, some conclusions are apparent from the work reported herein, and some improvements in the LTA test method appear possible. These are summarized on the following page:

Induced voltages are due primarily to magnetic flux and structural resistances, both caused by currents in the airframe. - This was apparent in comparisons of each of the induced voltage oscillograms with the airframe current that apparently caused them.

Voltages must be present to drive the airframe currents, but since less is known about lightning voltages than about currents, it seems best, for the present, to relate LTA test criteria to airframe currents. - Measurements of the lightning currents that actually flow in the aircraft during the leader attachment and return-stroke phases of the lightning attachment process must be obtained to ascertain the full threat levels that should be simulated or extrapolated to in future LTA tests. Measurement of airframe currents, however, is a much simpler task than measurement of airframe voltages, due to the absence of a reference.

Substantial current may flow in the airframe even if the aircraft is unterminated (floating) when subjected to a high voltage impulse. - In this case the current is solely related to the applied voltage via the airframe surge impedance. The duration of such currents is short, and they will oscillate back and forth along the airframe.

The frequency of oscillatory currents depends on:

1. The length of the airframe and

2. The characteristics of the attached lightning generator circuit.

Test circuit generated traveling waves appear to travel at 50% to 80% of the speed of light through an airframe. - The actual velocity appears to depend on the diameter of the fuselage or wing structure, and the configuration of the return conductors. It may not be possible to identify a definite relationship between an aircraft test circuit and traveling wave transit times, due to the complex geometries involved, but this not necessary since precise simulation of induced voltage frequencies is not necessary for assessment of component damage effects.

Lightning current surges may either. -

1. Travel once through the airframe, from entry to exit point.

2. Enter the airframe, reflect back and forth, and exit.

3. Enter and reflect back and forth only.

What happens in a particular case may depend on the characteristics of the attached lightning channels.

REFERENCES

1. Lloyd, K.J., Plumer, J.A. and Walko, L.C.: Measurements and Analysis of Lightning-Induced Voltages in Aircraft Electrical Circuits. NASA CR-1744, 1971.

2. Plumer, J.A.: Analysis and Calculation of Lightning-Induced Voltages in Aircraft Electrical Circuits. NASA CR-2349, 1974.

3. Walko, L.C.: A Test Technique for Measuring Lightning-Induced Voltages on Aircraft Electrical Circuits. NASA CR-2348, 1974.

4. Maxwell, K.J., et al.: Computer Programs for Prediction of Lightning-Induced Voltages in Aircraft Electrical Circuits. AFFDL-TR-75-36, Volume I, 1975.

5. Plumer, J.A., Fisher, F.A. and Walko, L.C.: Lightning Effects on the NASA F-8 Digital Fly-by-Wire Airplane. NASA CR-2524, 1975.

6. Plumer, J.A.: YF-16 #1 Lightning Transient Analysis Test Report. General Dynamics Report 16PRO51, 1975.

7. Space Shuttle Program Lightning Protection Criteria Document. JSC-07636, Revision A, 1973.

8. Cianos, N. and Pierce, E.T.: A Ground-Lightning Environment for Engineering Usage. Stanford Research Institute Technical Report No. 1, 1972.

9. Nanevicz, J.E., Bly, R.T. and Adamo, R.C.: Airborne Measurement of Electromagnetic Environment near Thunderstorm Cells. Proceedings of the 1977 IEEE International Symposium on Electromagnetic Compatibility, IEEE Publication 77CH 1231-0 EMC.

10. Bewley, L.V.: Travelling Waves on Transmission Systems, Second Edition, Dover Publications, Inc. 1963.

11. Fisher, F.A.: Geometric Model Studies of KSC Launch Facilities. General Electric Report SRD-76077.

12. Fisher, F.A.: Feasibility of Geometric Models for the Determination of Shielding Effectiveness. General Electric Report, 1966.

13. Crouch, K.E.: Lightning Current Distribution on a Scale Model Space Shuttle Rocket Engine. General Electric Company Corporate Research and Development Report SRD-73-177, 1973.

14. Fisher, F.A.: Geometric Model Studies of KSC Launch Facilities. General Electric Company Corporate Research and Development Report SRD-76-077, 1976.

15. Crouch, K.E.: Lightning Protection Evaluation of Launch Complex 36A Using Model Techniques. Lightning Technologies, Inc. Report LT-78-07, 1978.

16. Little, P.F., Hanson, A.W. and Burrows, B.J.C.: Test Techniques for Simulating Lightning Strikes to Carbon (Graphite) Fibre Composite Structures. Proceedings of the 1979 Federal Aviation Administration-Florida Institute of Technology Workshop of Grounding and Lightning Technology.

17. Kim, D.G., Dubro, G.A. and Tessler, L.P.: Transmission Line Theory Applied to Aircraft Lightning Interactions. Proceedings of 1977 IEEE International Symposium on Electromagnetic Compatibility, 1977.

18. Little, P.F.: Transmission Line Representation of a Lightning Stroke. Journal of Applied Physics, Vol. 11, 1978, pp. 1893-1910.

19. Strawe, D.F.: Non-Linear Modeling of Lightning Return-Strokes. Proceedings of the 1979 Federal Aviation Administration-Florida Institute of Technology Workshop on Ground and Lightning Technology.

20. Fisher, F.A. and Plumer, J.A.: Lightning Protection of Aircraft. NASA Reference Publication 1008, 1977.

21. Hess, R.F.: EMP Coupling Analysis Using the Frequency (Transfer Function) Method with the SCEPTRE Computer Program. IEEE Transactions on Electromagnetic Compatibility, 1975.

22. Berger, K.A.: Novel Observations on Lightning Discharges: Results of Research on Mount San Salvatore, Franklin Institute, 1971.

1. Report No. NASA CR-3329	2. Government Accession No.	3. Recipient's Catalog No.
4. Title and Subtitle IMPROVED TEST METHODS FOR DETERMINING LIGHTNING-INDUCED VOLTAGES IN AIRCRAFT		5. Report Date September 1980
		6. Performing Organization Code .
7. Author(s) K. E. Crouch and J. A. Plumer		8. Performing Organization Report No. LT-80-59
9. Performing Organization Name and Address Lightning Technologies, Inc. 560 Hubbard Avenue Pittsfield, Massachusetts 01201		10. Work Unit No. 512-51-14
		11. Contract or Grant No. NAS4-2613
12. Sponsoring Agency Name and Address National Aeronautics and Space Administration Washington, D.C. 20546		13. Type of Report and Period Covered Contractor Report
		14. Sponsoring Agency Code H-1126

15. Supplementary Notes

NASA Technical Monitor: Wilton P. Lock, Dryden Flight Research Center

Final Report

16. Abstract

Tests performed on aircraft at reduced lightning current levels to measure the magnitude of voltages induced on the electrical cables have used standard lightning current generators which produce double exponential current waves. A lumped parameter transmission line with a surge impedance (Z_0) matching that of the aircraft and its return lines was evaluated as a replacement for the earlier current generators. Various test circuit parameters were evaluated using a 1/10 scale relative geometric model. Induced voltage response was evaluated by taking measurements on the NASA-Dryden Digital-Fly-by-Wire (DFBW) F-8 aircraft. Return conductor arrangements as well as other circuit changes were also evaluated, with all induced voltage measurements being made on the same circuit for comparison purposes. The lumped parameter transmission line generates a concave front current wave with the peak di/dt near the peak of the current wave which is more representative of lightning. However, the induced voltage measurements when scaled by appropriate scale factors (peak current or di/dt) resulting from both techniques yield comparable results.

17. Key Words (Suggested by Author(s)) Lightning Transients Induced voltages Test techniques	18. Distribution Statement Unclassified - Unlimited Subject category 05		
19. Security Classif. (of this report) Unclassified	20. Security Classif. (of this page) Unclassified	21. No. of Pages 107	22. Price* $9.00